2011

Aspects of the contemporary and Quaternary hydrology of the Lake Eyre Basin, central Australia

Joshua Redder Larsen
University of Wollongong

Aspects of the contemporary and Quaternary hydrology of the Lake Eyre Basin, central Australia

Joshua Redder Larsen

This thesis is presented as part of the requirements for the award of the Degree of

Doctorate of Philosophy

From the School of Earth & Environmental Sciences
University of Wollongong

November 2011

THESIS DECLARATION

I, Joshua Redder Larsen, declare that this thesis, submitted in fulfilment for the requirements for the award of the award of Doctor of Philosophy in the School of Earth and Environmental Sciences, University of Wollongong, is wholly my own work unless otherwise acknowledged. This document has not been submitted for qualifications at any other academic institution.

The chapters of this thesis constitute papers submitted or published within academic journals, and where co-authors are present remain approximately 80% my own work. I developed the ideas, aims and methods for each chapter, conducted all the analysis, and wrote all the text. Whist this text was subject to the review of my supervisors, co-authors, editors and journal reviewers, in general this only changed the presentation and interpretation of results and not the overall aims, methods, or conclusions.

Joshua Larsen

Gerald Nanson

November 2011

"Whatever idea I might have had of the character of the country into which we penetrated, I certainly was not prepared for any so singular as that we encountered…"

Charles Sturt, Australian explorer (1795 – 1869).

ABSTRACT

The availability of surface water resources is of fundamental concern globally, especially in dryland environments where these resources are particularly vulnerable to over-exploitation. Determining the extent and quality of this water also requires some knowledge about the susceptibility of these resources to change. This thesis aims to improve our understanding of the water balance in dryland environments, in particular within the Lake Eyre Basin (LEB) in central Australia, both in terms of modern processes and the factors that may have resulted in changing hydrological conditions during the Late Quaternary.

The dissolved load in the contemporary dryland rivers of the LEB is assessed and indicates that evaporation does not significantly modify the ionic content or solute concentration despite large transmission losses to the surface water budget (~64% of mean annual flow). The source of these solutes is investigated and shows that although rainfall and dust account for the bulk of them, silicate weathering also plays a surprisingly important role. This suggests that dryland environments should also be included estimates of the global silicate-weathering cycle. A comprehensive investigation into the cause and fate of the large catchment transmission losses, and their role in the water budget within the LEB is undertaken. The semi-confined alluvial setting caused by the large mud-dominated multiple channel and floodplain system in many parts of the LEB, and in particular the Channel Country of Cooper Creek, has resulted in at least three distinct shallow groundwater recharge pathways. These control recharge rates, the distribution of freshwater lenses, and the evolution of high groundwater salinities. This highlights the importance of preferential flow in semi-confined alluvial settings, and suggests that where hydrological variability is typically high, such as dryland environments, groundwater recharge is perhaps better considered as a probability of occurrence instead as an average rate. Furthermore, the sum of these probabilities may in turn best account for the observed transmission losses in the water budget.

The current hydrology of the LEB is complex, making it difficult to interpret the conditions that prevailed during the dramatic changes in climate and hydrology associated with the Late Quaternary. This aspect of the study investigates runoff

conditions required to maintain the system of terminal lakes. Strzelecki Creek, a distributary of Cooper Creek originating at Innamincka, has a record of fluvial deposition that broadly matches the fillings of the Lake Mega-Frome system. This confirms the ability of the headwaters of the LEB to deliver runoff to both the Mega-Frome and Eyre terminal lakes at various stages of the Late Quaternary. The magnitude of change required to balance the water and energy budgets implied by the existence of much larger lakes throughout the Late Quaternary in central Australia is quantified. The acute sensitivity of surface water hydrology to small changes in climate within dryland environments is highlighted. The results indicate relatively small changes (~ 27 %) in mean basin rainfall can fully account for the existence and maintenance of the largest recorded lake systems. These results have important implications for the interpretation of Late Quaternary climate changes, the impact of early human arrival on the landscape of the LEB, and the role of climate in the extinction of Australia's megafauna. Previous assessments have largely overlooked the non-linear relationships and potential feedbacks between hydrology and climate, and this has led to some unlikely proposals for palaeo-environmental change during the Late Quaternary. This work can guide future research that combines data-driven and modelling approaches to the investigation of modern and Late Quaternary water balances, especially in the dryland regions of the world.

ACKNOWLEDGEMENTS

Firstly, and not least because of their enduring patience, the biggest thanks must go to my main supervisors Gerald Nanson and Dioni Cendón, for persevering with my short attention span, and somewhat delayed writing inspiration. I trust the extended tenure has resulted in a finer vintage than would have otherwise been produced by a more rapid completion, which on last inspection has not yet turned to vinegar. It has truly been an inspirational collaboration, and a course from which I have perhaps learnt how to finally be a scientist.

For my equally patient and ever supportive family, I guess this is finally it. So, Dad, Mum, Melinda, Grandma, and Grandad, all of this, is as much yours as it is mine. Although the text itself may not bear the hallmarks of your advice or effort, to have begun in the first place, and most definitely to have reached the end, was only made possible because of it.

To all willing and unwilling field participants, who in no order of effort or timing include: Martyn Hazelwood, Tim Grey, Anna Halbeck, Sarah Woodward, Tom Gill, Rebecca Jackson, Luke Morley, and Oscar Garrett. It was also a privilege to work and learn in the field with so many accomplished and capable scientists: John Jansen, Tim Cohen, Jan-Hendrick May, and of course my supervisors, Brian Jones, Gerald Nanson, and Dioni Cendón. In this regard I must also make special mention and thanks to Brent Peterson, without whose technical expertise, not a single sample would have been yielded from that sordid, dusty, and beautifully brutal landscape. Trevor Whitelaw and SANTOS provided much needed field assistance and logistical support, and the staff from both Moomba and Ballera are also thanked for site access and support. Kidman properties at Nappa Merrie and Innamincka, and also the station owners at Merty Merty and Moolawatana, are gratefully acknowledged for providing access and much needed assistance with vehicles, trailers, and tires.

I am grateful to the institutional support provided by the University of Wollongong (UOW) and the Australian Nuclear Science and Technology Organisation (ANSTO), especially for providing matching and top-up scholarships, respectively. Funding from the Australian Research Council and Faculty of Science also supported most of the work. When all samples and hope seemed lost, I thank Paul Carr, Lesley Head, Colin Murray-Wallace, the Dean Will Price for their assistance, and of course Gerald

Nanson, who managed to galvanise a full advance in the face of what surely seemed an inevitable retreat.

I am indebted to the jovial and upbeat OSL lab facilities at UOW provided by Bert Roberts and Zenobia Jacobs, and especially the support and training from Terry Lachlan. However, it is to the infinite generosity of the Risø luminescence group, especially Andrew Murray, Jan-Pieter Buylaert, Mayank Jain, and Rezza Sobhati, to which I owe any ability to analyse and interpret some aspect of the black-magic world of OSL. Risø is truly a wonderful place to be. I also thank the various lab staff at ANSTO, especially the radiocarbon lab, for the provision of crucial facilities, and also for accommodating the odd OH&S nightmare.

In some misguided twist of fate, I have also begun employment as a post-doctoral researcher prior to the completion of the actual doctorate, which apart from being quite absurd has also been both a blessing and a curse. I thank my new employers at the Water Research Laboratory (University of New South Wales), especially Martin Andersen and Ian Acworth, for their continued patience, and especially for the provision of new research directions which have become endlessly distracting and fascinating.

Finally, to my wife, without whom, it is safe to say, this work would have stayed in the back lots of near completed and half thought out ideas, never seeing the full roundness of scientific reason. I would never have had the courage to pick everything up and put it together, to trust in some ability to find something worth saying, or even the need to get up in the morning, without this wonderful woman. Annegret, with all my heart, thank you.

TABLE OF CONTENTS

LIST OF FIGURES

LIST OF TABLES

1 INTRODUCTION

1.1 General overview

The availability of surface water resources is of fundamental concern globally, especially in water limited environments where these resources are particularly vulnerable to over-exploitation. Determining the extent and quality of water availability in these environments also requires some knowledge of the susceptibility of these resources to change. Moreover, the fate of precipitation in the dryland areas of the world is not well understood, conceptually, and actual measurements of many aspects of the water cycle are rarely compared to those of better-watered regions. Additionally, because of the contrast offered, it is in world's dryland areas where some of the most dramatic evidence for wet climates in the earth's recent past can be found. Here past changes can be quantified and the future scenarios can be better predicted.

Within the broader problem of water resources, there are substantial scientific insights to be gained from the investigation of the hydrological processes operating in dryland areas. The large uncertainties in rainfall and streamflow, both in timing and magnitude, yield unique hydrological and ecological systems. However, our perspective is short, and in Australia monitoring of these regions for scientific purposes has been haphazard and, even then, only for the last ~ 50 years. The hydrological view from beyond the historical record and into the Quaternary has its origins with the first humans to settle Australia:

> *"According to the traditions of some Australian aborigines, the deserts of Central Australia were once fertile, well-watered plains. Instead of the present brazen sky, the heavens were covered by a vault of clouds, so dense that it appeared solid; where to-day the only vegetation is a thin scrub, there were once giant gum-trees, which formed pillars to support the sky; the air, now laden with blinding, salt-coated dust, was washed by soft, cooling rains, and the present deserts around Lake Eyre were one continuous garden."* Gregory (1906).

Gregory (1906) continues with Aboriginal stories that apparently originate with the Dieri people whose traditional lands included parts of Lake Eyre and lower Cooper Creek. These stories explain that the soils were once fertile and shielded from the sun by a dense canopy. The order in which Gregory (1906) goes on to describe the Dieri explanation for the disappearance of these better watered conditions suggests that the basic premise of feedbacks between the water and the energy balance of the earth's surface were understood, at least to some degree, by the Aboriginal people of central Australia, albeit repeated as myth and tradition.

Such an intense contrast between past and present in the Lake Eyre basin (LEB), and the unknown basis of many of the observed modern hydrological conditions, both offer unique scientific challenges and an opportunity to make progress in many aspects of the contemporary and palaeo-hydrological balance of dryland environments in general. In an attempt to address some of these challenges, this thesis presents four separate papers that have been prepared on a range of topics within this context. Although each addresses separate scientific problems at different temporal scales, they are all connected in an appeal to the fundamental processes governing our understanding of water resources in that drylands that constitute a third of the earth's land surface.

Much of the research of Gregory (1906) focussed on the large mammal fossils, members of the now extinct megafauna of Australia, found in close proximity to many of the terminal lakes in the LEB. He then wondered whether the environment of today could support them, or whether the environmental change as told by the Deiri people might be somehow responsible for their demise, and with considerable understatement suggested that:

> *"If therefore, the geologist can determine whether the extinct monsters of Lake Eyre correspond to those described in Aboriginal traditions, he can throw light on several interesting problems..."*

Although we can safely suggest this correspondence between the extinct monsters in Aboriginal tradition and those within the LEB sediments to be true, the shedding of light on several interesting problems, over 100 years later, remains the exact task of the work presented here.

1.2 Aims and outline

The title of this thesis sets a broad range of investigation, and through building upon a smaller series of questions it is hoped that critical gaps in our knowledge concerning the contemporary and palaeo-hydrology of the LEB can be investigated. The transfer of water, sediment, and solutes from catchment headwaters to their termination in the ocean or in lakes, are fundamental processes which we seek to understand as hydrological systems. This will enable us to project this understanding on the records of hydrological change that occur in a variety of environmental archives. In the case of intra-continental drainage basins, such as the LEB, the transfer of solutes is concentrated in terminal lake systems that have developed as saline playas. The origin and transfer of solutes in the rivers that drain to these lakes, and their relationship to the surface water balance, remain poorly understood. Chapter 2 (submitted date to *Global Biogeochemical Cycles*) attempts to answer these questions using data on the dissolved load from all the major tributaries in the Lake Eyre Basin. It also provides a general framework for analysing water quality trends and changes within dryland environments as well as suggesting possible management implications where surface water resources are yet to be developed.

Given the relative lack of knowledge concerning surface water resources in the Lake Eyre Basin, it is perhaps not surprising that beyond its existence, very little is known about the shallow groundwater resources in the basin. Chapter 3 attempts to address this knowledge gap by addressing the relationship between the large transmission losses in the surface water budget and the shallow groundwater recharge rates estimated from geochemical tracers. The role of preferential flow paths, maintenance of freshwater lenses, and the general evolution of near-surface saline groundwater in semi-confined aquifer environments of the river floodplains are also investigated.

The climatic controls governing the distribution of water resources are well understood in terms of basic principles, however, this is not necessarily the case for our interpretations of the past where the evidence for the magnitude and extent of water resources relies mostly upon proxy environmental evidence. One major difficulty is how to gauge which climate factors, such as rainfall or potential evaporation, have changed, and by how much, relative to the present. Chapter 4, recently published in *Quaternary Australasia*, provides a general outline of this problem and also addresses specifically the misuse of evaporation in palaeo-

hydrology investigations that attempt to balance the water budget, particularly at the time of the Last Glacial Maximum (LGM).

Continuing this palaeo-hydrology theme, Chapter 5 examines the Late Quaternary river dynamics of Strzelecki Creek and its relationship with the palaeo-hydrology of the terminal lake system. This chapter aims to combine the environmental proxy approach with the quantitative tools available from contemporary hydrology in order to investigate the Late Quaternary water resources of the LEB. This approach sheds light on the scale of past environmental change and illustrates the sensitivity of surface water resources in dryland landscapes to small changes in climate.

2 WHAT DETERMINES THE DISSOLVED LOAD OF DRYLAND RIVERS? THE CASE FOR WEATHERING, RAIN, DUST, AND ABSENCE OF EVAPORATION IN THE LAKE EYRE BASIN, CENTRAL AUSTRALIA.

2.1 Abstract

The source of the dissolved load in global rivers is often debated in terms of the contribution from weathering and cyclic salts, however, rivers within the arid and semi-arid regions of the world have received comparatively little attention in this regard. Here, we compile data from the major rivers of the LEB in central Australia, which is an endoreic basin draining $1/7^{th}$ of the Australian continent. These dryland rivers appear to maintain a mostly constant concentration of ions with increasing discharge, and are appreciably distinct from solute sources such as rain, and the soluble fractions of windblown dust and soils. Assuming all the Cl in the dissolved load of the rivers is derived from rain and dust, a combined mass balance reveals these sources can account for 22 – 75% of the major ions in the rivers. The remaining fraction of solutes must then be attributed to silicate and/or carbonate weathering, which we quantify based on deviation from an idealized silicate weathering relationship between Na, Ca, Mg, and HCO_3. These results demonstrate silicate weathering can account for the majority of the remaining ions (10 – 70%), with minor contributions from carbonate weathering, except in one catchment with a small area of carbonate lithology, which exerts a strong influence on the dissolved load. In addition, despite large transmission losses (64%) over the lower reaches of these rivers, we find no significant role for evaporative modification of the dissolved load, and instead attribute these losses to shallow groundwater recharge and flood routing to terminal wetlands. These results have implications for our understanding of the global silicate weathering cycle, which has previously concentrated on more temperate climates or areas of significant topographic relief, and suggests that the dryland rivers of the world might also make an important contribution. Furthermore, a comparison with other dryland rivers in Australia suggests any significant development of flow regulation is likely to cause a dramatic decline in water quality and aquatic habitat functionality, and should be taken into account in any future management of these basins.

2.2 Introduction

The large dryland rivers of the world, defined here as rivers in arid and semi-arid regions, are often allogenic, meaning that their waters are fed mostly from outside their predominantly dryland setting. This may in turn determine their dissolved and suspended loads, as well as flood magnitude and frequency, and when originating in tropical-monsoon regions are commonly strongly skewed towards the low frequency, high magnitude end of the range. Such highly variable flow regimes and flood hydrology determine the distinctive ecologies (Leigh et al., 2010) and fluvial processes (Tooth, 2000) present in these system, with patterns in water quality also likely to have large effects on the composition of dryland ecosystems (Marshall et al., 2006). Research concerning the nature and origin of the dissolved load of these systems is, therefore, critical in order to properly understand these processes.

Compared to their better watered counterparts, we still know very little about the major hydrological processes, ion sources and controls both between and within dryland river catchments (Powell, 2009), and yet conceptually they should be beholden to the same potential processes and trends as other surface waters. The initial work of Gibbs (1970) explained the composition of the dissolved load of rivers and lakes around the world as being the result of mixing between two main sources of ions, rainfall and rock weathering, and the modification processes, evaporation and crystallization. Gibbs (1970, 1971) suggested that because of mid-range total dissolved solid (TDS) concentrations and low Na / (Na + Ca) ratios, the origin of major ions in dryland rivers was most likely dominated by rock weathering, prior to being modified by evaporation and crystallization processes as the waters travel downstream. Feth (1971) also highlighted that ion contributions from springs are often proportionately higher in dryland rivers and that, using the method of Gibbs (1970) this composition is difficult to distinguish from the effects of evaporation. Mixing with saline shallow groundwaters has since also been found to be a significant modification process in some semi-arid rivers where high water tables can be maintained through irrigation and land use change (Herczeg et al., 1993).

The dominance of rock weathering as the origin of the major ions in the larger streams and basins has become well established (Meybeck, 2003; White, 2003). As such, studies of many catchments around the world with substantial topographic relief have attempted to quantify the type of weathering (i.e. silicate, carbonate or

evaporite) responsible for the composition of rivers (Gaillardet et al., 1999; Garrels and Mackenzie, 1967; Jacobson et al., 2003; West et al., 2005). Gaillardet et al. (1999) concluded dryland rivers such as the Murray River in Australia and the Limpopo River in SE Africa exhibit very low rates of silicate weathering; and that the former in particular is dominated by ions that are rainfall derived. In these studies, the attribution of the dissolved load to specific kinds of weathering is achieved using either a mineral mass-balance approach (Bowser and Jones, 2002; Garrels and Mackenzie, 1967), or inverse mathematical methods based on major ion ratios, usually with Na as the denominator (Gaillardet et al., 1999; West et al., 2005). Most studies of the sources of the dissolved load of rivers, however, neglect the input from dry dust deposition, largely because of the shortage of data on the soluble content of regional dust sources, and is potentially a large source of error in the attribution of ions sources within the dissolved load of arid rivers.

Despite the importance of rock weathering in determining the composition of the dissolved load, and setting the backdrop for water quality in a large proportion of surface waters around the globe, most studies within Australian catchments have concluded that rainfall is the major source of ions in the dissolved load (Jolly et al., 2001). As a result, a rainfall origin for solutes has become the dominant paradigm for the interpretation and management of water quality in Australia. This is in contrast to earlier studies suggesting rock weathering was an important source in arid, semi-arid, and temperate areas of the continent (Gunn and Fleming, 1984; Gunn and Richardson, 1979; Wopfner and Twidale, 1967), and for determining shallow groundwater compositions in some semi-arid areas (Herczeg et al., 2001). Also, more recent studies in the headwaters of major agricultural river basins in Australia have demonstrated that rainfall is not necessarily the major source of ions in shallow ground and surface waters (Acworth and Jankowski, 2001; Herczeg et al., 1993; White et al., 2009). In addition, dry deposition of dust is rarely considered as a source of solutes, despite Australia being a continent with significant dust activity (McTainsh, 1989), and the previous work of Simpson and Herczeg (1994) which suggested that up to 50% of Cl in the western Murray River basin is derived from dry deposition of dust. Since most of the Australian continent is semi-arid to arid, correctly interpreting the balance and sources of solutes in these rivers is of relevance

not only to the management of Australian river systems, but also to better understand arid and semi-arid catchments worldwide.

In this study, we focus on the endoreic Lake Eyre Basin (LEB) (Figure 1), whose rivers receive most of their water from the Australian summer monsoon, and provides runoff that reaches all the way to Lake Eyre only about once a decade. We combine datasets of water chemistry and the potential major ion sources in this region, including: rainfall, dust, soils and bedrock, in order to elucidate the potential sources of ions which constitute the dissolved load. The aim of this paper is therefore to quantify the contribution of these various sources to the dissolved load of dryland rivers, and determine the mechanisms responsible for the delivery and modification of this load in order to expand our knowledge on the functioning of dryland catchments.

2.3 Regional Setting

2.3.1 Climate and rainfall

The LEB is an intra-continental drainage basin covering ~1/6th of the Australian continent. It spans a large longitudinal and latitudinal range, and although most of its climate is almost entirely arid to semi-arid, the northern headwaters of the basin are able to receive large magnitude rain events from incursions of the summer monsoon (Figure 1). The Cooper Creek and Georgina-Diamantina catchments are the most significant catchments in this basin, draining the north and northeastern portions. Minor floods are usually experienced every summer (wet season), and major floods occur typically during La Niña phases of ENSO (Kotwicki and Allan, 1998a).

Mean annual rainfall varies between ~530 and ~450 mm yr-1 in the upper Cooper Catchment above Longreach, after which mean annual rainfall decreases to Currareva (~361mm yr-1) and even further to Nappa Merrie (~200 mm yr-1). This inland decrease in mean annual rainfall in part reflects the southern limit of summer low pressure incursions, however, most of these large rainfall events are infrequent and there is potential for significant easterly derived rainfall to occur during winter. Rainfall is spatially sporadic, and only a small percentage of rainfall from these events is converted to runoff, thus it is difficult to predict and describe the conditions necessary for large magnitude discharge events to occur (McMahon et al., 2008a). It is generally observed, however, that rainfall of greater than 200 mm in 72 hours

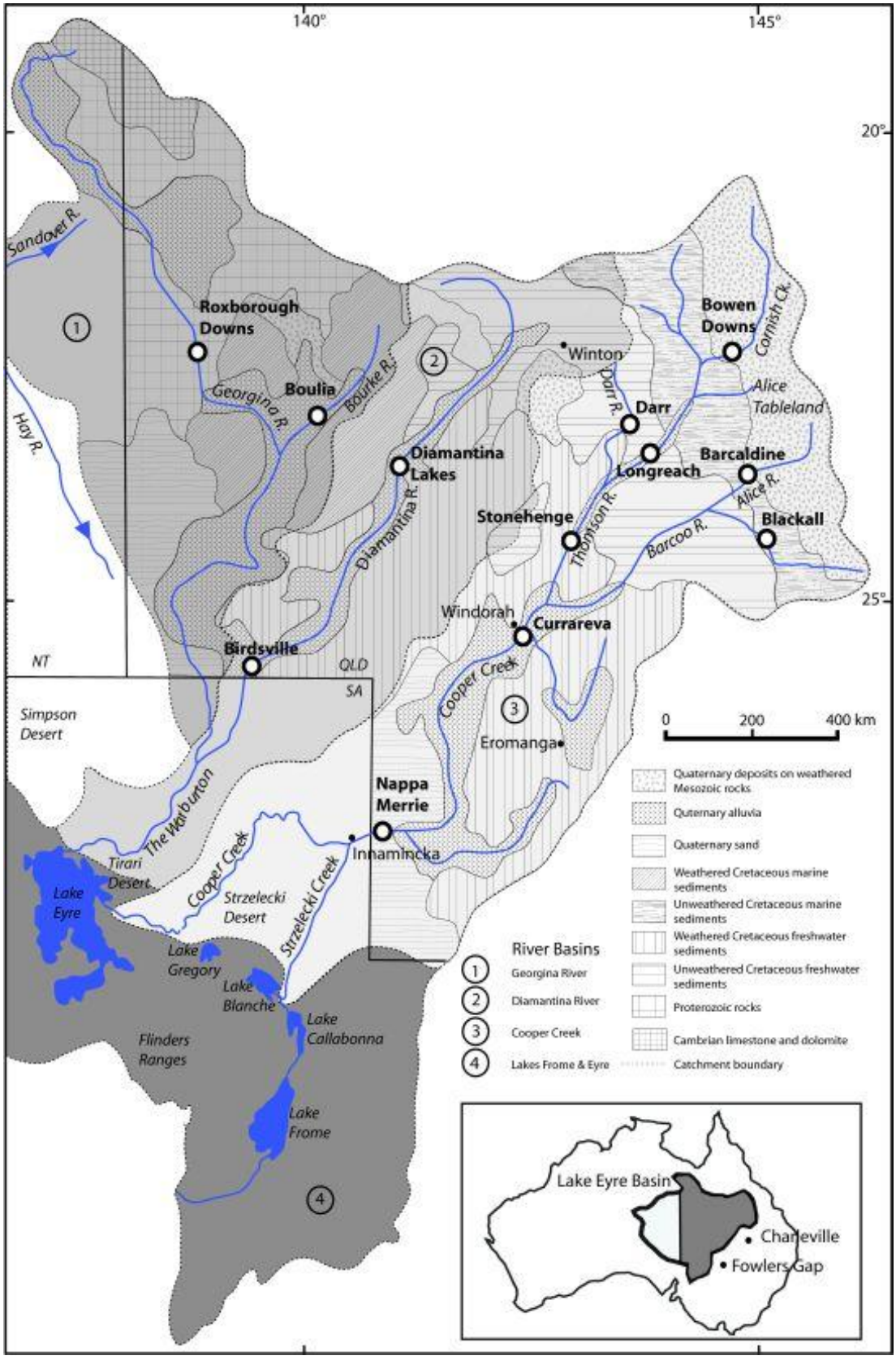

Figure 1. Geomorphology, geology, and major catchments of the eastern LEB. Discharge and sampling station locations are shown as large circles, with Table 1 and Figure 3 referring to these stations by the name of the River from where the

measurements were taken. Base map substantially modified from Gunn and Fleming (1984).

within a confined region of the catchment can lead to large flows connecting most of the channels and floodplains of the system up to the edge of the major dunefields of the Strzelecki, Tirari and Simpson Deserts. Once flows reach these deserts, the sandy river channels experience large transmission losses through infiltration and inter-dune flood routing to numerous clay pans and terminal playas. However, precise transmission losses are difficult to determine since few flow data exists, especially in these dunefields (Bullard et al., 2007). Potential evaporation exceeds actual evaporation in all parts of the LEB, except in the very headwaters of Cooper Creek (Ceplecha, 1971), with potential evaporation rates ranging from 2.2 m/yr in the very north east to almost 4 m/yr in the downstream reaches of Cooper Creek and the Diamantina River.

2.3.2 Hydrology

As a result of the variable climate and rainfall distribution, rivers in the LEB are characterized by long dry periods between flow events of highly variable magnitude (Knighton and Nanson, 2001). However, the LEB remains completely unregulated in terms of flow, which means the flow and dissolved load data presented here can be interpreted as reflecting natural conditions. The event hydrographs for stations in the headwaters of these catchments are generally flashy and with larger peaks compared to stations farther downstream (Knighton and Nanson, 1994). During large magnitude flood events, downstream stations continue to receive flow for weeks and sometimes months following the peak in discharge because of the large, low gradient catchments that they drain. As a result, stations in the downstream more arid parts of the catchment typically have fewer days of no flow than those in the upper parts of the catchment, although these headwater stations can also experience minor flows from smaller winter rains. The discharge relationships are further complicated with increasing catchment area because as the hydrograph recessions become longer, the probability for additional rain events and tributary contributions increases and results in complicated compound hydrographs for many downstream stations (Bullard et al., 2007; Knighton and Nanson, 1994).

Although the Cooper Creek catchment has higher average peak discharges, it is the Georgina-Diamantina catchment which supplies most of the flow to Lake Eyre itself (Kotwicki, 1986). McMahon et al. (2008b) summarized all the available streamflow data in the LEB, with three points being particularly relevant to this study: 1 - discharge variability is approximately double that of the average for all other dryland rivers in the world; 2 - discharges increase until the mid-catchments where heavy transmission losses diminish flows for the remaining stream length; and 3 - the median contribution of baseflow to total daily discharges over the full range of flow durations is 7%, indicating groundwater is only a minor contributor to stream discharge.

The rivers of the LEB possess unique habitats and ecology, especially in their mid reaches where they adopt a large anastomosing river style, and the many waterholes in enlarged channel segments provide relatively large aquatic refugia during periods of low or no flow (Bunn et al., 2006; Hamilton et al., 2005a). Like many dryland rivers of the world, we know very little about the water quality or balance in these catchments, and the processes which control them. Sheldon and Fellows (2010) recently analyzed the major ion composition from a number of waterholes in the mid-reaches of Cooper Creek and the Warrego River, and found Na-Ca-HCO_3 type waters with low TDS, even during no flow periods, which they attributed to groundwater discharge following mixing with carbonate-rich sediments. This is a similar result to that found by Cendón et al. (2010) for surface waters farther downstream in Cooper Creek, yet in their analysis of the shallow groundwaters they could find no evidence for groundwater contribution to surface flow, a conclusion similar to that of Hamilton et al. (2005a).

2.3.3 Geology

The headwaters of the LEB are composed mostly of shallow weathered and unweathered marine and freshwater sedimentary rocks that form the uppermost sequences of the Eromanga Basin. The sediments which comprise these formations are largely volcaniclastic, derived from a large silicic volcanic province off the east coast of Australia (Bryan et al., 1997). The depositional environments of these sediments range from marine to freshwater, with the most extensive and youngest being the Cretaceous – Late Palaeocene freshwater Winton Formation. In the Late

Palaeocene drainage was re-arranged, forming the continental Lake Eyre Basin, and various fluvial and lacustrine facies were deposited (Alley, 1998). Throughout the Quaternary, however, a general trend towards increasingly arid conditions has been observed (Nanson et al., 2008; Nanson et al., 1992).

Extensive weathering and mobilization of ions certainly occurred sometime between the Early – Mid Cenozoic in the LEB, and in many other parts of the Australian landscape (Pillans, 2007). In the LEB this weathering is often manifest in thick kaolinitic soil profiles with alternating ferruginous and palid zones (Senior and Mabbutt, 1979) and abundant silcrete formation, which is the result of multiple phases of silica and iron mobilization (Alley, 1998). The timing of these events remains speculative, although a recent study by Fujioka et al. (2005) demonstrated that some of this silcrete must have formed prior to the development of the stony desert pavements 2 - 4 Ma ago. The basin is tectonically stable on global standards, however, gentle warping may explain landscape doming features, particularly in the silcrete-capped terrains, and the preferential stripping of the lower surfaces. The timing and magnitude of warping remains speculative, however, the high temperature shallow granites beneath the sedimentary basins may provide an on-going source of thermal uplift, such as the Innamincka Dome which has been shown to be rising at greater than 36 m/Ma (Nanson et al., 2008).

In the upper and middle reaches of the Cooper and Georgina-Diamantina catchments much of the weathered terrain has been stripped at some time in the Late Cenozoic to expose fresh bedrock, over which, in places, a more recent soil profile has developed (Figure 1) (Gunn and Fleming, 1984). Prior to ~400 ka, much of the northern Australian landscape had bedrock valleys without extensive sediment cover (Nanson et al., 1993), and the stripping of the weathered mantle in some areas of the LEB was probably contemporaneous with this. Since this time, both sand- and clay-rich alluvium of greatly varying depth has been deposited in the broad fluvial valleys, and has been reworked to varying degrees in the lower reaches of the LEB by aeolian activity to form the large linear dunefields of the Simpson, Tirari and Strzelecki Deserts (Nanson et al., 2008).

2.4 Data compilation and uncertainties

The raw hydrochemical data were obtained from the Queensland Department of Environment and Resource Management (QDERM), which collected water samples

from the various catchments during 1973 – 2000. The samples were collected and analyzed using standard techniques, with checks routinely performed to assess the quality and accuracy of the results. The quality of this data was also checked in a previous independent study (McNeil et al., 2005). The mean daily discharge records and annual flow statistics for each station were also obtained from QDERM.

Prior to data analysis, the data was processed to exclude samples extensively modified by evaporation. Given the climatic conditions, the natural modification of the solute concentrations by evaporation is inevitable and indeed is an important process that this study aims to investigate. However, as far as possible samples were selected which were representative of the flood waters that reached a particular location in order to assess evaporative processes acting at the catchment scale. Plotting the daily discharge against TDS shows that some samples collected under low flow conditions, regardless of their position in the catchment, have TDS concentrations trending towards significantly higher values than the rest of the record, which remains within a 0 - 250 mg/l TDS range under a wide range of discharge conditions (Figure 2). The samples with TDS above 250 mg/l were therefore assumed to have been substantially modified by evaporation in situ, rather than during flood procession, and were excluded from further analysis. Samples collected under no flow conditions were also excluded. The exclusion of TDS > 250 mg/l is further supported by previous research, which included surface water samples from Cooper Creek collected under no flow conditions that had a measured TDS of 275 mg/l and a considerably enriched $\delta^{18}O$ and $\delta^{2}H$ signature relative to floodwaters (Cendón et al., 2010). The charge balance for all remaining samples was also calculated, and samples with error greater than 15% were also excluded (for n = 129 samples, 116 were less than 10%, and 13 were between 10 and 15%).

Water chemistry sampling in this study is inevitably biased towards low flow conditions, which is a reflection of the remote location and access difficulty at most sites. Nonetheless, given the large inter-site, and intra-site variability in major ion concentrations at both low and high flows (Tables 1 and 2), we contend that the range of variation present in this database is representative of the full range of concentrations likely to be found during varying discharges at each site. This is because of the generally chemostatic relationship of the major ions with increasing discharge (Figure 2); a phenomena increasingly evident in catchments worldwide

(Godsey et al., 2009). The mean ion concentrations were used without flow weighting, both because of the low flow bias, and because those flows contributing the most water also have considerable variability in concentrations. These mean concentrations are, therefore likely to be more representative of the long term trends in solute concentrations at each site, and more useful to distinguish any long term differences between sites, which is part of the aim of the present study.

Dust samples and analysis used in this study are from Kiefert (1995), which were collected from Fowlers Gap (NSW) and Charleville (QLD). The soluble fraction of the dust was extracted and analysed using standard techniques, and the TDS of this soluble fraction was found to be between 11 and ~14% by weight of the dust from these locations (Table 3). The soil and bedrock samples used in this study are from Gunn and Fleming (1984), which provided 145 weathered and unweathered bedrock and 35 soil analysis from various soil types throughout the eastern Lake Eyre Basin, again obtained via solute extracts (Table 3). Although these may not represent the total ion concentrations within the bedrock samples, they do provide a good estimate of the most readily dissolved ions present and, therefore, the proportion most likely to contribute to the surface water chemistry data analysed here.

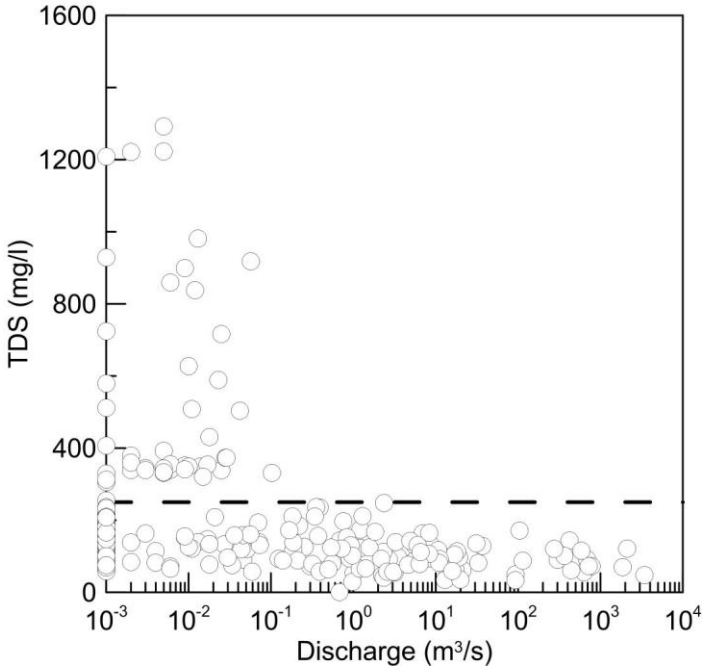

Figure 2. TDS concentrations of all available samples from the LEB plotted against mean daily discharge. Samples above the dashed line (250 mg/l) or collected during no flow conditions were excluded from further analysis.

2.5 Data analysis and interpretation

2.5.1 The solute chemistry of Australian dryland waters

The TDS of the Cooper and Georgina-Diamantina catchments are moderate by world freshwater river standards (Meybeck, 2003) but low compared to other large drainage basins in Australia such as the Murray-Darling (Herczeg et al., 1993; Meredith et al., 2009). TDS are also low compared with other dryland rivers in the world (Feth, 1971; Gibbs, 1971), where concentrations can be substantially modified by saline groundwater discharge and anthropogenic disturbance. Such factors are minimal in the mid-upper reaches of the catchments studied here. Mean TDS concentrations in the Cooper catchment are relatively constant in the headwaters (Darr River, Alice River, Barcoo River, and Cornish Creek, range = 119 ± 8 – 124 ± 10 mg/l), and then decrease downstream until Stonehenge (90 ±12 mg/l), after which TDS increases slightly to Currareva (103 ± 8 mg/l), and then increases by ~50% as the flows reach Nappa Merrie (146 ± 6 mg/l) (Figure 3a). Approximately the opposite trend is true of mean annual discharge, which is low in the headwaters, then increases until Currareva, after which the discharge declines dramatically towards Nappa Merrie (Figure 3a). Although the lowest average TDS concentration is at Stonehenge, and the highest mean annual discharge is not reached until farther downstream at Currareva, a strong inverse relationship between the two remains and demonstrates the first order control of discharge on the solute chemistry of these waters, especially as catchment area increases and the stream chemistries become highly mixed. It is important to note that the maximum change in TDS of ~62% between the lowest and highest mean concentrations is quite small considering the two orders of magnitude increase in discharge between the tributaries and the start of the main stem of the Thomson River at Longreach. For the Georgina-Diamantina catchment, a rapid increase in TDS and corresponding decline in mean annual discharge is also found with increasing catchment area, however, the much more limited data set means the trend in TDS and discharge at smaller catchment areas cannot be determined (Figure 3b).

Investigating the major ion trends with increasing catchment area reveals that HCO_3 is the only major ion with changes in concentration that match the trend of TDS concentrations in both the Cooper and Georgina-Diamantina catchments (Figure 3c & d). Excluding the headwater streams, where concentrations are fairly constant,

changes in HCO_3 concentrations account for 45%, 73%, and 73% of the changes in TDS between Longreach and Stonehenge, Stonehenge and Currareva, and Currareva and Nappa Merrie, respectively, in the Cooper Creek catchment. Although a change in HCO3 must be in balance with the other ions since there are no corresponding changes in pH, most of the other major ions display no systematic trends downstream, indicating the processes of cation addition and/or anion depletion to accommodate changes in HCO_3 are not consistent downstream, nor probably at individual sampling locations.

Location	Catchment Area (km^2)	n	Na	K	Ca	Mg
Cooper Creek						
Darr River	2700	4	532.8 ± 28	87.6 ± 7	283.2 ± 35	66.9 ± 8
Alice River	7918	8	571.4 ± 89	137.8 ± 16	245.1 ± 31	138.3 ± 22
Barcoo River	8782	14	530.0 ± 71	102.7 ± 7	258.2 ± 17	130.8 ± 12
Cornish Creek	22825	10	708.1 ± 148	103.1 ± 7	179.9 ± 23	148.1 ± 20
Thomson River - Longreach	57587	27	574.0 ± 47	87.1 ± 4	185.5 ± 12	88.7 ± 5
Thomson River - Stonehenge	87811	20	510.2 ± 103	73.9 ± 8	161.1 ± 22	81.9 ± 14
Cooper Creek - Currareva	150220	10	473.7 ± 39	95.4 ± 5	222.3 ± 30	110.3 ± 9
Cooper Creek - Nappa Merrie	236985	12	649.5 ± 31	134.9 ± 6	295.7 ± 18	156.2 ± 10
Georgina –Diamantina						
Bourke River	14846	3	143.5 ± 61	92.1 ± 11	307.7 ± 58	101.5 ± 28
Diamantina Lakes	54130	5	528.1 ± 56	84.9 ± 12	164.2 ± 24	96.3 ± 22
Diamantina River - Birdsville	115205	9	1072.0 ± 117	125.6 ± 12	235.7 ± 22	144.5 ± 18
Georgina River – Roxborough	118398	7	865.0 ± 163	110.0 ± 5	572.1 ± 49	309.8 ± 37
Longreach X	-	-	589.5 ± 48	81.7 ± 3	159 ± 10	73.8 ± 4
Stonehenge X	-	-	538.1 ± 108	74.5 ± 8	162.5 ± 22	89.7 ± 15
Currareva X	-	-	214.2 ± 18	230.0 ± 13	614.9 ± 83	289.5 ± 23
Nappa Merrie X	-	-	374.7 ± 18	73.1 ± 3	181.0 ± 11	84.4 ± 5

Table 1. Major cations of the rivers in the LEB (µmol/l). Values are the mean and standard error for each major ion within the Lake Eyre Basin. Number of samples used in the calculation and catchment areas are also shown. X = Back-calculated ion concentrations using the discharge mass balance between stations.

However, Na, Ca, Mg, K and Si do show slight increases between Currareva and Nappa Merrie, and interestingly Cl remains constant within standard errors over the same distance (Figure 3c), which is discussed in detail later. Notably, still in the headwaters of the Cooper catchment, Cornish Creek has the highest mean concentrations of Na, Si and Cl, but very low HCO_3 compared to other headwater streams. HCO_3 is the dominant anion in all LEB streams studied here, although Cl is

also high in some streams such as Alice River and Cornish Creek in the Cooper catchment, and Roxborough in the Georgina-Diamantina catchment (Tables 1 and 2). Na is the dominant cation and Ca is the next most abundant cation, although it is consistently ~200 to ~300 µmol/l less than Na throughout the Cooper Catchment (Figure 3c). Si, measured as SiO_2, is also quite high, while Mg, K and SO_4 are all consistently low in these catchments (Table 1). The relationships between major ions are similar in the Georgina-Diamantina catchment, except for the Bourke River where Ca is higher than Na, and at Roxborough, which has much higher concentrations of all ions, especially Na and Cl (Figure 3d).

Location	Cl	SO_4	HCO_3	SiO_2	TDS	pH
Cooper Creek						
Darr River	79.7 ± 18	65.8 ± 16	1064.6 ± 132.7	356.6 ± 14	2183.3 ± 183	7.6
Alice River	345.5 ± 49	75.0 ± 18	923.2 ± 103.7	214. 5 ± 31	2438.3 ± 242	7.6
Barcoo River	190.0 ± 36	125.6 ± 19	912.3 ± 63.9	240.3 ± 20	2250.8 ± 173	7.7
Cornish Creek	467.7 ± 115	85.2 ± 18	705.3 ± 82.4	371.1 ± 79	2399.3 ± 381	7.3
Thomson River - Longreach	238.8 ± 31	105.0 ± 12	679.2 ± 40.8	280.7 ± 15	1960.0 ± 129	7.3
Thomson River - Stonehenge	239.3 ± 79	75.0 ± 8	585.3 ± 91.4	265.3 ± 24	1727.2 ± 295	7.0
Cooper Creek - Currareva	216.9 ± 31	95.3 ± 8	738.2 ± 97.4	249.6 ± 25	1953.3 ± 167	7.3
Cooper Creek - Nappa Merrie	187.8 ± 23	102.2 ± 17	1251.4 ± 79.5	285.2 ± 30	2779.5 ± 119	7.4
Georgina –Diamantina						
Bourke River	221.9 ± 101	88.5 ± 60	602.9 ± 283.7	249.6 ± 51	1559.7 ± 187	7.6
Diamantina Lakes	258.4 ± 11	147.8 ± 41	462.6 ± 126.0	359.5 ± 19	1742.5 ± 222	7.3
Diamantina River - Birdsville	502.6 ± 58	162.3 ± 23	938.2 ± 108.3	416.1 ± 23	3182.3 ± 301	7.3
Georgina River – Roxborough	1160.5 ± 264	207.5 ± 33	1234.1 ± 59.2	259.2 ± 31	4461.4 ± 546	7.5
Longreach X	256.1 ± 33	97.8 ± 11	596.7 ± 35.9	295.0 ± 15	-	-
Stonehenge X	282.2 ± 93	63.3 ± 7	585.2 ± 91.4	290.9 ±26	-	-
Currareva X	60.2 ± 9	225.4 ± 18	1688.8 ± 222.8	153.3 ± 16	-	-
Nappa Merrie X	233.5 ± 29	91.4 ± 15	448.6 ± 28.5	229.8 ± 24	-	-

Table 2. Same as for Table 1(µmol/l), but for anions, pH and TDS. Total dissolved solids (TDS) are calculated as the sum of the major ions including SiO_2 (mg/l). Standard errors for pH values are all approximately 0.1.

1.1.1 Balancing the water and solute budgets

As noted earlier, discharge in the Cooper catchment increases downstream until Currareva, after which it declines rapidly, losing 64% of the mean annual flow before Nappa Merrie. Additional discrepancies in the water balance occur in the Thomson River at Longreach and Stonehenge, and in Cooper Creek at Currareva, which receive 74%, 51% and 13% of their mean annual discharge, respectively, from non-

gauged tributaries. A decline in tributary contribution downstream is probably due to the accompanying decline in annual rainfall and also the declining tributary size. Nonetheless, these additional runoff sources are significant because they must also contribute to the solute chemistry of each downstream station, and need to be accounted for before potential solute sources can be elucidated.

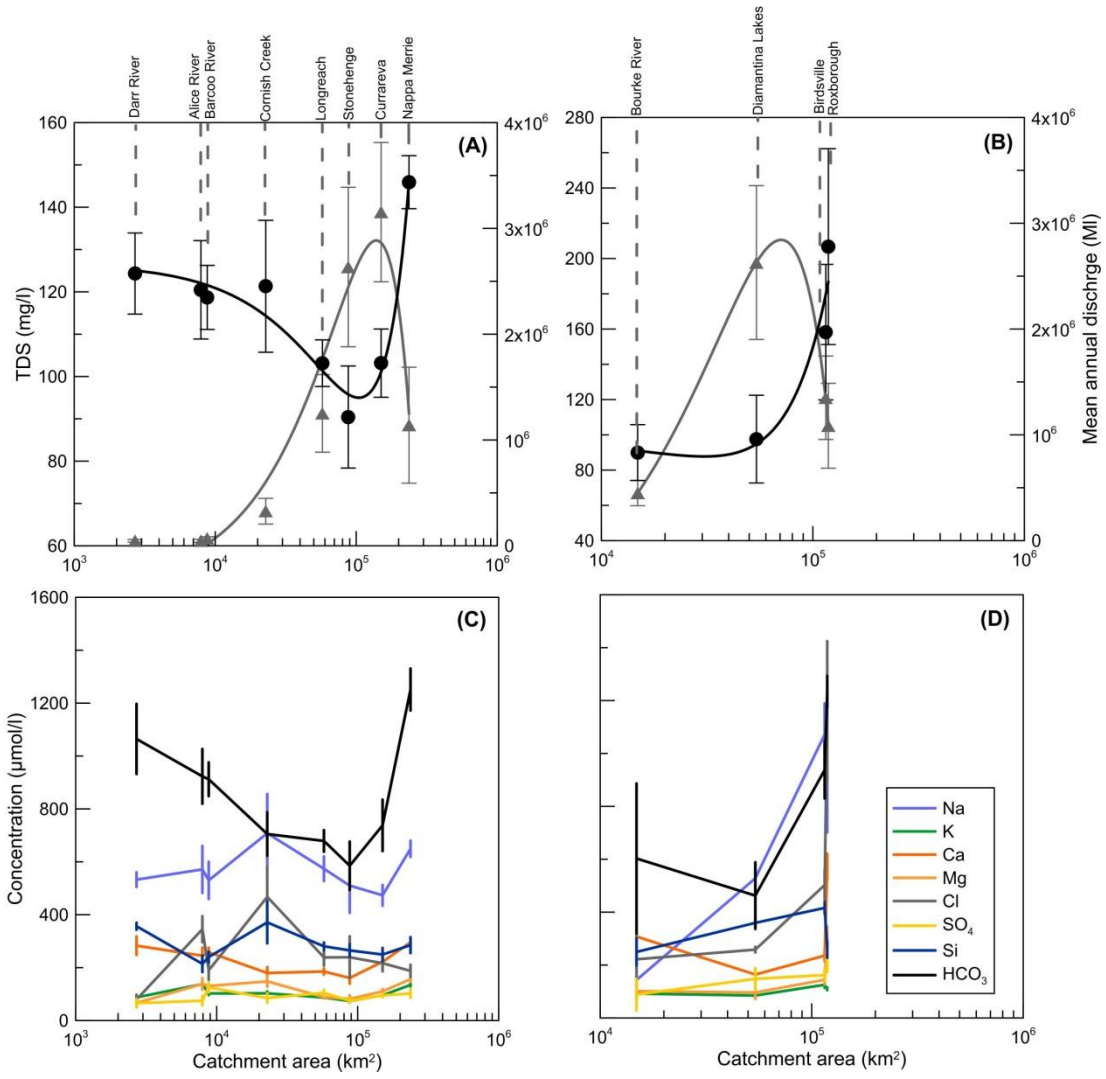

Figure 3. TDS concentrations (black circles) and mean annual discharges (grey triangles) for (a) the Cooper Creek catchment, and (b) the Georgina-Diamantina catchment with respect to catchment area. The dotted grey lines join the station names to their corresponding catchment area. The solid black and grey lines are simple polynomial fits to the TDS and discharge data, respectively, with r^2 values for (a) of 0.95 and (b) 0.94, respectively. Major ion concentrations (µmol/l) are also shown for stations in the (c) Cooper Creek and (d) Georgina-Diamantina catchments. All error bars represent standard errors.

The major ion chemistry of the sum of these contributing (or losing, as is the case between Currareva and Nappa Merrie) waters can be back-calculated using the

discharge mass balance between stations, and the major ion concentrations in the upstream and downstream stations. The discharge required to complete the water balance between stations, Q_x, is simply the difference between the station discharge (Q_d) and the sum of the separate contributing upstream discharges (Q_i):

$$Q_x = Q_d - \sum_{i=1}^{n} Q_i \qquad (1)$$

where n is the number of separate contributing stations available. Since in each case Q_x must have major ion concentrations which contribute to the total downstream concentration $[C]_x^j$, the concentration of any ion in Q_x is, therefore, calculated as:

$$[C]_x^j = \left[[C]_d^j - \sum_{i=1}^{n} [C]_i^j \left(\frac{Q_i}{Q_d}\right) \right] / \left(\frac{Q_x}{Q_d}\right) \qquad (2)$$

whereby $[C]_x^j$ is estimated as the mass balance between the downstream $[C]_d^j$ minus the sum of upstream $[C]_i^j$ concentrations of ion j proportional to the fraction of contributing discharge, which ensures $[C]_x^j$ is also dependent on the overall contribution of each component to the water balance. The results of these tributary calculations are shown in Table 1, and are labelled as LongreachX, StonehengeX, CurrarevaX and Nappa MerrieX to distinguish them from the actual station data. In order to estimate the legitimacy of these calculations, the ion charge balance (% error) of each solution was calculated and found to be between 1.2 and 6.4%. Both LongreachX and StonehengeX have major ion compositions similar to the downstream and upstream stations, suggesting these solutes have similar sources to the waters from other upstream tributaries. CurrarevaX, however, has a major ion composition with elevated Ca, K, Mg, SO_4 and HCO_3, and much lower Na and Cl. Nappa Merrie has experienced a net loss in mean annual discharge of 64%, therefore Nappa MerrieX represents the concentration of ions that must be within these losses in order for the ions to balance between Currareva and Nappa Merrie, assuming no other significant tributary input of solutes. Equation (2) is then rearranged such that the concentration at Currareva $[C]_i^j$ is equal to Nappa Merrie $[C]_d^j$ proportional to discharge (Qd/Qi) plus the concentration of ions in the water loss $[C]_x^j$ proportional to the lost discharge [$(Qi - Qd)/Qd$], to get:

$$[C]_i^j = [C]_d^j \left(\frac{Q_d}{Q_i}\right) + [C]_x^j \left(\frac{Q_i - Q_d}{Q_d}\right) \quad (3)$$

where Q_d is the mean annual discharge at Nappa Merrie and Q_i is the mean annual discharge at Currareva. Solving for $[C]_x^j$ results in the Nappa MerrieX concentrations shown in Tables 1 and 2, which are very similar to those at the upstream stations with the only difference being slightly lower Na and HCO_3 concentrations. This simple approach thus provides a reasonable method of estimating the concentrations within unknown flow components associated with both large transmission gains and losses, and ensures tributary input with potentially distinctive chemistries is accounted for.

These calculations assume that no in-stream modification processes, biological or otherwise, have contributed significantly to the variation in ion concentrations between stations, and that the addition of other surface water sources is the only modification to stream chemistry, thus allowing the source of these solutes to be further investigated. Evaporation is also an important modification process, however it can be seen in Figure 3c that there is no systematic increase in Cl with respect to any other ion downstream. Since Cl is a conservative ion, if evaporation were affecting the stream chemistry of these rivers then an increase in major ion concentrations with respect to Cl would be expected. The Georgina River at Roxborough is a possible exception to this, since it has on average much higher Na and Cl concentrations compared to other stations in the catchment (Figure 3d). Additionally, Cl concentrations decrease between Currareva and Nappa Merrie, despite a dramatic loss in flow and for which there are only two possible explanations: 1. halogen uptake of Cl by organic matter, or 2. Cl concentrations are considerably diluted with respect to other ions as mixing between remnant channel waters and new flood waters takes place. We consider the latter process to be the most likely given Cl uptake by organic matter is not an obvious process in other parts of the catchment, and is only likely to be significant in environments where large amounts of organic matter are available, a situation not typically encountered in dryland areas. Therefore, the variations in the major ion concentrations in the Thomson River at Longreach and Stonehenge, and Cooper Creek at Currareva are a result primarily of variations in the composition of tributary waters, and the unknown

components can be estimated by discharge weighted mass balance of ion concentrations.

2.5.2 Major ions

2.5.2.1 Chloride ratios

The most common method to estimate and subtract the contribution of rainfall to the dissolved load of surface waters is a Cl mass balance approach, which assumes rainfall derived Cl is the only significant source of Cl (e.g. Stallard and Edmond, 1981). However, other sources of Cl, such as dust, are also potentially significant and need to be accounted for. Comparing these potential sources in the LEB, it is clear that rainfall and dust compositions are distinct, whilst in all soil types, weathered or unweathered, the major ion ratios with Cl are identical to rainfall (Figure 4a). This is remarkable given the range in concentrations of each ion within the different soils (Table 2), suggesting that any ions derived from dust or weathering have since been leached, and completely replaced and re-concentrated in the soil by the dispersion of rainfall derived ions over time. Compared to rainfall, dust concentrations are slightly enriched in most ions relative to Cl, except SO_4 which is almost equal to rainfall values, and K, which is slightly depleted. Furthermore, the high Na content of dust can be attributed to the importance of saline lake beds and clay pans as dust sources (McTainsh et al., unpublished data). Unweathered marine rocks are typically enriched in most ions/Cl (except K) compared to rainfall, especially SO_4 and Na, while unweathered freshwater rocks are mostly depleted in ions/Cl compared to rainfall (except Na). During weathering, SO_4/Cl and Na/Cl decline in marine sedimentary rocks, but a slight enrichment in SO_4/Cl and constant Na/Cl occurs in freshwater sedimentary rocks (Figure 4a). Mg/Cl is slightly enriched during the weathering of freshwater sedimentary rocks, and while Ca/Cl and K/Cl both show some variation during weathering, the changes are not large and so the ratios can be interpreted as remaining fairly constant.

The similarity of the rain, soil and much of the weathered bedrock Cl ratios means that any correction based on Cl mass balance cannot confidently distinguish between water derived directly from rainfall, or that which has passed through the soil or weathered profiles before being discharged into streams. However, low baseflow indices for the entire LEB suggest the contribution of this water during hydrograph

recession is not significant (McMahon et al., 2008b). Since this analysis is focused on dissolved loads, any period of extended residence in soil profiles by rain-derived waters would result in increased solute dissolution and much higher TDS concentrations than are found in the floodwaters investigated in this study. Furthermore, low TDS concentrations have been found in waters collected following large flow events (Sheldon and Fellows, 2010), with major ion compositions very similar to those described here, suggesting the receding limb of the hydrograph for these rivers is not especially distinct in TDS or major ion composition, and that storage and release of waters from saline soils or weathered profiles is not an important contributor to the water balance or to the dissolved load.

The ion/Cl relationships for the dissolved load of the Cooper Creek and Georgina-Diamantina catchments show considerable downstream variation in Na/Cl and Ca/Cl, and much less variation in Mg, K and SO_4/Cl ratios (Figure 4b). In all cases, however, the ion/Cl ratios are greater than those found in rainfall or soils, meaning additional sources for these ions are required. HCO_3 was excluded from Figure 4 because it is usually not detected in rainfall analysis, and its incorporation into the dissolved load of rivers is known to be via either the dissolution of carbonates or the conversion of soil CO_2 to carbonic acid. In the LEB, the only significant concentrations of HCO_3 are found in the unweathered soils, dust, and to a lesser extent in the unweathered freshwater and marine sedimentary rocks (Table 2), including small areas of limestone in the headwaters of the Georgina catchment (Figure 1). An important modification process which can potentially lead to erroneous Cl mass balance corrections, particularly for Ca and Na concentrations, is cation exchange within river and soil clays. To examine this, we calculated the mean sodium absorption ratios (SAR) for all water samples, which were on average very low (0.2-1.7), with the highest values from Cornish Creek (1.5) in the Cooper Creek catchment, and from Birdsville (1.7) in the Georgina-Diamantina catchment. We interpret this to mean most clay cation exchange sites are already saturated, and that this process is unlikely to significantly modify the dissolved load or affect the calculations presented here.

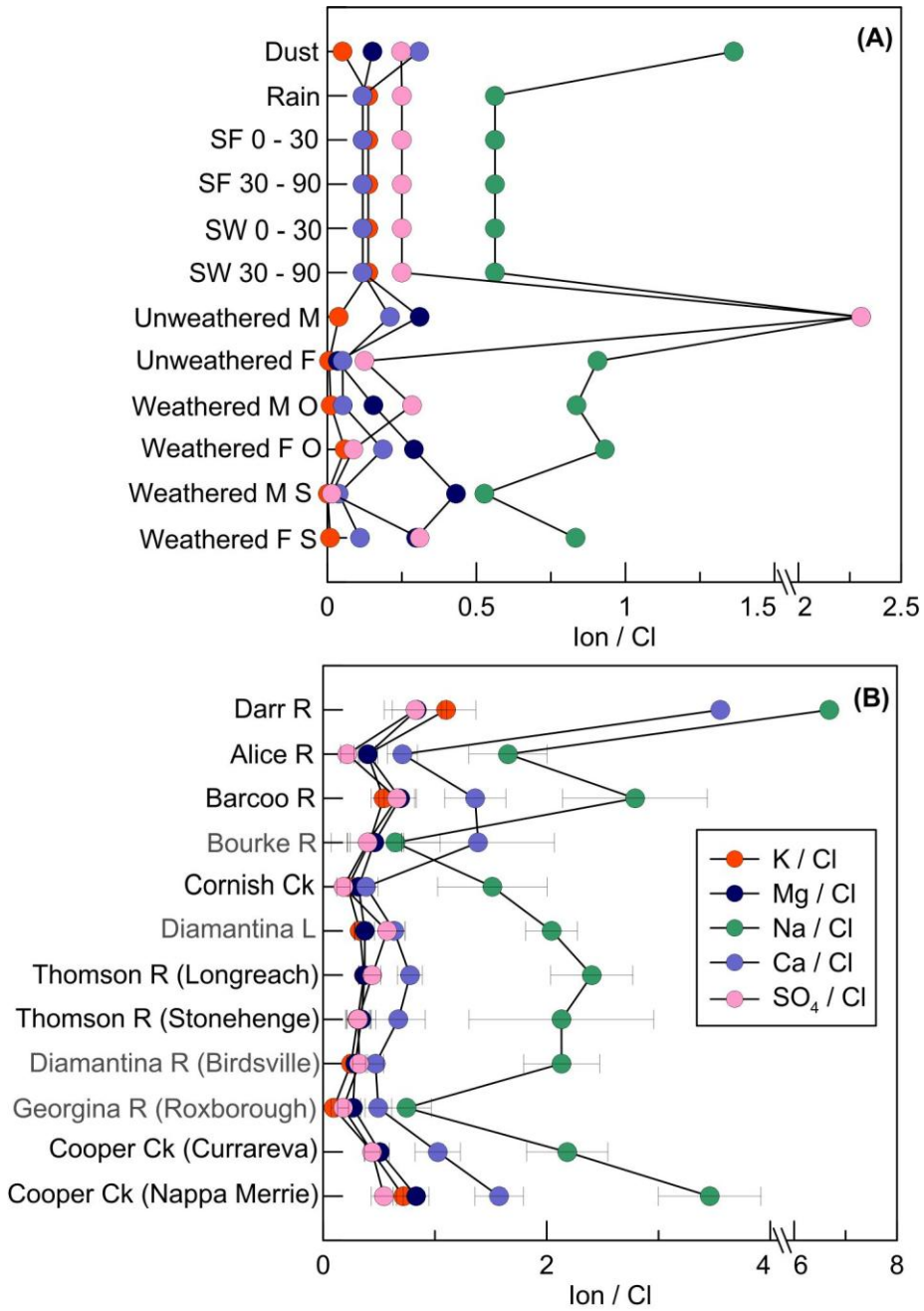

Figure 4. Major ion ratios (Ca, Mg, Na, K, SO_4) with Cl for (a) rain, dust, soil and bedrock, and (b) in the dissolved load of the river stations within the LEB. In (a), SF and SW are soil fresh, and soil weathered, respectively; M and F are marine and freshwater, respectively, for both weathered and unweathered bedrock types; and O and S are outcrop and shallow drill core samples, respectively. Black station names in (b) represent those within the Cooper Creek catchment, while those in grey are within the Georgina-Diamantina catchment, with all stations ranked in order of increasing catchment area. All error bars are standard errors, and note the break in scale on the x-axis in both (a) and (b).

2.5.2.2 Rainfall and dust

In order to constrain the sources of major ions, we first consider the role of cyclic salts derived from rainfall and dry deposition. The Table 3 ionic concentrations in monsoonal rainfall from Likens et al. (1987) represent volume weighted means collected from Katherine, in the Northern Territory of Australia. Although this rainfall is not directly within the LEB, we expect it to be similar because the main rainfall source in the LEB is also the summer monsoon. This rainfall is relatively dilute in major ions, and we consider these ion concentrations to be a good representation for the purposes of this study as the headwaters of the LEB are also a similar distance from the coast and, therefore, also likely to be diluted via this continental effect. There remains considerable uncertainty, however, in the composition of rainfall over much of the Australian continent. In southern Queensland, for example, Biggs (2006) found much higher concentrations of all major ions in rainfall than those used here, even for rainfall sampled farther inland. We believe these rainfall values are not as relevant to this study because of major differences in the source and volume of the rainfall from these two areas.

A second important source and transport mechanism is dry deposition of solutes within windblown dust. Since the rivers of the LEB do not empty to the ocean, solutes derived from rainfall cannot be considered truly cyclic, save for the small fraction that would be delivered back to the atmosphere via evaporation from salt lake surfaces. However, the transport of sediment by rivers into the interior of the basin and subsequent entrainment and re-deposition of a small percentage of this sediment as dust in the headwaters of the catchment is the only mechanism by which salts in this basin can be recycled effectively. Suspended dust in eastern Australia has been measured to be up to ~50% by weight soluble salts (Kiefert, 1995), and thus regions under the long term major dust transport pathways, both of which emanate from the LEB (McTainsh, 1989), could potentially have dry deposition as a significantly more important contributor to soil and water solute loads than rainfall, depending on the deposition rate.

Assuming all Cl in the river dissolved load is derived from rainfall and dust sources, the percentage of rainfall + dust derived ions within the dissolved load, $[C]^{j}{}_{\%R+D}$, of the LEB is calculated as:

$$[C]^{j}{}_{\%R+D} = [C]^{j}_{W} - \left[\left(\frac{[C]^{j}_{R+D}}{[Cl]_{R+D}}\right)[Cl]_{W}\right] \qquad (4)$$

where $[C]^{j}_{W}$ is the concentration of ion j in the dissolved load of the river (Table 1), $[C]^{j}_{R+D}$ is the sum of j measured in the composite rain and dust sources (Table 2), $[Cl]_{R+D}$ is the concentration of Cl in the composite rain and dust sources (Table 2), and $[Cl]_{W}$ is the concentration of Cl in the dissolved load. The results of these calculations are shown in Table 3.

Source	Ca	Mg	K	Na	Cl	HCO_3	SO_4
Rain [a]	0.95	0.95	1.1	4.5	8.00	-	2
Dust [b]							
Fowlers Gap	360	185	20	1710	1310	280	315
Buronga	360	170	100	1480	1030	530	265
Soil [c]							
Fresh 0-30 cm	430	170	220	2880	60	4040	4160
Fresh 30-90 cm	830	560	230	17790	4960	3160	24660
Weathered 0-30 cm	4850	1300	310	21600	30500	1600	2800
Weathered 30-90 cm	11700	6750	550	89500	114400	1100	12200
Bedrock [c]							
Unweathered M	4950	7300	910	54400	23600	2710	54400
Unweathered F	5250	3550	600	93300	102900	2100	12800
Weathered M O	4250	12600	940	68200	81600	160	23200
Weathered F O	17150	26750	5400	85700	92000	0	8000
Weathered M S	11350	127150	720	310000	589000	0	8400
Weathered F S	2850	7750	500	43300	52000	80	16100

Table 3. Representative concentrations of the major ion sources in the LEB (µmol/l). For unweathered and weathered sedimentary bedrock samples, M = marine, F = freshwater, O = outcrop and S = shallow (30-90 cm depth) samples. [a] Litkens et al., (1987) Volume weighted mean monsoonal rainfall concentrations from Katherine, NT, Australia [b] Data from Kiefert (1995) [c] Soluble extract data from Gunn and Fleming (1984).

Whilst there is some variation in $[C]^{j}{}_{\%R+D}$ between stations, the rank of these percentages between the different ions from highest to lowest is consistent throughout the LEB, such that: $[C]^{j}{}_{\%R+D}$ [SO_4 > Na > Ca > Mg >> K > HCO_3]. The high contribution of SO_4 from rainfall + dust derived sources is most likely to be from the dissolution of dust size gypsum, which stoichiometrically would also provide equal amounts of Ca to the dissolved load. Since Ca concentrations in the

LEB rivers are generally > 2 x SO_4 (Table 2), an average of 41% (range = 21 – 73%) of Ca derived from rainfall + dust sources is consistent with a gypsum source for SO_4. As a consequence, it appears that any weathering of evaporite or sulfide (outcrop) sources does not occur at a significant rate to influence the solute chemistry of the LEB rivers. This calculation of a combined rainfall + dust source also incorporates the dissolution of other salts contained within dust, such as halite and carbonates, however, it is difficult to distinguish between rainfall Na, which is the major cation in rainfall, and Na from the dissolution of halite within dust, which are both likely large contributors to the high percentage of rainfall + dust derived Na (Table 4). If all the data in Table 4 is combined, rainfall and dust are able to account for 22 – 75% of the dissolved load of the LEB rivers as a fraction of TDS, and for ions other than SO_4, silicate and carbonate weathering are clearly required as sources of the remaining solutes.

	Na	K	Ca	Mg	SO_4	HCO_3	Total
Cooper Creek							
Darr River	20.3 ± 5	4.8 ± 1	9.1 ± 3	18.9 ± 5	31.7 ± 7	2.8 ± 1	31.2
Alice River	81.4 ± 7	13.9 ± 3	44.7 ± 6	47.2 ± 13	87.9 ± 7	13.3 ± 2	64.7
Barcoo River	44.7 ± 5	10.0 ± 2	24.7 ± 6	21.2 ± 4	46.6 ± 10	6.7 ± 1	42.3
Bowen	82.2 ± 6	23.2 ± 6	73.3 ± 11	46.5 ± 7	92.7 ± 7	21.0 ± 3	73.1
Thomson River	54.4 ± 4	14.0 ± 2	39.1 ± 4	39.2 ± 4	57.7 ± 6	12.2 ± 1	52.7
Stonehenge	56.4 ± 6	14.5 ± 3	43.0 ± 7	38.7 ± 7	51.0 ± 6	17.7 ± 5	53.5
Currareva	61.2 ± 7	12.2 ± 2	34.4 ± 7	29.4 ± 3	55.0 ± 7	11.9 ± 2	50.7
Nappa Merrie	39.8 ± 5	7.3 ± 1	21.0 ± 4	19.2 ± 3	49.8 ± 8	5.7 ± 1	40.5
Georgina-Diamantina							
Bourke River	100.0 ± 0	11.6 ± 4	25.3 ± 14	31.4 ± 7	83.5 ± 17	36.9 ± 32	67.5
Diamantina Lakes	68.7 ± 6	17.0 ± 2	53.2 ± 9	50.2 ± 11	53.4 ± 14	27.7 ± 9	62.0
Birdsville	65.4 ± 6	21.3 ± 2	66.7 ± 6	55.9 ± 6	74.1 ± 8	22.9 ± 6	67.7
Roxborough	99.6 ± 0	54.1 ± 12	59.8 ± 12	52.3 ± 8	90.8 ± 8	32.3 ± 7	81.5

Table 4. Percentages (%) of ions derived from rainfall and dust within the dissolved load of LEB rivers.

2.5.2.3 Silicate and carbonate weathering

The remaining percentage of ions in the dissolved load of these rivers not accounted for by rainfall or dust deposition must be the result of either silicate or carbonate rock weathering, or the dissolution of carbonates and other salts not present in dust. Previous studies often use ratios with Na as the denominator to derive the proportion of silicate and carbonate weathering contributions to the dissolved load, which is

calculated using either inverse mathematical methods, or mass balance using a representative silicate source ratio (e.g. Ca/Na in plagioclase). Here, we adopt a different approach and assume some proportion of the remaining ions in the dissolved load must be derived from silicate weathering, and that this weathering can be adequately described by a generic silicate weathering reaction such as:

$$2NaAlSi_3O_{8(s)} + 9H_2O_{(l)} + 2H_2CO_{3(aq)} \rightarrow Al_2Si_2O_5(OH)_{4(s)} + 2Na^+_{(aq)} + 2HCO_3^-{}_{(aq)} + 4H_4SiO_{4(aq)} \quad (5)$$

which produces major cations in equal proportion with HCO_3, although reactions of Ca and Mg silicates with carbonic acid can also have a stoichiometry distinct from Na silicates. Thus the sum of these cations should be roughly equal to HCO_3 if silicate weathering were solely responsible for the remaining dissolved load concentrations. Prior to correction for rain and dust derived solutes, Na + Ca + Mg are clearly in excess with respect to HCO_3 concentrations (Figure 5a), however, after correction (subtraction of rain + dust derived sources), a good relationship emerges between the sum of these cations and HCO_3 (Figure 5b). Ca and HCO_3 are plotted separately using uncorrected concentrations in Figure 5c, which demonstrates dissolution of carbonates is not a major source of these ions, except for Roxborough in the Georgina-Diamantina catchment, which displays a strong carbonate dissolution signal above that of a background HCO_3 concentration of ~ 653 µmol/l. This is consistent with a small area of Cambrian dolomite and Cenozoic limestone outcrops occurring in the headwaters of the Georgina River (Figure 1), and supports the validity of the calculations. Silicate weathering therefore appears to be sufficient to explain the majority of the dissolved load concentrations after the removal of rain and dust derived sources, however, carbonate dissolution and weathering may also provide an additional source of Ca and HCO_3 that is not necessarily strongly overprinted on the dissolved load chemistry, but nonetheless may be responsible for some of the scatter about the 1:1 line in Figure 5b.

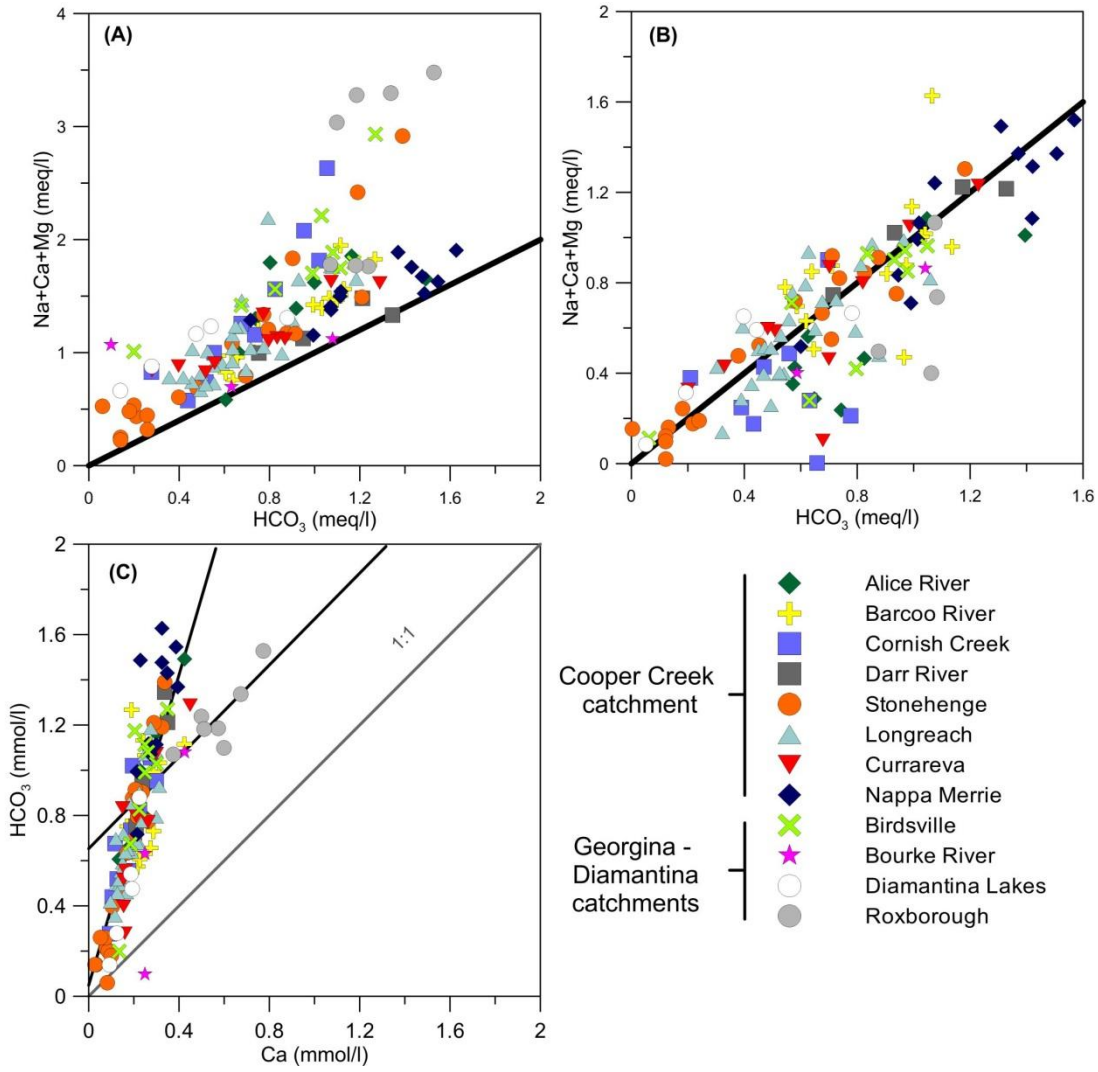

Figure 5. All available chemical data for the LEB, showing Na + Ca + Mg versus HCO_3 for (a) raw concentrations, and (b) concentrations corrected for rain and dust input. The solid black line in (a) and (b) is a 1:1 line. Since we are concerned with the products of reactions with acids and bases (Equation 5), the data presented in (a) and (b) are in meq/l. (c) Ca versus HCO_3 for raw data, with a regression line ($y = 3.43x + 48.8$) through all data except Roxborough having an r^2 of 0.7. The regression line through the Roxborough data has an r^2 of 0.71, and a slope identical to the 1:1 line. The Roxborough y-intercept value of 0.65 mmol/l (653 µmol/l) is interpreted as the HCO_3 concentration in the dissolved load prior to carbonate dissolution. In this case, since we are only concerned with the relationship between Ca and HCO_3 and its molarity, and not the number of available charges, the data in (c) is presented in mmol/l. Note 1 sample from Cornish Creek, 1 sample from Stonehenge, and 3 samples from Roxborough are not included in (b) because they plot below zero on the y-axis, indicating factors other than rain, dust and silicate weathering are contributing to, or modifying the dissolved load.

In order to quantify the proportions of the dissolved load derived from silicate and carbonate weathering, the distance from each point normal to the 1:1 line in Figure

5b is calculated, with the resulting normalized distribution shown in Figure 6. The distances from the 1:1 line to the data points at Roxborough are shown as outliers in the histogram, and since we can assume that the majority of the ions in these samples are sourced from carbonate weathering and dissolution (Figure 5c), they provide a 100% carbonate weathering end-member to the distribution. The normalized distribution in Figure 6 therefore provides an estimate of the degree of silicate (0 = 100% silicate) versus carbonate (1 = 100% carbonate) weathering responsible for solutes in the dissolved load. With a median normalized value of 0.07 and 90th percentile value of 0.25, this calculation estimates that silicate weathering alone can explain at least 75% of 90% of the normalized data, and can therefore be attributed as the major source of ions in the dissolved load of these dryland catchments after rainfall and dust contributions are accounted for.

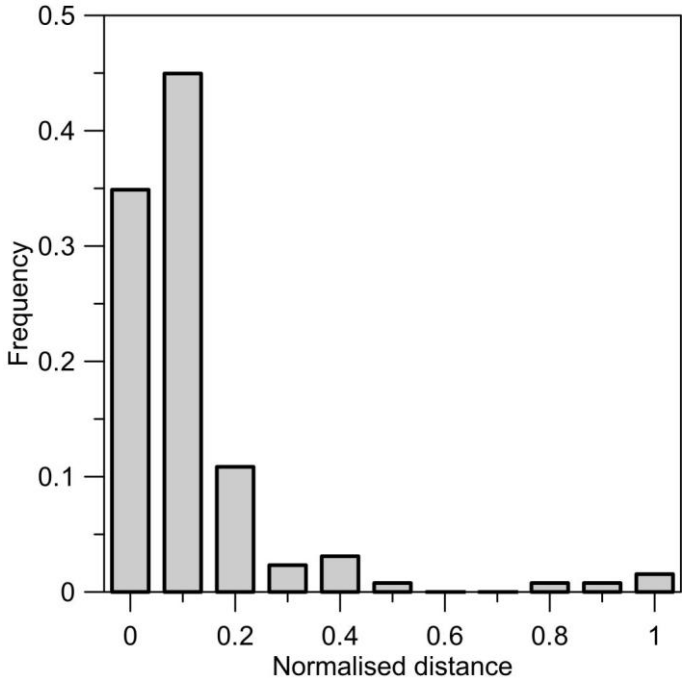

Figure 6. Histogram of calculated distances between data points (n = 129) and the idealised silicate weathering 1:1 line in Figure 5b normalised to between 0 (100% silicate weathering) and 1 (100% carbonate weathering). The right side of the distribution characterising the carbonate dissolution end-members also includes the 3 outliers from Roxborough and the 1 outlier from Stonehenge not plotted in Figure 6b.

2.6 Weathering and evaporative contributions to the dissolved load of dryland rivers

2.6.1 Weathering in the LEB

Combining all the calculated percentages of the potential ion sources shows considerable variation in the relative contribution of these sources to the dissolved load of the LEB rivers (Figure 7). The decreasing variation in solute sources with increasing distance downstream in the Cooper Creek catchment can be attributed to a corresponding increase in effective mixing of floodwaters. In most cases, weathering or dissolution of carbonates is only a minor contributor to the dissolved load in the LEB, however, an unknown fraction of the dust derived source will also be from carbonate dissolution. These contributions from carbonate weathering may derive from carbonate dissolution of minor limestone areas in the case of the Georgina River (Roxborough), sedimentary rocks or Quaternary alluvial cements (calcrete) in the case of other rivers ($Ca:HCO_3$ = 1:1), or the direct weathering of carbonates by carbonic acid, which would instead produce $Ca:HCO_3$ at ratios of 1:2 via:

$$H_2CO_{3(aq)} + CaCO_{3(s)} \rightarrow Ca^{2+}_{(aq)} + 2HCO_3^-{}_{(aq)} \quad (6)$$

however, Figure 5c indicates that $Ca:HCO_3$ for most of the LEB rivers is approximately 1:3.5, and although these reactions contribute to the direct weathering of carbonates, Ca must also be released during silicate weathering via replacement with Na in Equation (5) as part of the Albite-Anorthite solid series. Moreover, the good match between the estimates of solute sources in Figure 7 and catchment lithology, the contribution of Equation (6) reactions to the carbonate weathering proportion of the dissolved load is probably relatively minor.

Nonetheless, the important contribution of silicate weathering to the dissolved load of these dryland rivers, between 10 - 70%, is somewhat surprising given it is generally not discussed as an important process in dryland hydrology, since it implies a largely unrecognized component of water-rock interaction which must be obtained via bedrock fracture flow contributing to runoff generation in the headwaters of these catchments. Intuitively, it is also a simpler explanation for the dominance of HCO_3 and relatively high SiO_2 (as a fraction of TDS) in the dissolved load of these rivers,

rather than groundwater discharge as suggested by previous studies in the large floodplain and channel areas of lower Cooper Creek (Sheldon and Fellows, 2010).

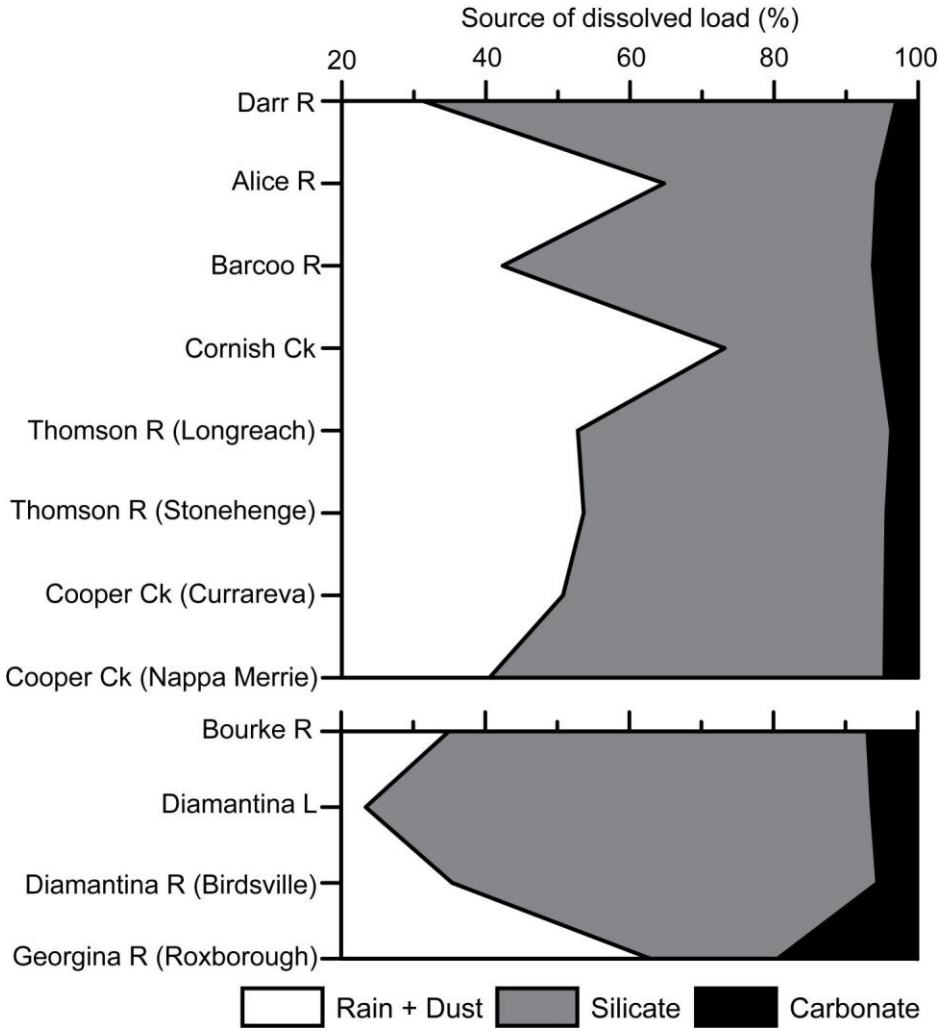

Figure 7. Percentages of sources in the dissolved load of the Cooper Creek (top) and Georgina-Diamantina (bottom) catchments, with the stations on the y-axis plotted with catchment area in increasing order. Rain + dust sources are calculated from the sum total of the percentages of each ion in the dissolved load (not including silica) derived from rainfall and dust (Table 3), including 100% contribution from Cl. Silicate and carbonate weathering sources are then attributed to the remaining fraction according to the percentages calculated in Figure 6. Standard errors are not shown, but range between 2.8 - 9.0% for rain + dust, 2.1 - 4.6% for silicate weathering, and 0.1 - 3.2% for carbonate weathering in both catchments.

Where shallow groundwater has been studied in this area, the watertable lies below the base of the channels and therefore makes no known contribution to surface flow (Cendón et al., 2010) (Chapter 2). The differences in the percentage of solute sources across the catchments can best be explained by variations in the rates of

rainfall/runoff and dust deposition within the catchments, as well as access to suitable bedrock and the depth to the base of the weathered profile (Figure 8).

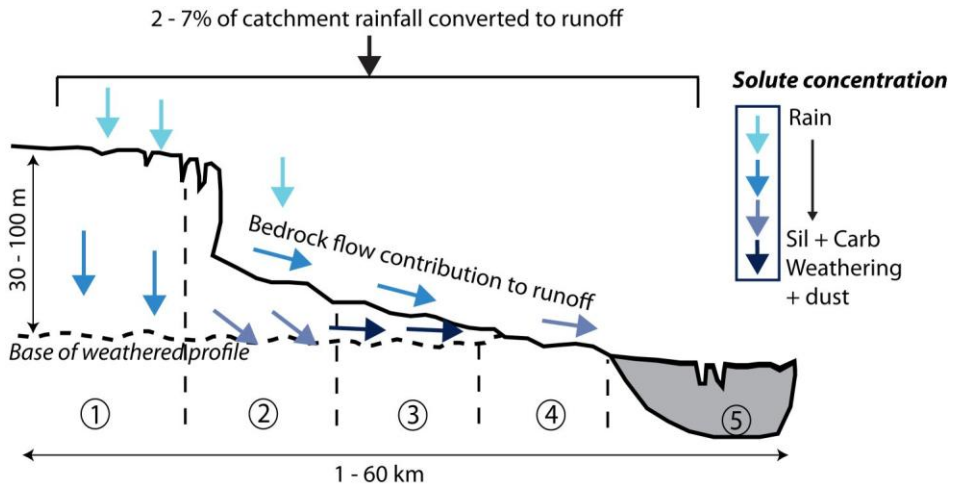

Figure 8. Conceptual model of infiltration and runoff interaction with a generalised geology and geomorphology of the Lake Eyre Basin (zones 1 – 5). Descriptions of these zones based on Gunn and Fleming (1984) are as follows: (1): Weathered marine and freshwater Cretaceous, Triassic or Jurassic sedimentary rocks, with or without Quaternary cover, or Neogene silicification. These typically form the scarps or isolated mesas throughout the basin. (2) and (3): Cretaceous marine and freshwater sedimentary rocks, which can be expressed in the landscape as debris slopes and pediments (2), or lower slope gently undulating terrain (3). (4): Low slope unweathered marine and freshwater sedimentary rocks. (5): Mixed sand and mud Quaternary alluvial deposits. The soils developed on (2) and (3) can have considerable stores of soluble salts (Na and Cl dominate), and especially on (3), develop strong gilgai soils (also on (5)). The soils developed on (4) generally have a very low store of soluble salts and are dominated by Na, Ca and HCO_3. Soils on (5) can be salt affected where isolated from flow, but are generally alkaline. Relative magnitude of solute concentrations indicated by shade of blue arrows. Relatively dilute rainfall can interact with dust directly, or on its path through the weathered profile, as it brings carbonic acid into contact with fresh bedrock. These waters then incorporate silicate (Sil) and/or carbonate (Carb) weathering derived ions along their flow path, before being discharged at topographic discontinuities and incorporated with the dissolved load of rainfall and dust dominated runoff. Adapted and modified from Gunn and Fleming (1984).

Fresh minerals in the volcaniclastic sedimentary rocks provide a suitable source of silicate weathering within the LEB, and fracture flow in the silicified weathered profiles most likely facilitates the transport of carbonic acids to the top of the fresh bedrock from the surface. Water richer in HCO_3 and SiO_2 is then transported as bedrock fracture flow during runoff generation in large storm events to the base of the slopes, which have generally developed as piedmonts or low gradient alluvial

fans (Coventry, 1978), where it mixes with surface flow before entering the streams as discharge. This scenario is consistent with the water balance of the headwaters of these catchments, which have runoff co-efficients of only 2-7% (McMahon et al., 2008b), and the fact that the rivers have equilibrium solute concentrations despite orders of magnitude changes in discharge (Figure 2).

2.6.2 Transmission losses and evaporation

There is little evidence that the large transmission losses experienced in the Cooper Creek catchment are the result of evaporation, although the effects of evaporation on the dissolved load are difficult to quantify. The changes in TDS as a result of such large transmission losses are comparatively small and, importantly, there is no corresponding decrease in ion/Cl ratios in the Cooper Creek catchment downstream (Figure 4b). Waters remaining in large waterholes between floods also exhibit no significant changes in water chemistry (Sheldon and Fellows, 2010). Thus although the storage potential within waterholes in the ~430 km between Currareva and Nappa Merrie is large (Bunn et al., 2006), there is only minor evaporative enrichment between floods, leading to only slightly higher TDS in waterholes that are then mixed and diluted in the next flood event. This is supported by electrical conductivity (EC) measurements in the rising stage of floodwaters between Currareva and Nappa Merrie, which show high concentrations at the beginning of flow, followed by dilution just prior to the flood peak (Nanson, unpublished data), suggesting the higher ion concentrations in pre-existing waters are being transported at the beginning of the flood wave, before the arrival of the well-mixed flood peak. This is consistent with previous studies of event based changes in dryland zone floodwater chemistry in NW India (Sharma et al., 1984) and in Namibia (Jacobson et al., 2000). This data demonstrates that although annual pan evaporation is almost always higher than mean annual discharge throughout the LEB (Ceplecha, 1971), its relationship to actual evaporation during flooding events in this environment is not well matched.

Without evaporation to account for the large transmission losses in the Cooper Creek catchment, we instead suggest this water is recharged into the shallow groundwater table following scour of the channel bed during flooding events. This is supported by the presence of freshwater lenses beneath the multiple channels of Cooper Creek,

which occur within otherwise relatively saline regional shallow groundwater (Cendón et al., 2010), and these transmission loss pathways are discussed in greater detail in Chapter 3. Additional sources of flow loss include flood routing into terminal wetlands, and soil moisture storage in the large area of floodplain sediments. The same conclusions are difficult to draw for the Georgina-Diamantina catchment given the much smaller dataset, but since the hydrology, subsurface stratigraphy and major ion processes appear similar, at least for the Diamantina River, it is reasonable to expect that this scenario applies partly to the Diamantina as well. On the other hand, the large increase in Cl, and the dominance of rain, dust and carbonate weathering at Roxborough on the Georgina River, suggests evaporation and precipitation of salts during the dry season, followed by subsequent dissolution in the next flood event, are important in determining the dissolved load at this location. Of course, as these rivers enter the large desert dunefields en route to Lake Eyre, we expect transmission losses would increase (Costelloe et al., 2007), however, it is unclear what, if any, modification to the major ion chemistry is experienced in these farthest downstream reaches. Although it is clear that once the terminal playa of Lake Eyre is reached during a very large flood event, mixing with salty brines, and high potential evaporation rates acting on a standing body of water, results in a fairly rapid attainment of halite saturation (Gunn and Fleming, 1984).

2.6.3 Implications

Dryland rivers are often defined on the basis of the regional climatology, but it is clear that most large dryland rivers are large (in discharge) because they are allogenic, i.e. they don't receive their water from a dry climate, and flooding is usually the product of climatic excursions from monsoons, large summer rains, or even snow melt. Therefore, provided suitable bedrock is available, on the basis of water availability many dryland rivers have just as large a potential for incorporating weathering products into their dissolved load as do their tropical or temperate counterparts. However, since the delivery of water is mostly seasonal, usually highly variable, and generally accompanied by higher losses, it is reasonable to expect silicate weathering processes to be comparatively slower, and generally limited by the supply of carbonic acid to mineral surfaces. Nonetheless, this study demonstrates silicate weathering is potentially an important contributor to the dissolved load of

dryland rivers, and that these regions need to be considered within the domain of future weathering studies.

Another important feature of dryland rivers worldwide is the well documented downstream decline in discharge, however, the relationship between this and the processes operating within the dissolved load itself are not well understood. This study demonstrates that large transmission losses do not necessarily correspond to a change in water quality, indeed no Na – Cl surface-water types are found in the mid to upper catchments of the LEB. This is remarkable given that Australia's largest river, the Murray River, which is mostly within semi-arid and temperate climates, experiences substantial modification to its dissolved load, and is dominated by Na – Cl type waters in its lower reaches. Since this is largely the result of saline groundwater discharge to the river, enriched by evaporation during irrigation (Herczeg et al., 1993), it demonstrates that any large industrial or agricultural water use within the LEB would almost certainly result in a dramatic decline in water quality towards Na – Cl type waters. Given the greater variance of the water cycle in the LEB, it would also likely be more severe than the impacts in the Murray-Darling basin.

2.7 Conclusions

Factors controlling major ion chemistry are poorly understood in dryland river basins compared to temperate and tropical basins. Most models for changes in major ion chemistry assume evaporation and crystallization are the dominant processes, however, here we demonstrate that for the Lake Eyre Basin in central Australia, the effects of evaporation on flow are not detectable at most locations, even following large transmission losses. Instead, we attribute these losses mainly to recharge of the shallow groundwater tables via scouring at the base of channels where mud layers are present (Chapter 2) and flood routing into smaller terminal wetlands.

An evaluation of all the potential major ion sources contributing to the dissolved load of the LEB demonstrates that rain and dust contribute between 22 – 75% of the TDS, the most significant being SO_4, and the least being HCO_3. The remaining ions are the product of silicate weathering and carbonate dissolution, which we separate on the basis of generic silicate and carbonate mineral stoichiometry. Silicate weathering accounts for 10 – 70% of the dissolved load of LEB rivers, a process not previously

quantified in dryland environments, and accounts for the dominance of HCO_3 and the high concentrations of SiO_2 in the dissolved load.

This has important implications for our understanding of silicate weathering processes, which usually focus on tropical rivers or tectonically active terrains. Since at least one third of the world's land surface is arid to semi-arid, a lack of knowledge about weathering processes in these environments results in a large deficit in our understanding of chemical weathering processes as a whole. It is also important for the management of dryland rivers, which may rapidly decline in water quality if their water resources are over exploited or improperly managed.

2.8 Acknowledgements

JRL was supported by a UOW and ANSTO PhD scholarship. Due to its long gestation time this paper has benefited from many discussions with various colleagues, too many to name, but no less appreciated. Annegret Larsen is thanked for providing Figure 1. This research would not have been possible without the many Queensland state government employees who collected and analysed water samples over ~30 years.

3 SURFACE - GROUNDWATER INTERACTIONS AND RECHARGE PROCESSES IN DRYLAND, SEMI-CONFINED, ALLUVIAL AQUIFERS

3.1 Abstract

The major factors controlling the water balance within dryland catchments remains a considerable challenge to determine, and is crucial for effective management of this limited resource. Within the semi-confined and multi-channel alluvial system of Cooper Creek, in the arid to semi-arid Lake Eyre Basin of central Australia, large transmission losses significantly reduce surface water availability. In this study we investigate shallow groundwater resources within the semi-confined aquifer in order to determine to what degree groundwater recharge can account for these losses. We find large changes in groundwater quality that largely depend on the distance to the nearest channel (waterhole), however, the pathways taken by infiltrating water and the mechanisms controlling these changes in quality are not straightforward. It appears that recharge is dominated by three distinct flow pathways: 1. within large channels where basal mud can be sufficiently scoured, 2. within smaller channels, however, only during exceptional flow events, and 3. via desiccation cracks in the mud dominated floodplain surface. These pathways can be differentiated on the basis of tracer (^{14}C and ^{3}H) derived recharge rates, major ion and stable isotope ($\delta^{18}O$, $\delta^{2}H$, and $\delta^{13}C$) composition, and the redox state of the groundwater. Relatively high recharge rates (^{3}H derived = 30.8 ± 16.1, ^{14}C derived = 41.4 ± 24.4 mm/yr) can occur through the base of sections of larger channels that have a suitable morphology for high flow efficiency and erosive power, which in turn maintains the low TDS and heavily reduced groundwater below. In contrast, smaller channels have lower average recharge rates (8.3 ± 5.2 - 22.6 ± 5.7 mm/yr) which infiltrate into a permanent unsaturated zone above a higher TDS and oxidised groundwater table. The large un-channelised floodplain facilitates only very low recharge rates (< 1 mm/yr) and beneath which is the most saline groundwater found in this study, with the main distinction between this third pathway and the second one being the ability of larger flow events to provide higher infiltration fluxes through the base of the smaller channels and the unsaturated zone below. These results have implications for mechanisms of groundwater salinisation, since direct surface evaporation and concentration of ions is largely absent, and therefore infiltration and dispersion of

recharge waters in the unsaturated zone with subsequent fractional leaching of ions are suggested an alternative. This work also highlights the importance of preferential flow in semi-confined alluvial settings, and suggests that where hydrological variability is high, which is typical of dryland environments, groundwater recharge is perhaps better considered as a probability instead of an average rate, and that the sum of these probabilities may in turn account for the observed transmission losses in the water budget.

3.2 Introduction

The increasing demand upon water resources in dryland environments is often transferred directly to the water available from aquifers. These may have received much of their recharge during infrequent flooding events (Dahan et al., 2007), or very slowly via large unsaturated zones (Walvoord et al., 2002). Some may also have been primarily recharged during significantly wetter climatic phases in the past (Edmunds et al., 2004; Edmunds et al., 2003). The high hydrological variability and low precipitation to evaporation ratio has resulted in relatively high-salinity groundwater from dryland areas (Simmers, 1997), however, it is the sparse distribution of lower salinity water which is crucial as a resource, and which almost exclusively occurs in close proximity to river channels in alluvial settings (Scanlon, 2004). The recharge of low salinity floodwaters to groundwater usually occurs as infiltration through an unsaturated zone of highly variable thickness (Rimon et al., 2007), although some connected, albeit loosing systems in drylands have been documented (Lamontagne et al., 2005). This recharge constitutes a loss to the surface water budget that in dryland environments can be significant over large distances and hence a measurable transmission loss to surface flows. Although transmission losses have been well documented in a variety of dryland settings, their relationship with actual groundwater recharge remains difficult to constrain (Lange, 2005; Shentsis et al., 1999). Moreover, studies that have successfully linked transmission losses and recharge are almost exclusively within unconfined aquifers (Dahan et al., 2007; Dahan et al., 2008; Morin et al., 2009). The role of a surface confining layer in controlling recharge in alluvial systems undergoing heavy transmission losses has not yet been explored.

Here we investigate these issues on a long reach of Cooper Creek within the Lake Eyre Basin (LEB) of arid to semi-arid central Australia. Cooper Creek has developed

as a large multiple-channel river with an extensive mud-dominated floodplain, and where the large transmission losses have been well documented (Knighton and Nanson, 1994, 2001; McMahon et al., 2008c). These losses, on average 64% of annual flow volumes, have been suggested to be the result of a combination of groundwater recharge (Cendón et al., 2010), flow routing into terminal wetlands (Costelloe et al., 2009), and direct evaporation (Knighton and Nanson, 1994). In addition, Larsen et al. (submitted) recently demonstrated that the transmission loss of floodwaters is not significantly influenced by direct evaporation, suggesting that some combination of shallow aquifer recharge, tree transpiration, floodplain soil moisture storage, and flood routing into terminal wetlands, must account for the bulk of these losses. In order to constrain this water balance, we investigate the potential recharge processes using a variety of geochemical tracers, including major ions, stable isotopes, and ^{3}H and ^{14}C. From this data we estimate recharge rates and the primary controls on groundwater salinization which are unique compared to those reported from other dryland settings. Furthermore, we conclude that both geomorphology and antecedent conditions are critical determinants of recharge pathways and processes, which in turn impact on the probability of transmission loss magnitude.

3.3 Regional setting

The Lake Eyre Basin is an internally draining basin covering ~1/7th of the centre of the Australian continent, of which the Cooper Creek and its tributaries is the second largest catchment (Figure 9). The lithology is dominated by marine and freshwater sedimentary rocks with highly variable degrees of weathering, which has also strongly influenced soil development and solute stores (Gunn and Fleming, 1984), as well as the dissolved load of the rivers (Larsen et al., submitted). Over the Quaternary period Cooper Creek was mostly a sand dominated meandering river system, until the Late-Pleistocene / Holocene when the sediment load became mud dominated, and resulted in an extensive mud-capping of varying depth over most of the alluvial plains (Maroulis et al., 2007; Nanson et al., 2008; Rust and Nanson, 1986). This is most apparent within the areas of the LEB known as the 'Channel Country', where the mud floodplain is typically very wide (15 – 60 km) and characterised by and extensive entrenched anastomosing channel network of varying morphology and a surficial braided and reticulate network over the floodplain

(Nanson et al., 1986; Rust and Nanson, 1986). Larger channel segments can retain water between periods of flow, and are known as billabongs or waterholes.

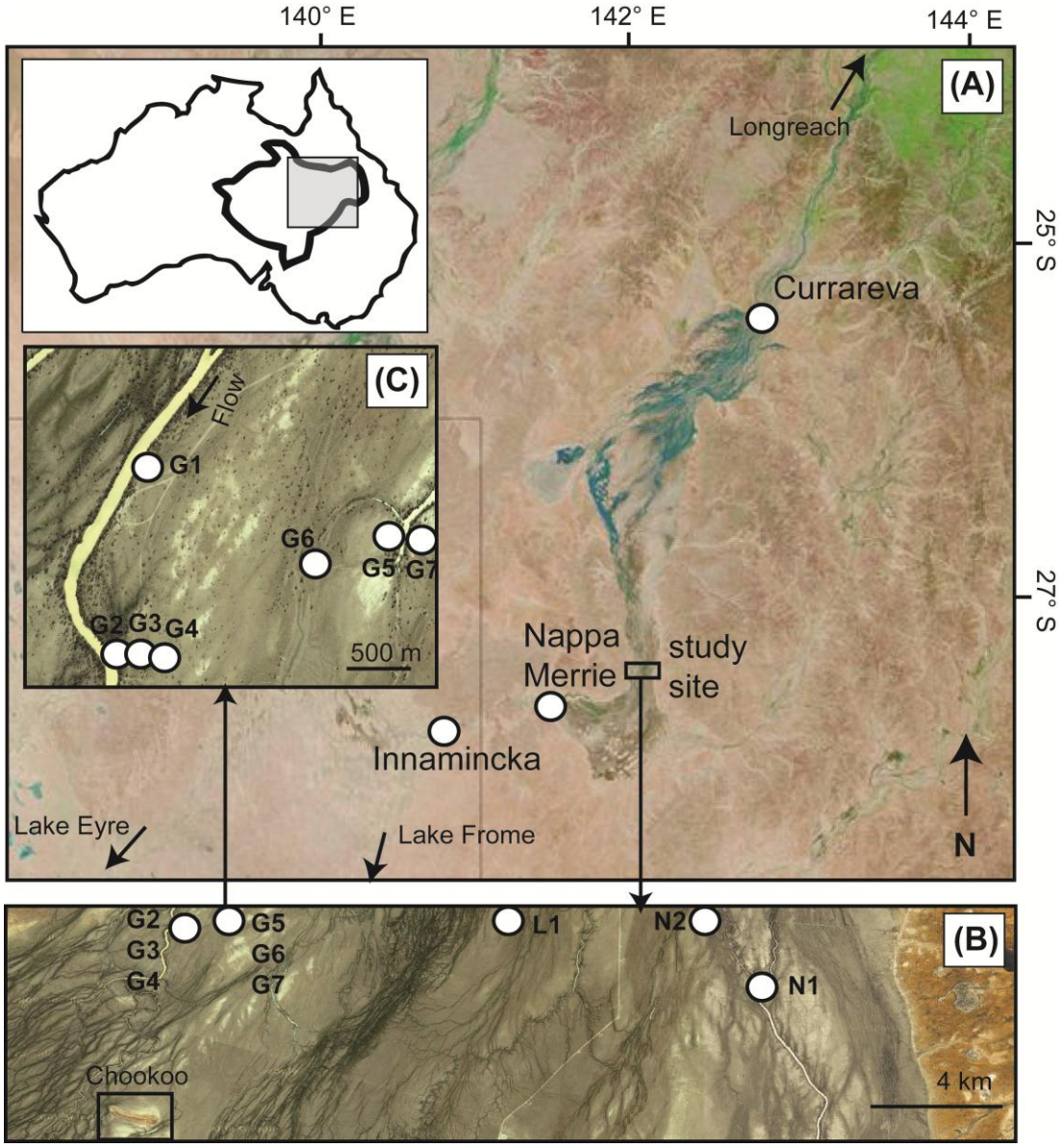

Figure 9. (a) MODIS satellite image of the Cooper Creek catchment during a minor flood in April 2006, inset map shows the Lake Eyre Basin (b) sampling locations across the ~18 km wide floodplain and channel network (also shown in cross section in Figure 10), with Goonbabinna Waterhole on the far left next to the G2,G3,G4 transect, and Naccowlah Waterhole on the far right adjacent to the N1 bore. (c) detailed locations of the bore network near Goonbaninna Waterhole (left) and North Chookoo Waterhole (right).

These are an integral part of the channel network, forming where flow energy is enhanced in a variety of settings, such as when anastomosing channels converge, where flow is confined between dunes, or where it is confined along the valley margins. With sufficient energy flow can scour through the mud deposits on the

channel bed and expose the Pleistocene sand sheet beneath (Knighton and Nanson, 1994, 2001). It has been proposed that during high flood stages these waterholes may recharge the shallow aquifer in the underlying sand sheet, but reseal with mud as discharges decline (Cendón et al., 2010) and hence they are also important ecological aquatic refugia during dry periods (Bunn et al., 2006). The shallow groundwaters studied here form a semi-confined aquifer, with the water table usually at 9 – 12 m depth, which is slightly beneath the base of the larger channels such as Goonbabinna and Naccowlah Waterholes (Figure 10).

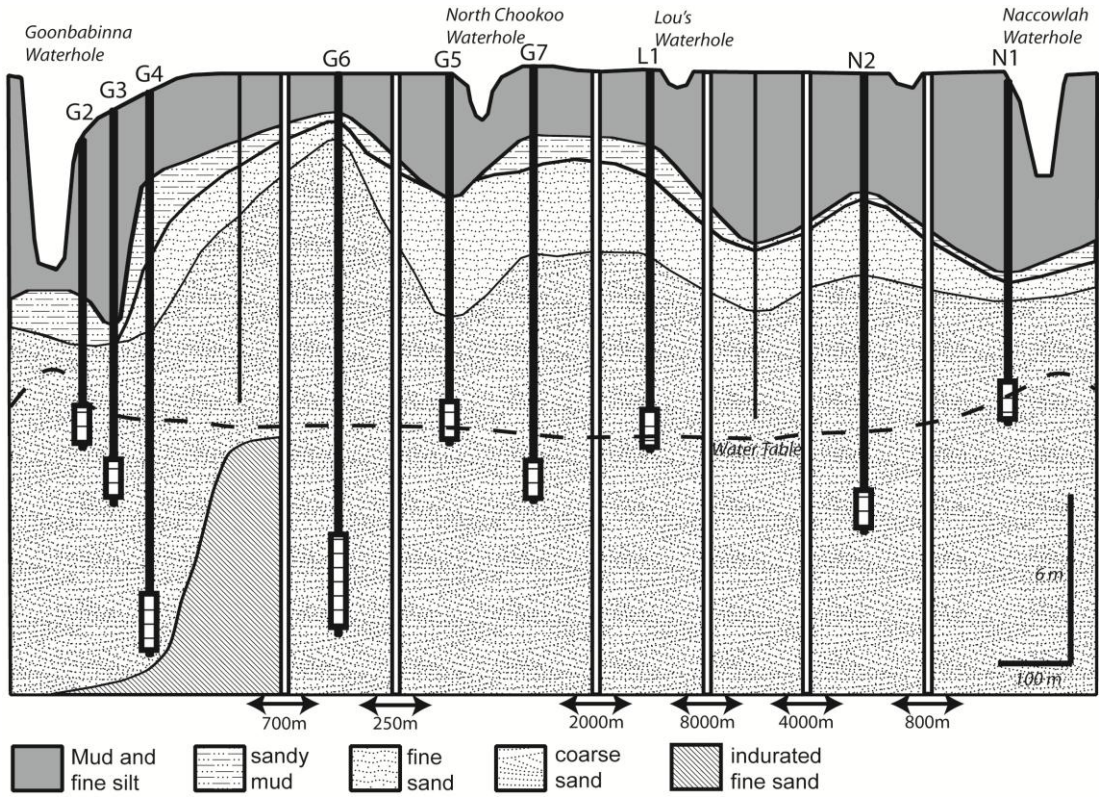

Figure 10. Stratigraphy, topography and variation in water table elevation within the floodplain transect investigated in this study. The vertical thick black lines with rectangles at the base are the bore location and depths, with the rectangles representing the approximate screen height, and the two thin black vertical lines are drill holes that did not reach the water table but provided stratigraphic information. Breaks in the horizontal scale are indicated by the white vertical sections, with the distances covered in each break given below. Note bore G1 from Figure 9 is not included.

Our study site, within the Channel Country of Cooper Creek, is between Currareva and Nappa Merrie, close to Ballera, and ~6 km upstream of the groundwater study by Cendón et al. (2010). The mean annual rainfall is 250-300 mm/yr at Currareva and Longreach, and decreases to 127mm/yr near our study area at Ballera, and mean

annual pan evaporation near Currareva is 2900 mm/yr. The heavy rainfall driving flows in Cooper Creek is strongly seasonal, occurring over the November-April summer monsoon period. Not directly within the tropics, the runoff in the headwaters relies mostly on incursions of the Australian summer monsoon, usually in the form of easterly low pressure troughs, to attract large rain events. The Australian summer monsoon is in turn modulated on the inter-annual timescale by ENSO, with higher rainfall events typically occurring during the La Niña phase (Kotwicki and Allan, 1998b). With virtually all of the runoff in the Cooper Creek catchment generated in the headwaters, the peak in catchment runoff occurs at Currareva ($31.5 \times 10^5 \pm 42.6 \times 10^5$ Ml/yr), which then decreases substantially over a 430 km reach as the flow reaches Nappa Merrie ($11.4 \times 10^5 \pm 27.3 \times 10^5$ Ml/yr). This represents a transmission losses of ~64% (2013168 Ml) of mean annual flow, and occurs almost entirely over the reach of the Channel Country (Larsen et al., submitted).

3.4 Methods

3.4.1 Field sampling and laboratory analysis

Following summer flooding lasting until late March-early April 2008, we collected surface water samples from flowing waterholes (major channels), and non-flowing waterholes (medium to minor floodplain channels). We used a drill rig to construct piezometer transects and sample shallow groundwaters across the ~16km floodplain (Figure 10). In each case, slug tests were undertaken to determine hydraulic conductivity, and groundwater was sampled by pumping following purging (3 x well volumes) except in cases where pumping was not possible, and bailers were used after rinsing with deionised water. Samples for G1, G3, and G4 were recollected in July 2008, and again in November 2009.

Prior to any collection or field analysis, all samples were filtered to 0.45μm. Total alkalinity concentrations were determined in the field by acid-base titration using a digital titrator (HACH). The Fe^{2+} concentrations were also determined using a portable colourimeter (HACH DR/890). Samples for anions and stable water isotopes ($\delta^{18}O$ and $\delta^{2}H$) analysis were collected in 125 ml and 30 ml HDPE (High Density Polyethylene) bottles, respectively. Samples for cations and trace elements analysis were collected in 125 ml and 250 ml HDPE bottles and acidified with double sub-boiled ~70% nitric acid (HNO_3). The $\delta\ ^{13}C_{DIC}$ samples were collected in 12 ml glass

vials (Exetainer) without head space and stored under dark and cool (~4°C) conditions and analysed within 2 months. Samples for ^{14}C and ^{3}H analysis were collected in 1L Nalgene HDPE bottles and were sealed with tape to eliminate atmospheric exchange during storage. The chemical composition of water samples were analysed at ANSTO by Inductively Coupled Plasma – Atomic Emission Spectroscopy (ICP-AES) and Inductively Coupled Plasma – Mass Spectrometry (ICP-MS) for cations and trace elements, respectively, and Ion Chromatography (IC) for anions. The saturation index (SI) of calcite and the derivation of total dissolved inorganic carbon (DIC, = $\sum HCO_3^- + HCO^{2-} + CO_2$)., was calculated using PHREEQC v2.1 (Parkhurst and Appelo, 1999). The $\delta^{18}O$, $\delta^{2}H$ and some $\delta^{13}C_{DIC}$ stable isotopes were analysed by Isotope Mass Spectrometry (IRMS) at Alberta Innovates, Canada. The $\delta^{18}O$ and $\delta^{2}H$ values were reported as per mil (‰) deviations from the international standard, V-SMOW (Vienna Standard Mean Ocean Water). The $\delta^{18}O$ and $\delta^{2}H$ measurements were reproducible to ±0.1 and ±1 ‰, respectively. The $\delta^{13}C_{DIC}$ results are reported as per mil (‰) deviation from the international carbonate standard, NBS19 ($\delta^{13}C$ = +1.95 ‰ V-PDB) with a precision of ± 0.1 ‰ and were analysed at Environmental Isotopes Pty Ltd. Alternative analysis of $\delta^{13}C_{DIC}$ and $\delta^{13}C_{DOC}$ were also done using Aurora total inorganic and total organic carbon analyser linked to an IRMS according to the method of (Assayag et al., 2006). In-house standards, established by runs with NBS18 and NBS19, are run as samples to allow the results to properly be reported versus VPDB. Results are accurate to ± 0.2 ‰.

Both ^{14}C and ^{3}H measurements were processed and analyzed for ^{3}H and ^{14}C activities at the Australian Nuclear Science and Technology Organization (ANSTO). For ^{3}H analysis, water samples were distilled and electrolytically enriched prior to being analyzed by the liquid scintillation method. The ^{3}H activities were expressed in tritium units (TU) with an uncertainty of ± 0.1 TU and an average quantification limit of 0.7 TU. Tritium was measured by counting beta decay events in a liquid scintillation counter (LSC). A 10 ml sample distillate was mixed with the scintillation compound that releases a photon when struck by a beta particle. Photomultiplier tubes in the counter convert the photons to electrical pulses that are counted over 51 cycles for 20 minutes.

For ^{14}C analysis, the total DIC was processed into CO_2 by acidifying the samples with H_3PO_4 and extracting the liberated CO_2 gas using a custom built extraction line. The CO_2 sample was then heated in a sealed glass tube, containing baked CuO and Ag and Cu wire, at 600ºC for 2 hours to remove any sulfur compounds that may have been liberated from the groundwater sample during the CO_2 extraction. The CO_2 sample was then converted into graphite by reducing it with excess hydrogen gas in the presence of an iron catalyst at 600ºC. The $\delta^{13}C$ isotopic composition of the graphite was determined using a Eurovector EA / Isoprime IRMS instrument with a precision of 0.1 ‰. This $\delta^{13}C$ measurement is solely used as a correction in the calculations related to the radiocarbon measurement and may not necessarily be the same as the $\delta^{13}C_{DIC}$ measured directly on the groundwater sample, and is not reported here. The ^{14}C activities were measured using the ANSTO AMS 2MV tandetron accelerator, STAR, and the ^{14}C results are given here as percent Modern Carbon (pMC) with an average 1 σ error of the AMS readings at ± 0.3 pMC.

3.4.2 Integration of discharge records

Our study site lies between two monitored discharge stations of differing length and duration, with the annual transmission losses (as a flood year) between them estimated to be on average 64% (Larsen et al., submitted). In order to obtain a broad estimate of the water available for shallow groundwater recharge over time we assess changes in transmission losses on a yearly basis from Currareva, which is ~250 km upstream of our site and has a mostly continuous record of daily flow volumes from 1948 – 1988, and Nappa Merrie, which is ~400km downstream of Currareva and has a discontinuous record daily flow volume record from 1968 – present. Additional flow volume records are also available from Longreach, which is ~280 km upstream of Currareva, and from Innamincka, ~40km downstream of Nappa Merrie. We first derive annual flow volume totals from integration of the daily data where it is continuous for the whole year. For annual totals not available because of missing daily data at Currareva or Nappa Merrie, we calculate the annual total for the missing year(s) using a simple linear regression of all available annual totals with one of the above supplementary stations, depending on availability. The regression statistics of annual flow volumes between stations are generally quite good (r^2 = 0.79 – 0.92), and although not the most robust estimate of annual flow volumes, it is nonetheless

the most practical one available given the limitations of the data, and is sufficient for the scope of this study.

3.4.3 ^{14}C and ^{3}H model description

The use of ^{14}C and ^{3}H as tracers in determining recharge rates is commonplace in groundwater studies, however, in arid and semi-arid areas this is often difficult to constrain because of the lack of general aquifer information. One approach in dealing with this limitation is to estimate the percentage of the aquifer mixed (renewal rate, R_n) during recharge events (R) using a general mixing model with annual time steps in order to constrain changes in the tracer concentration within the groundwater (C_{GF}) (Cartwright et al., 2007; Favreau et al., 2002; Le Gal La Salle et al., 2001; Małoszewski and Zuber, 1982), whereby:

$$C_{GF} = C_{GW_{(i-1)}}(1 - R_n)e^{-\lambda} + C_{A(i)}R_n \qquad (1)$$

and C_A is the atmospheric concentration of the tracer at year i (1900 – 2007), C_{GW} is the tracer concentration at year i, and λ is the decay constant ($^{14}C = 5730/\ln(2)$, $^{3}H = 12.43/\ln(2)$). In this study, we take the atmospheric concentrations of ^{14}C and ^{3}H from the Southern Hemisphere ^{14}C bomb calibration curve for the period 1955-2006 (Hua and Barbetti, 2004; Hua pers comm), and from rainfall weighted ^{3}H data from Alice Springs (1964-1986), Perth (1955-1987), Longreach (1970-1986), and Charleville (1970-1982) (Calf, 1988), with ^{3}H in rainfall since 1987 assumed to follow an exponential decay until 2007. Prior to bomb testing in 1955, ^{14}C concentrations were assumed to decrease from 99 to 97.5 pMC due to the Suess effect, and ^{3}H to be similar to the modern average of surface and event water samples collected here (Table 8) and elsewhere in the LEB (Tweed et al., 2011).

We can further relate recharge (R, mm/yr) and R_n by

$$R = R_n \varepsilon D \qquad (2)$$

where ε is the average porosity of the aquifer, and D represents the total aquifer thickness. Since we are concerned with constraining the concentrations of ^{14}C and ^{3}H near the top of the Quaternary sands aquifer, which potentially extends to large (> 30m), but relatively unknown depths (Nanson et al., 2008), the use of total thickness (D) would produce unreasonably high recharge rates. Therefore, we interpret D to be the effective depth mixed by R_n, which we define as being between 0.5 – 6m, and is probably more conceptually valid since the same aquifer may stratify both in age and

in general chemistry, depending on the effectiveness of mixing during recharge events and rates of lateral flow over depth.

Additional assumptions are that the transfer of ^{14}C from the atmosphere to the DIC within recharge water, via the terrestrial and freshwater organic carbon pools, is not significantly lagged from year to year. This may not be valid in environments with significant carbon reservoirs between the atmosphere and the aquifer, however, in the LEB, and indeed in many arid environments, turnover of organic carbon has been found to be relatively rapid (Burford et al., 2008). It is, therefore, reasonable to expect the ^{14}C of DIC, as originally derived from soil CO_2 and dissolved organic carbon (DOC), to be representative of atmospheric ^{14}C at the time of recharge. Nonetheless, even in the case of a significant time lag (~3 years) in the transfer of atmospheric ^{14}C to groundwater, this is only expected to vary input ^{14}C concentrations in our model by ~0.3 pMC (Favreau et al., 2002). We also assume porosity values (ε) of 0.4 in our model, which is a conservative estimate for unconsolidated and homogeneous medium to coarse sands (Freeze and Cherry, 1979). If, however, significant variation does occur in the aquifer, ε is linearly related to R so that a reduction in porosity to 0.3 would only result in a 10% reduction in R but, nonetheless, must be considered in any recharge estimates. Additional sensitivities relevant to this model are discussed in detail by Favreau et al. (2002).

3.5 Flood dynamics and transmission losses

Total transmission losses between Currareva and Nappa Merrie show considerable variation between 1955 and 2007 (Figure 11a) and, similar to the discharge statistics, have a standard deviation (23.1 mm/yr) higher than the mean (18.5 mm/yr). In general, trends in transmission losses mirror trends in discharge, with 1955 and 1974 being the most significant events in both cases. We also note that the transmission loss and discharge record we have constructed has more flood events above the mean between the 1955 – 1975 period than it does between 1976 – 2007. These periods are therefore termed ‘wet’ in the case of the former, and ‘dry’ in the case of the latter. These distinctions are also evident in the ratio of transmission loss and discharge (TL/Q), which is considerably more variable and with more events approaching one during the dry period (Figure 11a). Interestingly, this contrast between a wet and a dry phase also determines the behaviour of transmission losses with changes in total

flood volume. For large annual flows in both wet and dry years, transmission losses increase with increasing Q, however, at a much faster rate during the dry phase (Figure 11b). There is also a combined trend between TL/Q and Q for dry phase flows and most of the low flows, regardless of which phase they occur under. This suggests a similar level of reduced transport efficiency and high transmission losses under drier climatic conditions despite large variations in total discharge, and also for minor floods (low flows) which have a diminished flood wave transport capacity. These results also demonstrate the effectiveness of wetter antecedent conditions in increasing flood transport efficiency, and reducing overall transmission losses, in the annual water budget of large dryland river systems such as Cooper Creek, a point which was already suggested with a smaller dataset by Knighton and Nanson (1994).

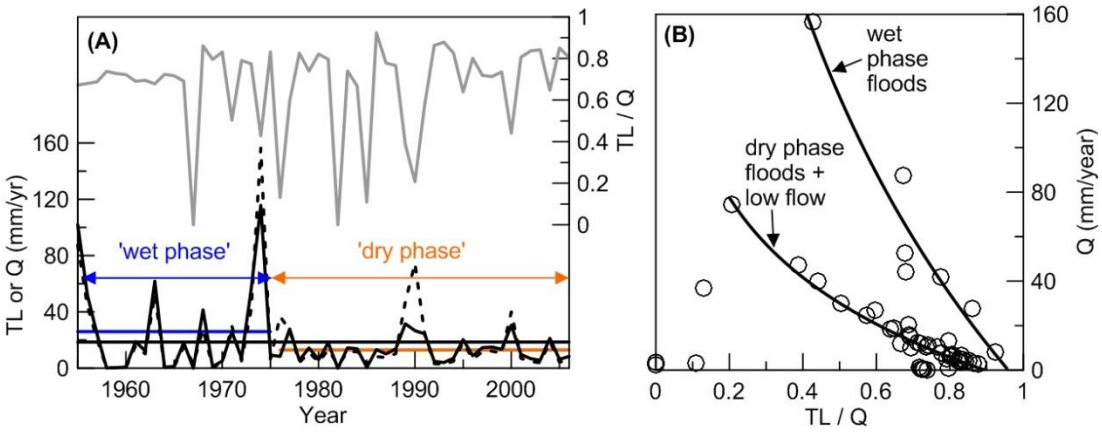

Figure 11. Dynamics of transmission losses in Cooper Creek. (a) Annual total transmission losses (black line) between Currareva and Nappa Merrie, and discharge (Q) at Currareva (dashed line) between 1955 and 2007. The straight black line through the TL and Q data is the mean TL (18.9 mm/yr) which has a standard deviation of 23.1 mm/yr. The discharge (Q) record is divided into a 'wet phase' (blue line, mean = 26.2 mm/yr), and a 'dry phase' (orange line, mean = 13.8 mm/yr). The light grey line above represents changes in the TL/Q ratio over the same period. (b) Plot of TL/Q against Q, showing distinct trends between dry phase and low flow TL/Q, and wet phase TL/Q, see text for further explanation.

3.6 Major ions and physical chemistry

The major ion chemistry of surface and groundwater samples at the study site can be grouped according to trends in concentration and spatial context (Tables 5 and 6; Figure 12). Similar to (Cendón et al., 2010) we define four main water quality trends: 1. *Surface waters*, low TDS (mean = 102.9 mg/l), dominated by Na, Ca, and HCO_3. 2. *Proximal groundwaters*, below or adjacent to major channels, relatively low TDS (mean = 315.9 mg/l), also dominated by Na, Ca, HCO_3. 3. *Intermediate*

groundwaters, with increasing TDS (mean = 888.6 mg/l) with the major ions now Na, HCO_3, and Cl. 4. *Regional groundwaters*, high TDS (mean = 14359.5 mg/l), and dominated by Na-Cl type waters.

Location	Ca mmol/L	Mg mmol/L	Na mmol/L	K mmol/L	Cl mmol/L	SO_4 mmol/L	HCO_3 mmol/L
Event water	0.06	0.05	0.55	0.12	0.13	0.02	0.56
Goonbabinna WH a	0.36	0.15	0.67	0.14	0.20	0.14	0.84
Goonbabinna WH b	0.20	0.08	0.46	0.10	0.14	0.09	0.51
Goonbabinna WH c	0.09	0.04	0.40	0.07	0.18	0.07	0.29
Noccundra WH	0.08	0.07	0.81	0.09	0.28	0.10	0.33
North Chookoo WH	0.43	0.25	1.08	0.20	0.24	0.05	1.44
Naccowlah WH	0.29	0.15	0.75	0.16	0.23	0.08	0.89
Lous WH	0.33	0.22	1.47	0.17	0.28	0.02	2.38
G2	0.50	0.44	1.25	0.16	0.17	0.03	2.08
G3a	0.89	0.99	1.76	0.09	0.31	0.09	3.64
G3b	0.77	0.87	1.74	0.09	0.34	0.07	4.00
G3c	0.88	0.90	1.73	0.08	0.37	0.11	4.03
G4a	0.71	0.51	2.58	0.10	0.56	0.17	3.16
G4b	0.63	0.51	2.44	0.10	0.56	0.02	3.25
G4c	0.59	0.53	2.50	0.09	0.59	0.14	3.08
N1	1.18	0.26	1.41	0.19	0.37	0.04	2.80
G1a	0.66	0.41	11.66	0.12	5.64	0.55	4.66
G1b	0.57	0.35	10.35	0.07	5.36	0.10	6.36
G1c	0.38	0.36	10.35	0.05	5.36	0.48	4.72
G7	0.37	0.32	11.74	0.04	6.77	0.42	4.46
N2	1.08	0.41	14.09	0.16	5.08	2.08	5.57
G5	4.14	3.85	61.33	0.11	64.87	5.31	7.02
G6	14.25	17.73	219.23	0.34	259.50	17.70	5.97
L1	23.83	20.98	245.76	0.42	332.84	16.66	5.18

Table 5. Major ions of surface waters and shallow groundwaters. The table is divided into 4 sections: 1. Surface water samples, 2. Proximal groundwater samples, 3. Intermediate groundwater samples, and 4. Regional groundwater samples. Explanation for classification is given in text. Location details are provided in Figure 9, and where alphabetical suffixes are present (a,b,c) they refer to separate sampling campaigns: (a) April 2008, (b) July 2009, and (c) November 2009.

These gradients in TDS and ion dominance are greater than that found by Cendón et al. (2010), probably because the proximal and intermediate groundwaters can be better distinguished in the groundwater transects in this study, however, the regional

groundwaters in Cendón et al. (2010) exhibited higher average TDS and are increasingly dominated by SO_4, which was not found in this study.

Location	TDS mg/L	Fe^{2+} mg/L	DO mg/L	pH
Event water	61.77	0	9.01	8.62
Goobabinna WH a	110.24	0	6.62	7.5
Goobabinna WH b	69.34	0	13.61	7.89
Goobabinna WH c	47.37	0	7.23	7.23
Noccundra WH	66.96	0	4.82	6.91
North Chookoo WH	157.44	0	9.38	8.31
Naccowlah WH	108.55	0	6.99	6.95
Lous WH	215.82	0	17.04	9.33
G2	201.79	1.62	0.4	6.4
G3a	345.34	2.36	0.7	6.59
G3b	357.85	0.57	0.7	6.82
G3c	369.94	0.48	0.7	6.63
G4a	333.02	0.03	2.0	6.8
G4b	317.79	0.70	2.0	6.81
G4c	319.54	0.38	2.0	7.01
N1	281.68	0.07	1.1	6.57
G1a	846.13	0.02	6.4	7.41
G1b	859.40	0.12	6.4	7.26
G1c	788.12	0.50	6.4	7.24
G7	846.28	0	1.6	6.7
N2	1103.17	0.01	5.7	8.07
G5	4911.67	0.02	2.4	7.06
G6	17319.20	0.03	3.4	7.01
L1	20847.60	0.00	7.3	7.37

Table 6. Same as Table 5, but for physical chemistry.

Interestingly, we also find distinct changes in the redox chemistry of the shallow groundwaters. Proximal groundwaters with low TDS in general also have very low

dissolved oxygen and high concentrations of Fe^{2+} (Table 6). In contrast, all intermediate, regional, and one proximal groundwater well (G4) have significantly higher concentrations of dissolved oxygen, and no measurable Fe^{2+}. These results indicate that besides having low TDS concentrations, proximal groundwater is also generally reduced, which we attribute to the availability of organic matter at the base of large channels.

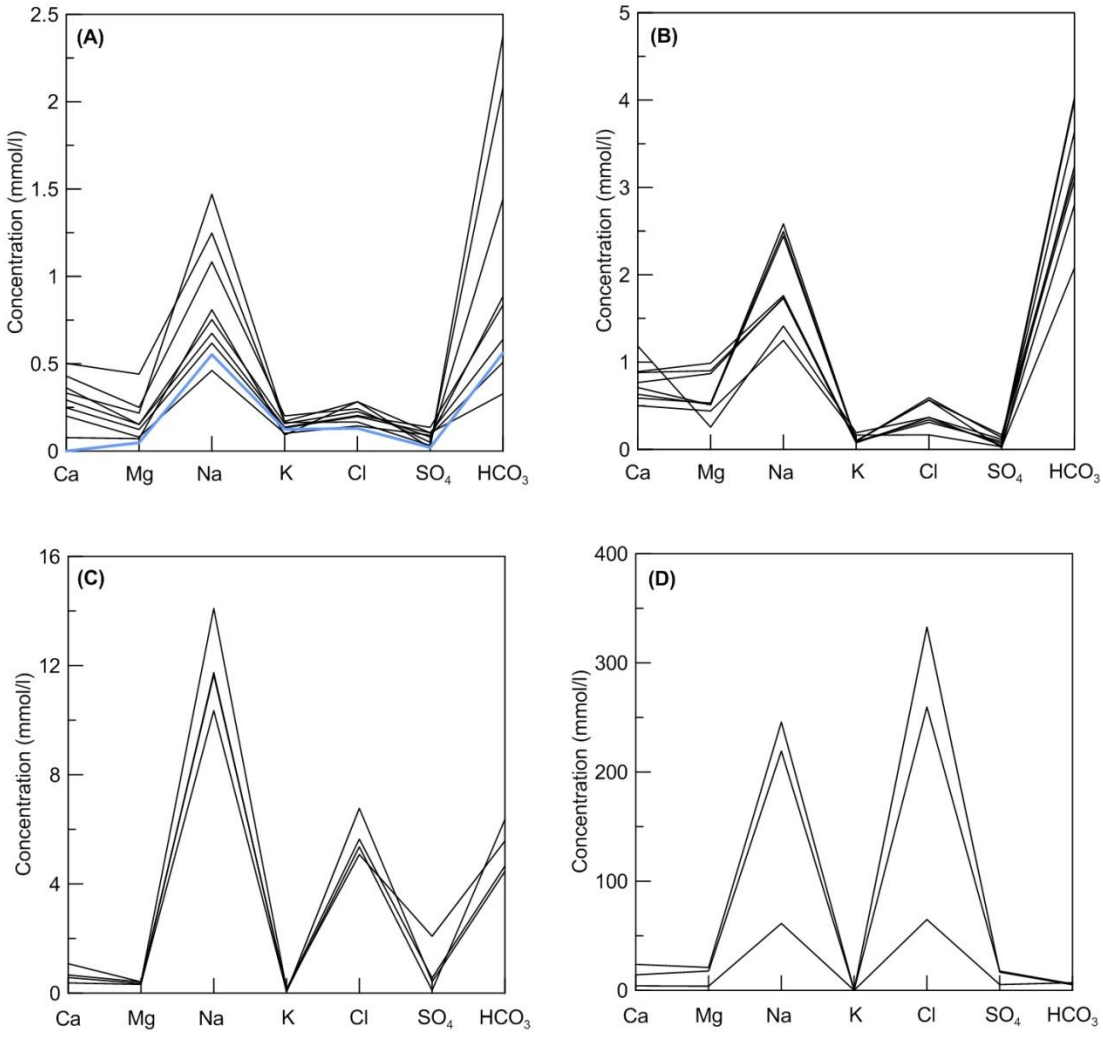

Figure 12. . Variation in major ion chemistry in surface water (a) and groundwater (b,c,d). (a) surface water samples from waterholes in low to no flow, and event water (blue line), with very low TDS and dominated by Na-HCO_3 and occasionally by Ca. (b) Proximal groundwater samples have a low TDS, and are also dominated by Na-Ca-HCO_3. (c) Intermediate groundwaters have a large increase in TDS and are now Na-Cl-HCO_3 type waters. (d) Regional groundwaters have a very high TDS, and are exclusively Na-Cl type waters.

Shallow groundwater with even a small concentration of organic matter can easily consume most available dissolved oxygen during organic matter degradation,

resulting in MnO_2, NO_3^-, SO_4^- and Fe^{2+} reduction. The development of low TDS and reduced shallow groundwater beneath and adjacent to Goonbabinna waterhole is indicative of two important points: first, there must be a reasonable degree of connection between the surface water and shallow groundwater without the development of a significant unsaturated zone for long periods of time, since the preservation of organic matter that can decay and consume oxygen is not likely under these conditions (Appelo and Postma, 2005); second, although a mixing zone has clearly developed between the low TDS and reduced proximal groundwater, and the oxidised and high TDS regional groundwater, recharge via the large channels such as Goonbabinna Waterhole and lateral transport beneath the floodplain is not occurring, since such a flow path provides no mechanism by which oxygen can be added to the groundwater. Therefore, additional flow paths for effective recharge of the high TDS, and oxidised regional shallow groundwater beneath the floodplain is required.

3.7 Stable and radiogenic isotopes

3.7.1 δ^2H and $\delta^{18}O$

The δ^2H and $\delta^{18}O$ composition of surface waters varies depending on channel and waterhole, and also upon sampling period (Figure 13). Samples collected following flooding in April 2007 all conform to a regression line to the right of the Alice Springs LMWL, while event water and waterhole surface waters collected during repeat campaigns are comparatively enriched in stable isotopes and much closer to the LMWL. Shallow groundwater samples also fit well to a single regression line, slightly offset to the right of the LWML. In addition, we observe a trend of isotopic depletion from the proximal groundwaters (mean $\delta^{18}O$ = -0.20‰, δ^2H= -14.75‰), to the intermediate groundwaters (mean $\delta^{18}O$ = -1.48‰, δ^2H= -22.41‰), regional groundwaters (mean $\delta^{18}O$ = -2.72‰, δ^2H= -28.58‰), and also the nearby high TDS regional groundwaters from Cendón et al. (2010) (mean $\delta^{18}O$ = -3.44‰, δ^2H= -33.49‰).

The relationship between increasing salinity and increasing stable isotope depletion is easiest to interpret in terms of mixing between two end member compositions that are themselves the result of different recharge pathways with different fractionation effects. Previous interpretations of stable isotope trends in this area (Cendón et al., 2010; Hamilton et al., 2005b) and in arid Australia generally (Harrington et al.,

2002), have compared the intercept of the groundwater regression line with the Alice Springs derived LMWL, which Harrington et al. (2002) noted becomes progressively more depleted with larger rain events. Since our groundwater regression line is identical to that of Cendón et al. (2010), their LMWL intercept values of $\delta^{18}O$ = -11.2‰ and $\delta^{2}H$= -74.7‰ also remains identical for this study, and suggests that if large flood events with heavily depleted stable isotopes are the main source of recharge, it only appears to be the case for the high TDS regional groundwaters.

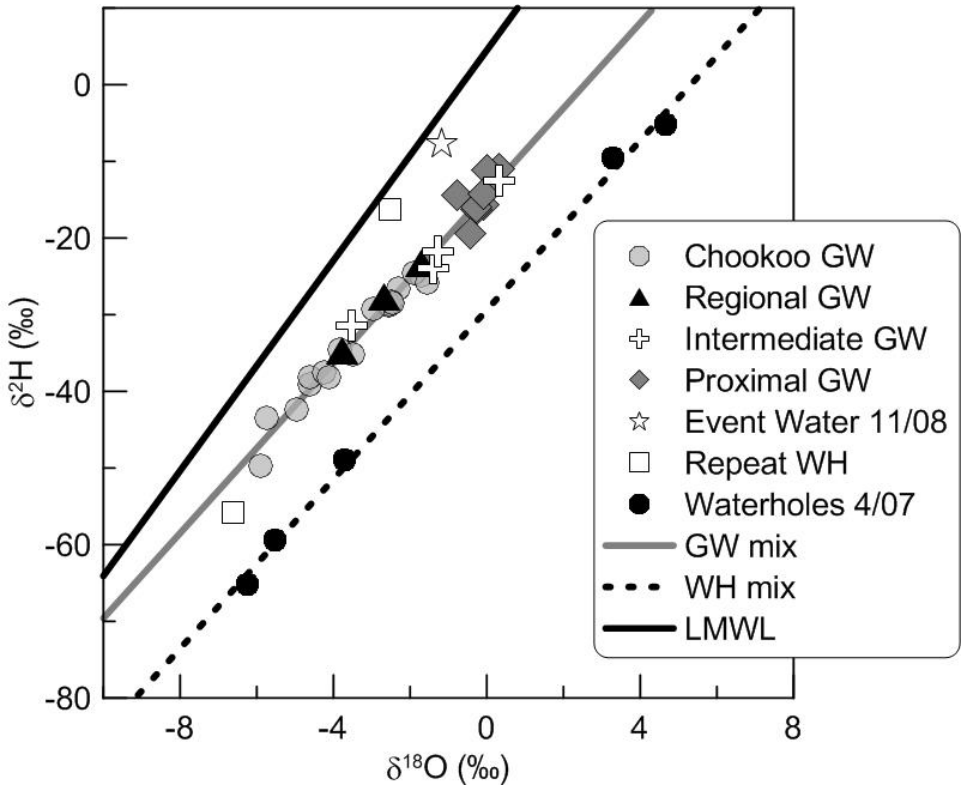

Figure 13. Ground and surface water stable isotope composition. Surface waters include the Waterholes sampled in April 2008, repeat sampling of Goobabina waterhole in July and November 2009, and event water also sampled in November 2008. Groundwater (GW) samples are divided according to major ion trends (Figure 12), and Chookoo GW is from Cendón et al. (2010). The groundwater mixing line (regression of all groundwater samples) is identical to that of Cendón et al. (2010)and the waterhole mixing line (regression of all April 2008 waterhole samples) is y =5.52 x - 29.36, r^2 = 0.99. The local meteoric water line is constructed from >100mm rainfall events in Alice Springs.

However, although these large events do occur, the majority of flow events are probably less depleted in stable isotopes, as is the case for the surface waters in this study that were not yet significantly influenced by evaporation (April 2007 samples), and the inclusion of this water in recharge occurring via the base of larger channels

also explains the origin of the less isotopically depleted, low TDS groundwater beneath and adjacent to them. In the case of recharge to high TDS regional groundwater, it is also important to note that the slope of the groundwater line (~5) does not indicate significant evaporation in the water column or in the unsaturated zone (Allison, 1982), thus differing from the results from unconfined aquifers in the LEB (Tweed et al., 2011).

Location	$\delta^{18}O$ ‰	$\delta^{2}H$ ‰	DIC mmol/L	DOC ppm	SI calcite	$\delta^{13}C_{DIC}$ ‰	$\delta^{13}C_{DOC}$ ‰
Modern Gastropod						-11.9	
Event water	-1.18	-7.67	0.55	-	-0.82	-7.02	-
Goonbabina WH a	-6.25	-65.23	0.90	-	-1.12	-9.90	-
Goonbabinna WH b	-6.62	-55.81	0.52	3.75	-1.25	-8.59	-24.26
Goonbabinna WH c	-2.53	-16.30	0.33	-	-2.28	-17.64	-
Noccundra WH	-	-	0.43	-	-2.76		-
Little G WH	3.29	-9.59	1.44	-	0.01	-11.41	-
Naccowlah WH	-3.72	-48.89	1.11	-	-1.66	-9.10	-
Lous WH	4.66	-5.26	2.11	-	0.95	-14.49	-
G2	-0.77	-14.43	3.90	-	-1.64	-16.98	-
G3a	-0.08	-15.59	5.57	-	-0.97	-16.45	-
G3b	0.01	-11.17	5.27	3.04	-0.78	-14.66	-22.24
G3c	-0.08	-14.20	5.96	-	-0.88	-16.44	-
G4a	-0.27	-16.28	4.22	-	-0.92	-14.65	-
G4b	-0.26	-15.99	4.32	21.56	-0.95	-13.70	-24.45
G4c	-0.44	-19.36	3.69	-	-0.75	-15.74	-
N1	0.31	-11.00	4.38	-	-0.96	-15.93	-
G1a	-1.13	-21.00	5.01	-	-0.26	-14.21	-
G1b	-1.28	-21.80	7.07	5.18	-0.34	-12.83	-26.72
G1c	-1.40	-23.96	5.26	-	-0.64	-15.04	-
G7	0.31	-12.49	6.25	-	-1.23	-18.53	-
N2	-3.54	-31.41	5.62	-	0.49	-14.37	-
G5	-1.72	-23.24	8.07	-	0.07	-14.93	-
G6	-3.77	-34.76	6.81	-	0.28	-9.87	-
L1	-2.67	-27.74	5.51	-	0.72	-11.80	-

Table 7. Water ($\delta^{18}O$, $\delta^{2}H$) and carbon ($\delta^{13}C_{DIC}$, $\delta^{13}C_{DOC}$) stable isotopes from surface and groundwater samples, with same division of data as Table 5.

3.7.2 $\delta^{13}C$

The $\delta^{13}C$ of dissolved inorganic carbon ($\delta^{13}C_{DIC}$), varies over a large range (-7.0‰ – -18.5‰) between both surface and shallow groundwater samples (Table 7, and Figure 14a). Within this variation, groundwater samples are generally more depleted in $\delta^{13}C_{DIC}$ than surface waters, although repeat sampling of Goonbabinna Waterhole revealed a depletion trend in surface water $\delta^{13}C_{DIC}$ with time since the last flooding event.

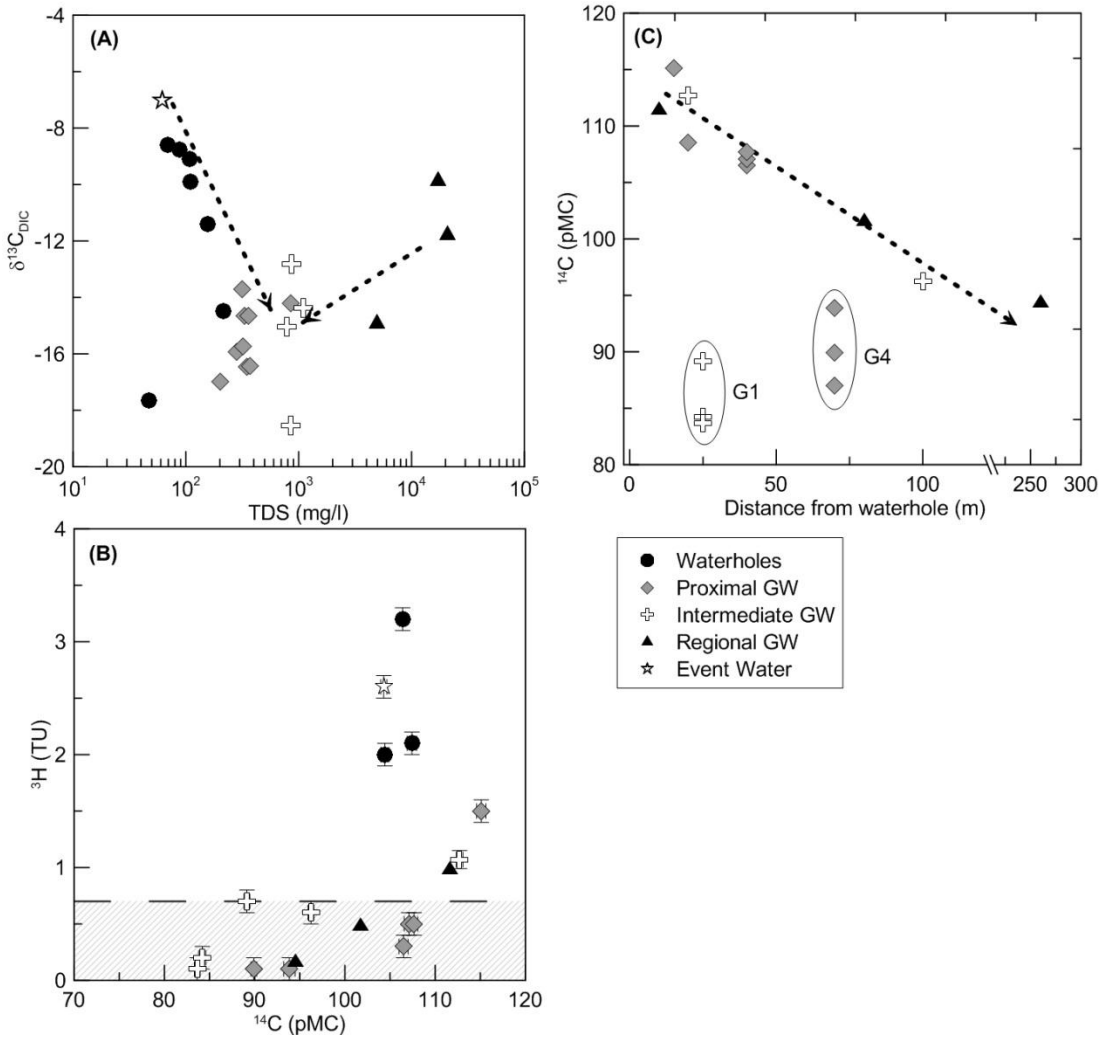

Figure 14. (a) Evolution of TDS concentrations and $\delta^{13}C_{DIC}$ from surface waters, to proximal, intermediate, and regional groundwaters. (b) ^{3}H and ^{14}C co-variation, the dashed area highlights ^{3}H samples below the detection limit (~ 0.7 TU). (c) Decrease in ^{14}C concentrations with increasing distance from waterholes of all channel sizes (note break in x-axis scale). Circled samples are separate from this trend and are from wells G1 and G4, which correspond to locations with a shallow channel in the waterhole, and deeper groundwater, respectively. Arrows in (a) and (c) indicate inferred trends discussed in text.

We also analysed other potential $\delta^{13}C_{DIC}$ sources including modern aragonite gastropod shells (-11.9 ‰), and dissolved organic matter ($\delta^{13}C_{DOC}$) in waterholes and proximal groundwater (4 samples, -22.2‰ – -26.7‰). Surface water $\delta^{13}C_{DIC}$ shows a depletion trend with increasing TDS concentrations, whilst in contrast as TDS increases from proximal to intermediate and regional shallow groundwater, there is an accompanying enrichment in $\delta^{13}C_{DIC}$ (Figure 14a). These results suggest that during the recharge process of proximal groundwater, and during waterhole evolution in no-flow periods, $\delta^{13}C_{DIC}$ is being increasingly sourced from reactions with DOC, which is in turn strongly depleted in $\delta^{13}C$ and indicative of C3 derived soil and plant organic matter. The modern gastropod shell $\delta^{13}C$ is similar to the average surface water value (-11.4 ‰), and our event water is the most enriched sample (-7.0‰), suggesting that the $\delta^{13}C_{DIC}$ of regular flood waters is mostly influenced by more enriched atmospheric sources. Calcite precipitation and dissolution is an additional factor which could influence the $\delta^{13}C_{DIC}$ composition, and indeed the surface water from one waterhole (Lou's Waterhole) is super-saturated with respect to calcite (SI = 0.95), higher than any of the groundwater samples. Not surprisingly, the groundwater directly below this waterhole (L1) has the highest calcite super-saturation within the shallow aquifer samples investigated here (SI = 0.75), with N1 and G6 being the only other groundwater samples found to be super-saturated in this study (SI = 0.49 and 0.28 respectively). The flow path of these waters could be expected to precipitate calcite, however this should result in a noticeable relative decline in HCO_3 and pH values (Appelo and Postma, 2005), which is not observed here, although this conclusion requires further investigation and sampling of the flow paths. Possible effects of calcite precipitation on the $\delta^{13}C_{DIC}$ ratios are noticeable in Lou's Waterhole (-14.49 ‰) which is the most depleted of any surface waters during the April 2007 sampling event, however, none of the super-saturated groundwater samples are distinct in $\delta^{13}C_{DIC}$ compared to other samples within a similar TDS range, indicating any calcite precipitation effects are probably minor with respect to groundwater $\delta^{13}C_{DIC}$ composition.

3.7.3 ^{14}C and ^{3}H

All ^{14}C percentage modern carbon (pMC) results are > 83.9 pMC, with proximal groundwaters distinguished by their > 100 pMC values, indicating atmospheric CO_2

during the post-1955 period of nuclear bomb testing has contributed to these DIC concentrations (Table 8, Figure 14b). Event water has a ^{14}C pMC of 104.3, while repeat sampling of waterholes yielded pMC values between 104.4 and 107.4.

Location	^{14}C pMC	error ±	^{3}H TU	error ±
Modern Gastropod	108.5	0.38		
Event water	104.3	0.34	2.6	0.1
Goonbabina WH a	107.4	0.52	2.1	0.1
Goonbabinna WH b	104.4	0.45	2	0.1
Goonbabinna WH c	106.4	0.34	3.2	0.1
Noccundra WH	-	-	-	-
Little G WH	-	-	-	-
Naccowlah WH	-	-	-	-
Lous WH	-	-	-	-
G2	115.1	0.51	1.5	0.1
G3a	106.5	0.5	> 0.3	0.1
G3b	107.1	0.53	0.5	0.1
G3c	107.7	0.4	0.5	0.1
G4a	93.9	0.62	> 0.1	0.1
G4b	87.0	0.32		
G4c	89.9	0.31	> 0.1	0.1
N1	108.5	0.52		
G1a	84.2	0.39	> 0.2	0.1
G1b	83.6	0.32	> 0.1	0.1
G1c	89.1	0.32	0.7	0.1
G7	112.7	0.37	1.07	0.08
N2	96.2	0.32	0.6	0.1
G5	111.6	0.35	1	0.1
G6	94.5	0.32	> 0.18	0.09
L1	101.7	0.38	0.5	0.1

Table 8. Same as Table 7, but for radiogenic isotope data (^{14}C and ^{3}H).

The modern gastropod shell we collected is very close to modern atmospheric ^{14}C at 108.53 pMC, and suggests this average is a good estimate of the range of modern

flood water ^{14}C concentrations, and that there is no noticeable reservoir effect. ^{3}H concentrations above the detection limit (~0.7 TU) are only present in surface waters and proximal groundwaters (Figure 14b), with the highest concentrations found in the waterholes, which in turn rapidly falls below the detection limit with increasing distance from Goonbabinna and Naccowlah waterholes. In contrast, there is a well-defined linear decline in ^{14}C with increasing distance from the nearest channel, or waterhole, with the exception of ^{14}C from wells G1 and G4 (Figure 14c). Despite this linear trend, given the large variations in major ion chemistry, as well as the co-variance of ^{14}C and ^{3}H, it seems that most of the samples < 100 pMC are the result of very low infiltration fluxes that mix with older (lower 14C concentration) groundwater upon arrival at the water table. The outliers in this mixing trend are from wells G1 and G4, which are both near Goonbabinna Waterhole; G1 groundwater is within lower hydraulically-conductive sediments (6.23 x 10^{-4} m / day), and G4 is from a deeper position within the aquifer. G1 also has the lowest ^{14}C concentrations found in the shallow aquifer and, if this is purely the result of radioactive decay, then the groundwater age (τ_{rad}) is equivalent to

$$\tau_{rad} = \ln\left(\frac{C_A}{C_{GF}}\right) \lambda^{-1} \qquad (3)$$

which gives an age of 1435 ± 30 BP. For the high TDS regional groundwater the oldest groundwater age is from well G6 at 455 ± 30 BP. Using Equations (1) and (2) this age implies that R_n < 0.1 %, such that short term variations in C_A have a negligible impact on C_{GF}, and if we assume shallow mixing depths (D = 0.1 - 0.5 m) thus yields recharge rates for G6 of < 1 mm/yr.

^{14}C concentrations are also known to be easily modified by dilution from inorganic or organic carbon in the aquifer matrix, methanogenesis, or even migration of geothermal CO_2 (Clark and Fritz, 1997), of which the latter two processes can be easily excluded. The question of matrix carbon is more difficult, however, on the basis of the $\delta^{13}C_{DIC}$ results and calcite saturation, there is no strong evidence of dilution from radiogenically deficient carbon sources in most samples analysed here, since groundwaters super-saturated with respect to calcite do not exhibit ^{14}C or depleted $\delta^{13}C_{DIC}$ concentrations lower than would already be expected given their distance from a waterhole or TDS range. However, any recharge occurring via an unsaturated zone will most certainly dissolve some proportion of older inorganic

carbon already present in the profile, and the degree to which this has affected ^{14}C concentrations needs to be estimated. Using unmodified pMC values our estimation of recharge rates for G6 appear consistent with very low mixing and reflective of long term average atmospheric ^{14}C concentrations, however, for G1 and G4 the same method would result in much lower recharge rates. In the case of G4, the deeper position suggests the lower pMC concentration is the result of mixing with waters increasing in age with depth. However, the shallow nature of G1 and its close proximity to Goonbabinna Waterhole suggests that this pMC concentration could be affected by mixing with older carbon. If we assume a 10% dilution effect, using Equations (1) - (3) then a new τ_{rad} of ~ 430 yrs BP, which is broadly consistent with that of G6, can be estimated. The remaining pMC concentrations can therefore be interpreted as the product of mixing between very low recharge regional groundwaters (well G6) and higher recharge rates closer to some parts of the channels (e.g. G2, G5, G7).

3.7.4 Model ^{14}C and ^{3}H recharge and renewal

The interpretation of groundwater ^{14}C concentrations that are the product of higher recharge rates, and are therefore influenced by post-1955 atmospheric nuclear testing remains difficult, since it is not a closed carbon system which, as with all groundwater radiocarbon interpretations, renders the use of calibration curves inappropriate. Instead, we can combine Equations (1) and (2) and examine the predicted concentrations of ^{14}C and ^{3}H with increasing recharge and mixing rates, as well as changes in assumed mixing depth, at the end of the model period (2007; Figure 15). An obvious contrast is the effect of λ on predicted ^{14}C and ^{3}H concentrations, whereby a high λ with increasing R results in unique estimates of ^{3}H at distinct D values, while a very low λ produces overlapping and non-unique estimates of ^{14}C for changing D. We also note that increasing recharge above ~37 mm/yr converges ^{14}C values to the modern atmospheric concentrations at shallow mixing depths (0.5m), and with the remaining range of D values also converging on modern atmospheric ^{14}C concentrations depending on R, with rates above ~500 mm/yr converging all groundwater ^{14}C model concentrations with modern atmospheric ^{14}C, regardless of mixing depth. Below 37 mm/yr, R_n is generally less than 10%, and the resultant ^{14}C concentrations are largely insensitive to D.

The predicted ^{3}H and ^{14}C concentrations from Equations (1) and (2) can be used to constrain a realistic range of recharge rates from the measured concentrations in groundwater samples with ^{3}H above the detection limit, and with ^{14}C pMC concentrations above modern atmospheric values, or 'bomb-pulse' ^{14}C in wells G2, G5, and G7 (Figure 14b,c). If we only consider those ^{14}C based recharge rate estimates derived from the ascending limb of the depth curves so as to avoid non-unique estimates (Figure 15a), then estimated recharge rates (mm/year) can be estimated (Table 9).

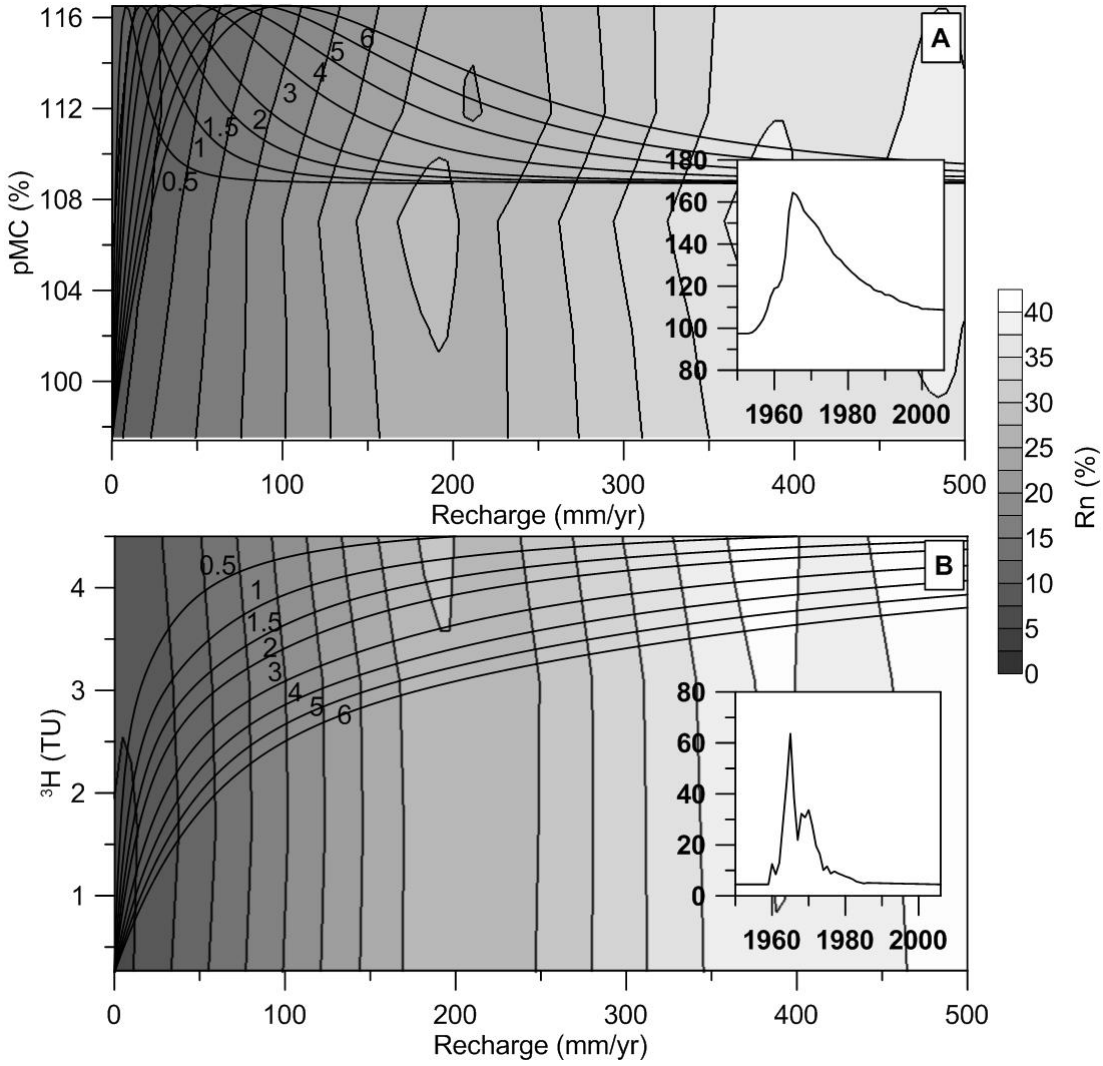

Figure 15. The relationship between recharge (R), R_n, and (a) predicted ^{14}C, and (b) predicted ^{3}H groundwater concentrations at the end of the model period (2007). Black lines and corresponding numbers represent equivalent changes in aquifer mixing depths (D, m). Inset figures are the atmospheric input (C_A) for the period 1950-2008 for (a) ^{14}C and (b) ^{3}H.

We note that in each case, the bomb-pulse ^{14}C recharge rate estimates are higher than the ^{3}H estimates, however, the differences in recharge rates between wells are consistent and suggest higher average recharge rates below the main channels (30.8 ± 16.1 – 41.4 ± 24.4 mm/yr) than the smaller floodplain channels (8.3 ± 5.2 – 18.4 ± 7.4 mm/yr), which is compatible with the major ion and stable isotope data, and also much greater than recharge beneath the floodplain (< 1 mm/yr).

	Recharge rate (mm/year)	
Well	^{3}H	^{14}C
G2[a]	30.8 ± 16.1	41.4 ± 24.4
G5[a]	8.3 ± 5.2	18.4 ± 7.4
G7[a]	8.3 ± 5.2	22.6 ± 5.7
G6[b]		< 1

Table 9. Estimated recharge rates constrained from observed and modelled ^{3}H and ^{14}C concentrations. [a] Recharge rates calculated using Equations (1) and (2) are reported as averages, and the errors are standard deviations. The analytical uncertainty on each ^{14}C and ^{3}H concentration, for each modelled depth (0.5 – 4m), was used as the input range. [b] Recharge rate calculated assuming constant atmospheric pMC, R_n > 0.1%, and D 0.1-0.5 m.

3.8 Implications

3.8.1 Recharge pathways and geomorphic controls

On the basis of variations in the major ion, stable and radiogenic isotope compositions, and estimated recharge rates, we identify three distinct recharge pathways (Figure 16): 1. temporarily connected recharge via some sections of *large channels*, 2. disconnected recharge via *small channels* during large events, and 3. diffuse and/or large event recharge via *floodplain mud-cracks*. The first pathway is distinguished on the basis of the reduced O_2 conditions, low TDS concentrations, and higher estimated recharge rates. The persistence of reduced oxygen conditions via organic matter decay requires at the very least an occasional hydraulic connection with the stream bed DOC, which the $\delta^{13}C_{DIC}$ trends demonstrate is the source of the organic matter, thus the development of any unsaturated zone must either be temporary or thin enough to allow the survival of DOC transport, which is otherwise easily consumed via diffusion of atmospheric O_2 (Appelo and Postma, 2005). The highest ^{3}H and ^{14}C concentrations and resulting recharge rates are also beneath a section of the largest channel, which further supports the case for relatively well connected conditions between the surface and shallow groundwater at this location.

The increase in TDS and dissolved oxygen, decrease in ^{14}C and ^{3}H, and slight enrichment in $\delta^{13}C_{DIC}$ with increasing distance from the large channel can be interpreted as the result of advective mixing with regional groundwaters, and thus marks the lateral limit of recharge via this pathway.

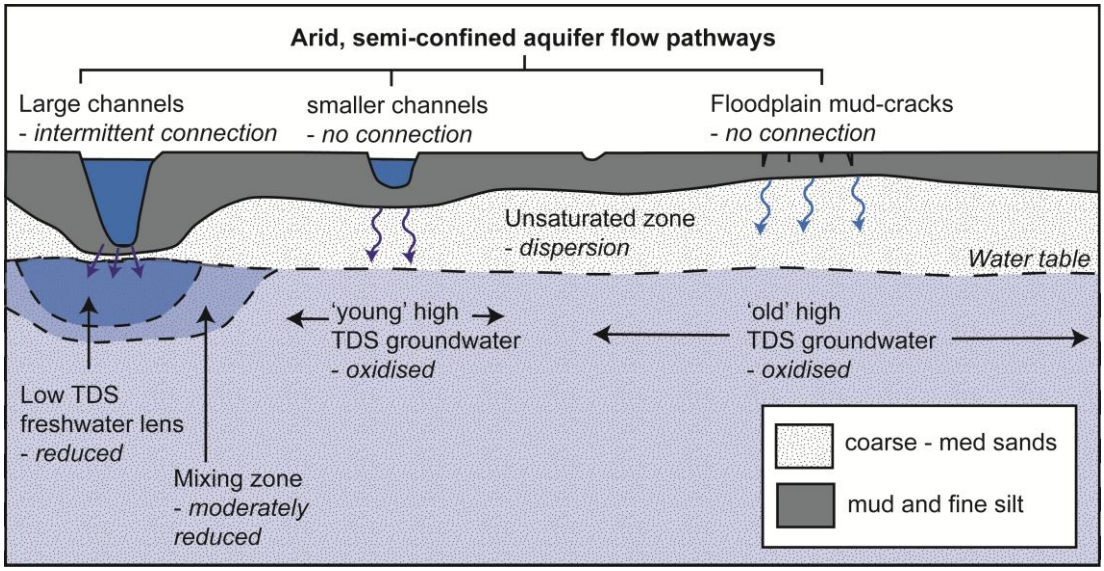

Figure 16. Conceptual illustration of the preferential recharge dominated recharge processes in the semi-confined aquifer system of Cooper Creek. The stratigraphic contrasts are given as homogeneous mud (dark grey) and coarse-fine sand (stippled) only, and are likely to be more variable in most cases. The water table and aquifer (dashed line, and light blue area) are not likely to be directly connected to the stream beds, even under the largest channels. However, the presence of low TDS and reduced groundwater beneath some sections of these large channels (darker blue) indicates this connection must be persistent enough to enable the survival of organic matter during recharge to the water table. Away from these fresh groundwater 'lenses', a mixing zone develops (intermediate blue) with the highly saline regional groundwater. This regional groundwater has developed high salinity via dispersion and fractional leaching in an unsaturated zone of variable thickness, however, this can occur at much higher rates beneath the smaller channels, presumably during large flood events, while the rate of recharge through the broader floodplain surface is likely to always remain low.

The second recharge pathway, via smaller floodplain channels, has a permanent unsaturated zone with occasional losses beneath the channel during large flow events. Transport of recharge water via the unsaturated zone explains two observations: 1. the development of higher TDS in regional and intermediate groundwater, whereby the unsaturated zone stores solutes through dispersion which is then fractionally leached during the passage of large events either via preferential

flow paths or as a wider pressure front. 2. The loss of organic matter, and the maintenance of oxidised groundwater conditions, which is most likely the result of atmospheric O_2 being more readily supplied relative to DOC in larger unsaturated zones (Appelo and Postma, 2005). A key distinction between this and the third pathway is the ability of larger events to provide a higher recharge flux to the aquifer despite the presence of a 5 – 10 m unsaturated zone, as indicated by the ^{3}H and ^{14}C data and the resultant recharge estimates (8.3 – 22.6 mm/yr).

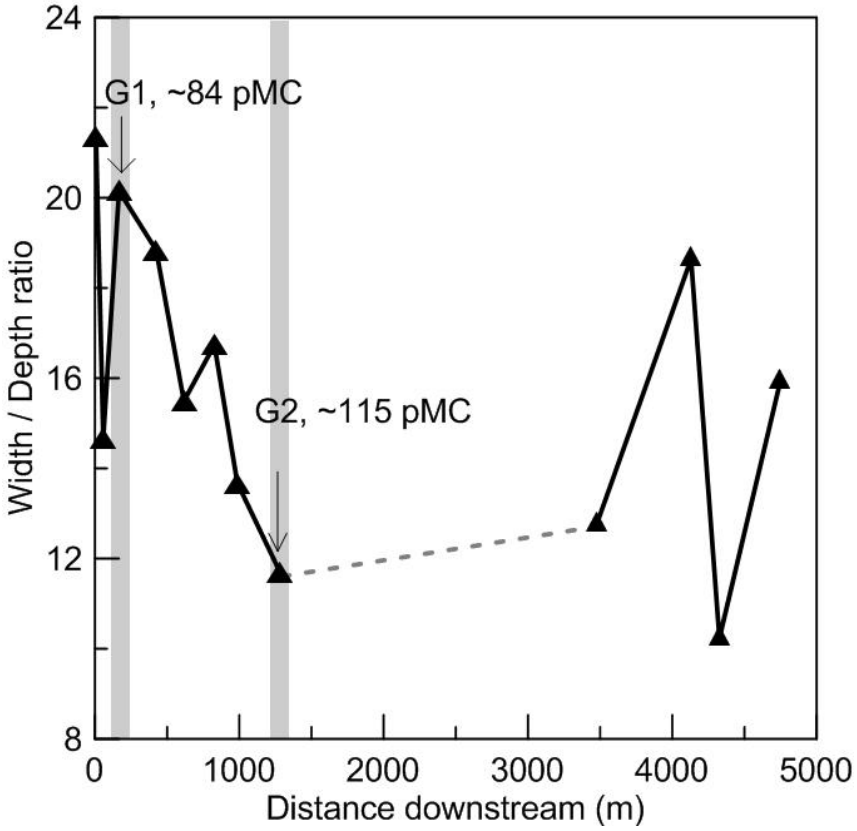

Figure 17. Changes in the bankfull width/depth ratio with increasing downstream distance in Goonbabinna Waterhole. The position of the G1 and G2 peizometeres and their respective ^{14}C pMC concentrations are also shown.

The difference in recharge rates between the first two pathways is interesting, and we propose that this is the result of geomorphic contrasts between the large and small channels. The former is entrenched deeper into the underlying sand body and is comprised of a much thinner deposit of mud on the bed that can be effectively transported as sand-sized mud pellets during most flow events or alternatively in suspension as individual grains (Maroulis and Nanson, 1996). The removal of this mud seal significantly increases the channel bed hydraulic conductivity during

floods. In contrast, smaller channels require more exceptional flow events to scour the mud base, or to provide sufficient infiltration through the presence of a low conductivity clogging layer. Such contrasts in channel size explain variations in recharge along the reach of Goonbabinna Waterhole, such that where the channel is wide and shallow (high bankfull width/depth ratio) the groundwater has the lowest ^{14}C concentrations (well G1), and as the channel becomes much deeper relative to its width recharge occurs via the first, and more effective pathway (Figure 17).

The final recharge pathway we identify occurs via preferential flow through the mud dominated floodplain surface, with many processes similar to the second pathway, except for the persistence of much lower average recharge rates (< 1 mm / yr). The development of desiccation cracks in the floodplain surface promote preferential flow during the initial stages of flooding, or during direct rainfall events, and are the only mechanism by which infiltration to the sand dominated unsaturated zone could effectively occur. The presence of the most depleted $\delta^{18}O$ and $\delta^{2}H$ groundwater values also suggests that only exceptional flood events, or direct precipitation on the floodplain surface similar in $\delta^{18}O$ and $\delta^{2}H$ to large rainfall events at Alice Springs, are responsible for groundwater recharge along this flow path. If infiltration via mud desiccation cracks is sufficiently rapid, then the long travel times through the sandy unsaturated zone below can occur largely unaffected by evaporative enrichment due to the presence of the surface confining layer, and thus preserving the depleted $\delta^{18}O$ and $\delta^{2}H$ composition. This is also supported by the similarity of the relatively enriched $^{13}C_{DIC}$ composition of the regional groundwaters to the surface water $^{13}C_{DIC}$, which is in contrast to the more $^{13}C_{DIC}$ depleted proximal groundwaters recharged via specific sections of large channels (first pathway).

3.8.2 Recharge probability

Large transmission losses are prevalent in most dryland river systems, however, their relationship to actual recharge rates remains difficult to constrain [e.g. *Dahan et al.*, 2008]. In the simplest case, for relatively shallow groundwater systems the water balance can be written as

$$TL = R - ET \qquad (4)$$

where ET is total evapotranspiration, either directly from the water surface or including the unsaturated zone. Although evaporative losses of actual discharge have

been shown to be minimal in the study area (Larsen et al., submitted), losses from the unsaturated zone via tree uptake are also undoubtedly a significant component of the water budget in these dryland floodplain environments (Costelloe et al., 2008). However, for the purposes of recharge analysis, and in the absence of the requisite evaporation data, we reduce Equation (4) to examine under what conditions $TL \approx R$.

As previously mentioned, the mean annual transmission loss for all events is 18.9 mm, however, given the large standard deviation (23.1 mm/yr) and multiple potential recharge pathways already described, the mean may not be a useful indicator of recharge occurrence in dryland environments. Inspection of the probability distribution (PDF) of the transmission loss data from Figure 11 shows an expected high magnitude tail (Figure 18a), however, the log of this distribution (logTL), appears bimodal in the low magnitude range (Figure 18b). A Q-Q plot of the logTL data shows that very low transmission losses (< 5 mm/yr), which are also coincident with very low flow events (Figure 11), are likely to be part of a separate distribution of flow events. Modelling studies have also demonstrated that very low transmission losses exhibit distinct flow behaviour, and in any case are likely to contribute little to overall groundwater recharge (Lange, 2005; Nanson et al., 1986). Removing very low transmission losses results in a similar PDF (Figure 18d), however, the log-transformed PDF now reveals slight skewness to high magnitude events, as would be initially expected from the original distribution (Figure 18e). Although the Q-Q plot of the > 5 mm/yr dataset does not fit a log-normal distribution perfectly at the very lowest and very highest losses (Figure 18f), it demonstrates that the bulk of the transmission losses are probably the result of many different loss rates multiplied together, which forms the basis of log-normally distributed populations. The slight deviation of high magnitude events from the log-normal distribution occurs only for losses > 40 mm/yr, suggesting that beyond this point, some threshold in loss mechanisms within this large alluvial system are exceeded.

If we consider the probability of transmission losses, with a mean of 18.9 ± 23.1 mm/yr, or the modified (> 5mm/yr) dataset mean of 23.2 ± 23.7 mm/yr, to be related to the sum of the probabilities of recharge occurring via the three recharge pathways outlined in section 3.8.1, then our understanding of the relationship between TL and R is much easier to explain. The probability of recharge via the larger channels is high for all but the smallest events, and in this case $R \propto TL$ and flood duration

(Dahan et al., 2008). On the other hand the probability of recharge via smaller channels is low unless transmission losses are high, however, the total rates remain comparatively lower. This may also partly explain the ~ 40 mm/yr threshold in transmission losses, above which the logTL distribution deviates from log-normal, and may therefore indicate the onset of recharge via this pathway.

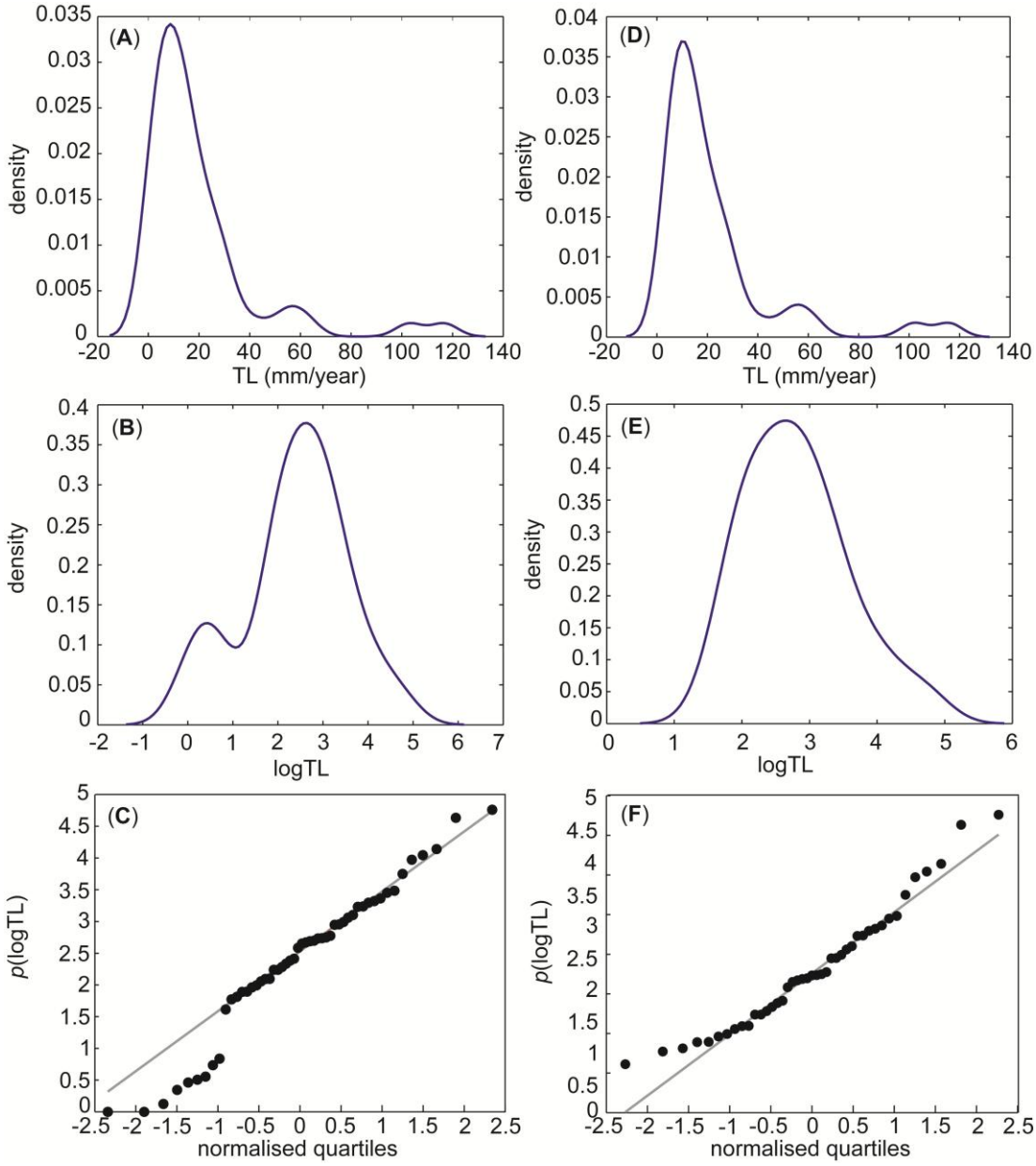

Figure 18. Probability distribution functions (PDF) for raw transmission loss (TL) data (a), and modified (> 5mm/yr) TL data (d). (b) and (e) are the log transformed (logTL) data of (a) and (d) respectively. (c) and (f) are normalised Quantile – Quantile (Q-Q) plots of the logTL data from (b) and (e) respectively.

Meanwhile a low probability of recharge for regional groundwater can be expected to remain relatively constant, because significant rainfall and event variability would be strongly dampened by diffusion and slow transport through the unsaturated zone. The role of antecedent conditions are also important in this respect, since we expect dry periods to facilitate recharge via desiccated mud pathways, and this may explain the faster increase in transmission losses as a function of discharge during these periods (Figure 11b). In contrast, we expect wetter conditions, and large flood events themselves, to be restrictive of this mechanism of recharge as the clay rich floodplain will swell and largely block infiltration, as has been demonstrated in other mud-dominated floodplains in Australia (Jolly et al., 1994).

3.8.3 Implications for groundwater salinisation

The development of high salinity groundwater in a dryland alluvial context has often been attributed to evaporative processes acting upon the shallow groundwater table directly (Cartwright et al., 2004; Herczeg et al., 2001; Lamontagne et al., 2005), bottom leakage from semi-confined, higher salinity groundwater and subsequent mixing with the shallow aquifer (Cartwright et al., 2007; Dogramaci and Herczeg, 2002), or extensive water-rock interaction if a fractured rock system is juxtaposed with, and receives recharge from, the alluvial one (Nativ et al., 1997). In the semi-confined system studied here, however, the surface confining layer and the promotion of at least three distinct recharge pathways has determined the spatial pattern in salinity and water quality, with the high salinity groundwater largely the result of preferential flow through the confining layer, dispersion in the unsaturated zone, and subsequent partial leaching of salts by sporadic recharge events which then reaches the shallow water table at very low rates (< 1 mm/yr). This is consistent with recent experimental results which demonstrate that although the percolation of flood water through the unsaturated zone results in solute leaching, this is normally incomplete, and over time provides a viable mechanism for the increase in salt stores within the unsaturated zone of alluvial dryland environments (Amiaz et al., 2011).

In contrast, higher recharge rates beneath the large channels has resulted in the development of fresh groundwater lenses, and although this has not transmitted the low TDS groundwater laterally for any significant distance beneath the floodplain, it does promote the development of intermediate groundwater chemistry through

advective mixing within 50-70 m of the large channels. Thus although unconfined aquifers in dryland environments display good evidence for the evaporative concentration of groundwater solutes (Tweed et al., 2011), the large extent of semi-confined alluvial aquifer systems, particularly in the LEB, suggests that salinisation in this setting requires some combination of preferential recharge processes described here. Moreover, the co-existence of relatively low TDS groundwater, the location of which is largely determined by channel geomorphology, is a crucial determinant of any available water resources from semi-confined aquifers within severely water limited environments.

3.9 Conclusions

The groundwater from a shallow semi-confined aquifer system of Cooper Creek in the arid to semi-arid Lake Eyre Basin exhibits marked changes in salinity and water quality with increasing distance from waterholes, however, the exact recharge pathways and mechanisms controlling these changes are not straightforward. We identify three main recharge pathways: 1. via large channels where the base can be easily scoured, 2. via smaller channels, and probably only during exceptional flood events, and 3. through desiccation cracks on the mud floodplain surface. Each of these pathways is distinguished on the basis of tracer (^{14}C and ^{3}H) derived recharge rates, major ions and stable isotopes, and redox chemistry. The first two preferential pathways are largely determined by channel morphology, and the last by antecedent conditions, which in turn explains variation in the large transmission losses along this section of Cooper Creek. Given the dominance of preferential flow pathways, our mean recharge rate estimates probably do not capture the true nature of recharge fluxes in this environment, and we instead suggest that recharge be considered in terms of probability. These results also have implications for the development of saline groundwater systems, since in this study it appears that surface evaporation plays a very minor role because of protection from confining layers, and that slow dispersion and fractional leaching in the unsaturated zone in the absence of isotopic enrichment appears to be the best explanation, and a process not commonly documented in dryland environments. It can therefore be concluded that the recharge of groundwaters in semi-confined alluvial settings are likely to be dominated by preferential flow processes, which is important if the water balance of dryland environments is to be determined with a higher degree of certainty.

3.10 Acknowledgements

JRL was supported by a UOW and ANSTO PhD scholarship. This research was funded by an ARC grant to GCN and BGJ, and ANSTO. No water would have been sampled without the expert and dedicated drilling service of Brent Peterson. We are also very much indebted to the field assistance provided by Thomas Gill, Rebecca Jackson, and Luke Morley. Many thanks to SANTOS for providing much needed field and logistical support in often trying conditions. We grateful to the Durham Downs station and Kidman properties for site access. Special thanks to the patience and support of the tritium and radiocarbon lab personnel at ANSTO, in particular Robert Chisari, Allan Williams, and Simon Varley. Gregoire Mertihoz and Martin Andersen provided useful discussions.

4 WAS EVAPORATION LOWER DURING THE LAST GLACIAL MAXIMUM?

4.1 Abstract

A critical aspect of the water balance in Australian palaeoclimatic studies is evaporation. During the Last Glacial Maximum (LGM), lower temperatures have been assumed to facilitate lower evaporation, which in turn is used to explain anonymously 'wet' hydrological conditions within many fluvial and lacustrine records from this time. Here, the evidence for this relationship is briefly reviewed, and examples from modern climates are given to argue for a revision of the role of evaporation in LGM hydrological balances throughout Australia.

4.2 Introduction

In 1965 RW Galloway published the now classic paper 'Late Quaternary climates in Australia' (Galloway, 1965), and ever since this time authors searching for climatic controls on hydrological conditions on the Australian continent during the Last Glacial Maximum (LGM) have embraced the notion of lower evaporation to explain a wide variety of hydrological conditions (Bowler et al., 1976; Coventry, 1976; Kemp and Rhodes, 2010; Singh et al., 1981; Williams et al., 2001). However, despite its ubiquity in the Australian palaeoclimatic literature, the assumption of lower LGM evaporation has never been tested explicitly as a plausible climatic scenario.

Galloway (1965) estimated evaporation during the LGM around Canberra in Australia to be roughly half the modern annual average, and was suggested to be the result of lower temperatures, despite acknowledging the importance of other factors. Lower evaporation was required by Galloway to balance the water budget for Lake George, where a 30m lake level shoreline was inferred to be LGM in age. Subsequent work by numerous authors have also demonstrated good evidence for fairly wet hydrological conditions during the LGM (Haberlah et al., 2010; Nanson et al., 1998; Nott and Price, 1994), although many lakes may have evolved to much drier conditions soon after the LGM (Bowler et al., 1976), however, the timing is not yet conclusive in many of these cases. Nonetheless, for better or worse the notion of lower evaporation during this time has remained.

4.3 Discussion

The case for lower evaporation could be made if the atmosphere were considered in isolation, that is, a colder atmosphere stores less water vapour, and therefore has less evaporative demand. This is a well-established thermodynamic relationship known as the Clausius-Clapeyron curve, whereby the saturation vapour pressure of the atmosphere increases as an exponential function of temperature (Figure 19a). However, since this relationship only describes absolute humidity, the resultant potential and actual evaporation can be considerably more complicated since the vital metric is relative humidity (or vapour pressure deficit), which is the saturation vapour pressure minus the actual (measured) vapour pressure. There are numerous equations to describe evaporation, and in terms of potential (or pan) evaporation, the penman equations are some of the most widely used. A model which uses modifications of these equations in an Australian context has recently been developed which accurately predicts measured pan evaporation rates across the continent (Roderick et al., 2007; Rotstayn et al., 2006). Using this model (PenPan), the Clausius-Claypeyron curve is incorporated into both a radiative and an aerodynamic component, which results in roughly contrasting effects in terms of changing temperature (Figure 19b). Crucial factors in determining evaporation which remain, namely net solar irradiance, wind speed, and the vapour pressure deficit, are therefore more likely to have the biggest impact on evaporation rates. In the modern climate for example, the observed decline in pan evaporation throughout Australia and many other parts of the world over the last ~30 years can be attributed to a decline wind speeds (Johnson and Sharma, 2010; Roderick et al., 2009). Although temperature most certainly plays an important role in evaporation, the simple relationship between temperature and evaporation which is assumed in the Australian palaeoclimate literature since the work of Galloway (1965) needs to be carefully revised.

Another important factor when considering evaporation in the context of water balances is the actual amount of evaporation versus the potential rate. Although the above mentioned equations can accurately describe potential evaporation, it is the relationship between potential and actual evaporation, and also precipitation and actual evaporation, which is crucial for the water balance. If potential evaporation is

greater than precipitation, then the rate of actual evaporation is limited by water supply.

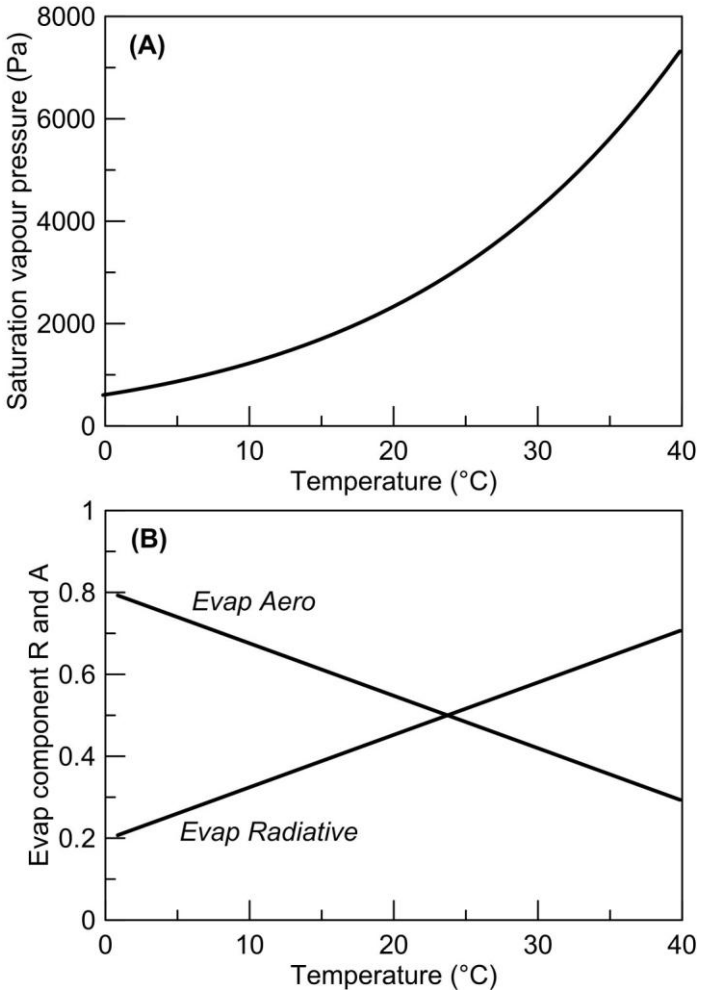

Figure 19. (a) The Clausius-Clapeyron curve for likely range of surface air temperatures throughout Australia during the LGM. (b) Increasing (or decreasing) temperature has an opposing effect on the separate radiative and aerodynamic components of evaporation. Although this does not include the effects of wind speed or vapour pressure on evaporation, it demonstrates that the direct effect of temperature on evaporation is potentially quite small. See Roderick et al., (2007) for a description and derivation of the full equations. Modified from Roderick et al. (2009)

If on the other hand potential evaporation is less than precipitation, then actual evaporation is limited by the amount of energy available for evaporation. Many Australian environments at first glance would be considered water limited, however, many areas of the country likely experience transitions between the two, since it is after all, a country of droughts and flooding rains.

This balance between potential evaporation, actual evaporation, vapour pressure, and precipitation is complicated, and depends on specific climatic forcings (van Heerwaarden et al., 2010).

Nonetheless, many arid and semi-arid areas of Australia display a good negative relationship between increasing precipitation and decreasing pan evaporation, while some semi-arid, and most temperate or tropical regions do not (Figure 20). The reasons for this relationship in arid and some semi-arid areas most likely relates to the fact that wetter years would also have on average greater cloud cover, which in turn reduces solar irradiance and therefore lowers the measured evaporation (Hobbins et al., 2008). Because the vapour pressure deficit is already very large in arid areas, a comparatively small change in other factors such as solar irradiance and wind speed has a proportionately larger effect on evaporation than more humid or tropical climates. The weaker correlations at some arid and semi-arid locations in Figure 20 most likely reflect the contribution of wind speed to total pan evaporation rates at these locations, which is not accounted for in these regressions.

It is important to remember that the measured evaporation in this data is from Class A pan weather stations, which by definition have no limit to their water supply. In reality, the actual evaporation would match this pan evaporation only in humid environments (Brutsaert and Parlange, 1998), or above open water bodies such as lakes and wetlands, whilst in semi-arid and arid climates it would be limited by the ability of the soil to provide water to the open atmosphere or plants, depending heavily on soil properties and antecedent conditions. However, if the local mean annual precipitation is reduced, and water can still be adequately supplied (e.g.: via more regionally supplied runoff in large basins), evaporation above lakes within arid or semi-arid areas could potentially increase, contrary to conditions generally assumed in Australian palaeoclimates.

In addition, the role of vegetation in palaeo-water balances for Australia remains largely unaccounted for. Many pollen studies point to a widespread reduction in tree density during the LGM, which would in turn allow a rise in water tables in many areas of the continent. This may be compensated for in many areas by an increase in actual evaporation from the soil, possibly via an increase in wind speeds if the surface roughness is reduced. If this effect is not uniform, then some areas may

experience an expansion in the area, and possibly rate, of ground and surface water connection, particularly following large storm events.

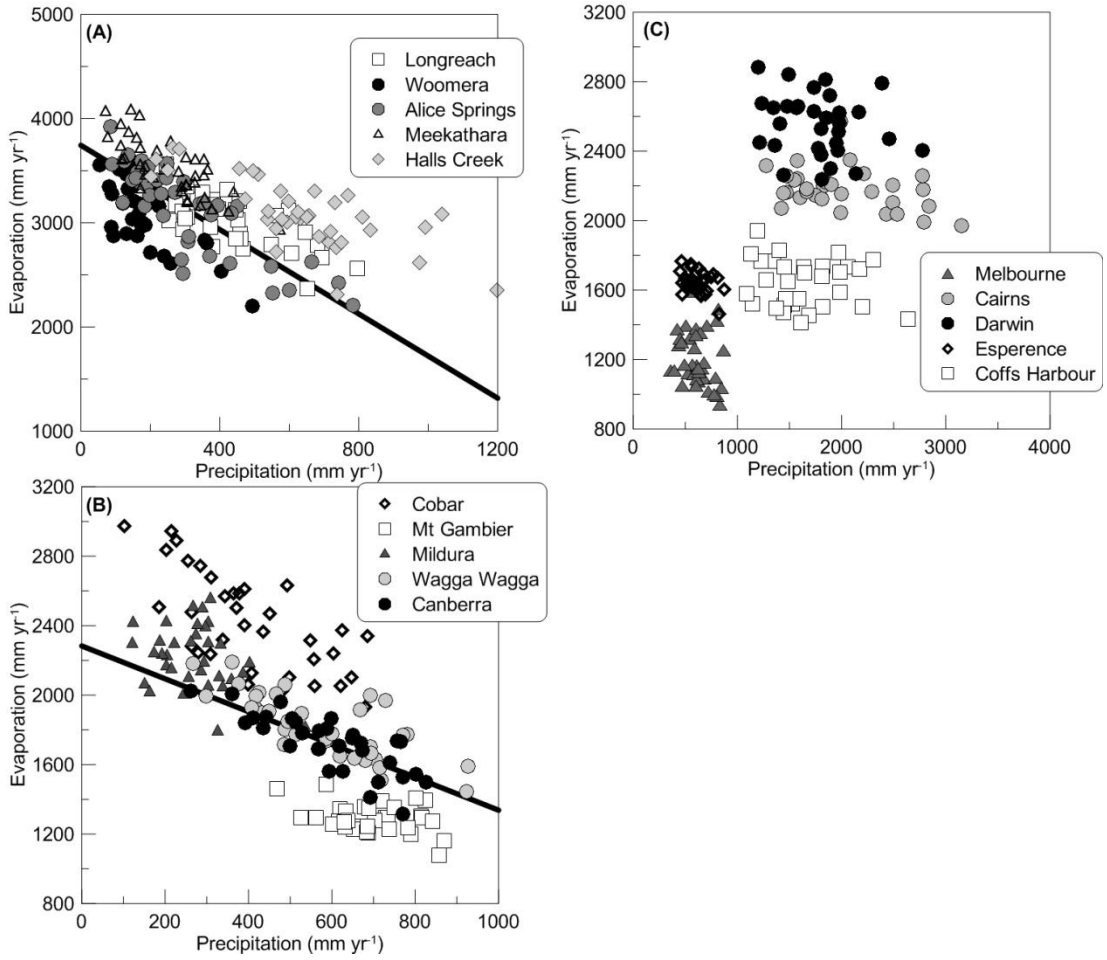

Figure 20. The relationship between total annual evaporation and rainfall as measured by the Australian Bureau of Meteorology at selected sites across Australia for the period 1970 -2009 (where available) for (a) arid, (b) semi arid, and (c) tropical and temperate stations across Australia. All arid stations (a) show good to weak correlations between total annual evaporation and rainfall (Longreach $r^2 = 0.51$, Woomera $r^2 = 0.50$, Alice Springs $r^2 = 0.70$, Meekathara $r^2 = 0.60$, Halls Creek $r^2 = 0.56$), however, only the regression line for Alice Springs is shown ($y = -2.02x + 3743$). For the semi-arid stations (b) only Canberra and Wagga Wagga have good correlations between total annual evaporation and precipitation ($r^2 = 0.62$ and 0.59 respectively, the regression line for Canberra is also shown, $y = -0.95x + 2283$), Cobar has a weak correlation ($r^2 = 0.49$) and Mildura and Mt Gambier display no correlation. All tropical and temperate stations (c) have no correlation between total annual evaporation and precipitation. Note the changes in scale between graphs.

This would also help explain the presence of some anomalously ‘wet’ hydrological conditions during the LGM, and demonstrates that understanding the coupling

between the land surface, atmosphere, and vegetation is crucial if we are to properly interpret glacial climates.

4.4 Conclusions

It is proposed here that the well-established drop in mean annual temperatures during the LGM may not have led to the corresponding drop in mean annual evaporation that researchers have generally assumed since Galloway's influential paper. Many researchers (including Galloway, (1965)) have also assumed and in some cases provided evidence for a decrease in precipitation during the LGM, which if true, would certainly limit the amount of actual evaporation, particularly for the majority of the continent's surface that is not permanently wet. However, for wet surfaces such as wetlands or lakes, whose palaeo-records are used to infer P/E conditions during the LGM, there is no *a priori* reason to suspect that evaporation would have been any lower. In addition, more recent studies suggest that strong, episodic precipitation could explain some apparently enhanced LGM pluvial conditions such as high lake stands, without the need for lower evaporation (Haberlah et al., 2010).

These conclusions highlight the lack of a robust conceptual model for LGM hydrological conditions, since precipitation and evaporation are almost always considered to be uniformly lower, and the role of vegetation is rarely considered. The difficulty of course is quantifying precisely how much, and for how long, these processes impact the terrestrial water balance. Nonetheless, greater flexibility in explaining P/E relationships and the overall water balance from LGM climate records, and not simply assuming lower evaporation, is clearly required of further research.

4.5 Acknowledgements

Support for JRL was provided from a UOW PhD scholarship, and an ANSTO postgraduate award. Many thanks to Michael Roderick for useful suggestions, and to Gerald Nanson and Dioni Cendón for constant support, and supervision. David Haberlah and an anonymous reviewer are thanked for their detailed comments and suggestions which greatly improved the paper.

5 QUANTIFYING CHANGES IN THE HYDROLOGY OF THE LAKE EYRE BASIN THROUGHOUT THE LAST ~130 000 YEARS

5.1 Abstract

Variations in the water resources within the Lake Eyre Basin of arid to semi-arid central Australia over the Late Quaternary are known to have been large, however, the distribution of this water within the basin and an actual quantification of these changes largely remain elusive. The supply of runoff to the terminal lake system of the basin, of which Lake Eyre and Lake Mega-Frome (a combination at ~10m depth of Lakes Frome, Callabonna, Blanche and Gregory) are the largest, is a critical aspect and here we demonstrate that Strzelecki Creek, a distributary of Cooper Creek, has a valuable Late Quaternary alluvial record which corresponds broadly with the shoreline record of lake high stands in the Mega-Frome system at its terminus. This confirms that substantial runoff was supplied from the northeast headwaters of the catchment during lake high stand phases, including the last full hydrological connection between Lake Mega-Frome and Lake Eyre. In combination, these two lakes when full represented the two largest interconnected bodies of standing water able to be maintained on the Australian continent in the past 50 ka. An accurate hydrological comparison of the two lakes is made by comparing the depths at which their volumes were equivalent. This reveals that Mega-Frome will fill and most likely overflow to Eyre while the same volume of water in Eyre will produce a very much lower lake level. Although the changes in lake level are not necessarily a good hydrological comparison, it is clear from changes in lake volume that large changes in lake inflow relative to the present are required to produce those levels recorded for the Late Quaternary. Assuming that the maintenance of such lakes has to be consistent with the water and energy balance between the land and the atmosphere, a simple framework comparing the basic catchment climate and hydrological parameters as ratios (potential evaporation / precipitation, and evaporation / precipitation) with the lake and catchment area ratios is developed, and shown to be consistent under modern climatic conditions. In order to apply this to the high stands in the Late Quaternary record, the sensitivity of the catchment conditions and major water fluxes (runoff and evaporation) to likely changes in precipitation and potential evaporation is examined. This illustrates that changes in potential evaporation have little effect compared to precipitation; the latter is always the

limiting factor. As a result, the change in precipitation relative to the modern mean required to maintain the largest recorded lake volume for Lake Frome is an increase of only ~ 9 %, while the corresponding change required to maintain the largest volume for Lake Eyre is an increase of ~ 27 %. Whilst the biggest impact on the water balance due to these changes is in terms of actual evaporation back to the atmosphere, the relative changes in runoff are also very large (22 – 55 % and 70 – 88 %, respectively) and demonstrate the hydrological sensitivity of arid and semi-arid climates to small changes in catchment forcings. These results have large implications for the interpretation of Late Quaternary climate, the role that human impact may have had on the landscape, and the role of climate change in the extinction of Australia's megafauna. Each of these contentious issues have previously been assessed by examining changes in climate in a qualitative way and this approach largely overlooked the non-linear feedbacks between climate and hydrology.

5.2 Introduction

The oscillation of surface water resources within Australia, currently the driest inhabited continent on earth, is an important phenomenon of the modern climate and hydrology. Evidence from a variety of sources indicates this oscillation was perhaps even more dramatic throughout the Late Quaternary (Bowler et al., 1976; Kershaw and Nanson, 1993; Williams et al., 2009), especially within the centre of the continent where the current salt dominated terminal lake system of the Lake Eyre Basin experienced large changes in the supply of fresh surface water (Bowler, 1986; Cohen et al., in press; Hesse et al., 2004; Magee et al., 2004; Nanson et al., 2008; Nanson et al., 1992).

These changes oversaw the arrival of humans on the Australian continent (Bowler et al., 2003; Roberts et al., 1994), the extinction of the large marsupial megafauna (Miller et al., 2005b; Roberts et al., 2001), and the decline of many inland river and lake systems to their current state (Cohen et al., in press; Magee et al., 2004; Nanson et al., 2008). Despite this dramatic environmental context, the actual magnitude of climate change responsible for the increase or decrease in runoff and lake size has never been addressed. Instead, the interpretation of evidence for larger rivers or expanded lakes is couched in terms of potential moisture sources and the re-arrangement of broad synoptic trends (Cohen et al., in press; Shulmeister et al., 2004;

Turney et al., 2006; Williams et al., 2009), which by implication have a changing degree of effectiveness attached to them. This is in contrast to modern hydrology, in which the effect of changes in precipitation or other climatic forcings on surface water resources are the subject of intense scrutiny and debate (Budyko, 1974; Dooge, 1992; Nêmec and Schaake, 1982; Roderick and Farquhar, 2011). The requisite tools now exist to examine palaeo-hydrological change within a consistent catchment water and energy balance.

This chapter seeks to combine both approaches in an effort to clarify and progress the debate surrounding the actual quantity of water available to rivers, lakes and plants over the last ~130 000 years, which until now has been addressed only qualitatively on the basis of comparisons of proxy evidence. The first section investigates the potential for, and timing of, discharge transmitted from a northerly source in the headwaters of the Lake Eyre basin, via a previously un-investigated route along Strzelecki Creek to the terminal lake system that includes Lake Frome. This rich fluvial record is then compared with the record of lake highstands from Lake Eyre and Lake Mega-Frome, and it is demonstrated that although the records are broadly consistent in timing, the hydrological requirements for high lake stands on Mega-Frome are small compared to those for Lake Eyre. A simple water and energy balance framework for the modern climate, hydrology, and lake areas is then presented, which is shown to be internally consistent, and suggests the method is robust and can be easily applied to past lake changes. Using estimates of lake area ratios, the aridity index, and other catchment parameters, the effect of a change in mean climate conditions upon the surface water resources of the basin is quantified, and demonstrates these climates need not be so extraordinarily different to the present in order to effect large changes in the water balance of the interior of the continent.

5.3 Regional setting

5.3.1 Geography, climate, and hydrology

The LEB is an internally draining basin covering ~1/7th of the centre of the Australian continent, with a large northern drainage system feeding a series of terminal lakes at the southern end of the basin (Figure 21). At -15m at its deepest point, Lake Eyre itself is the lowest point in the basin and in Australia, and receives

flood waters from the Australian summer monsoon mainly via the Georgina-Diamantina catchments.

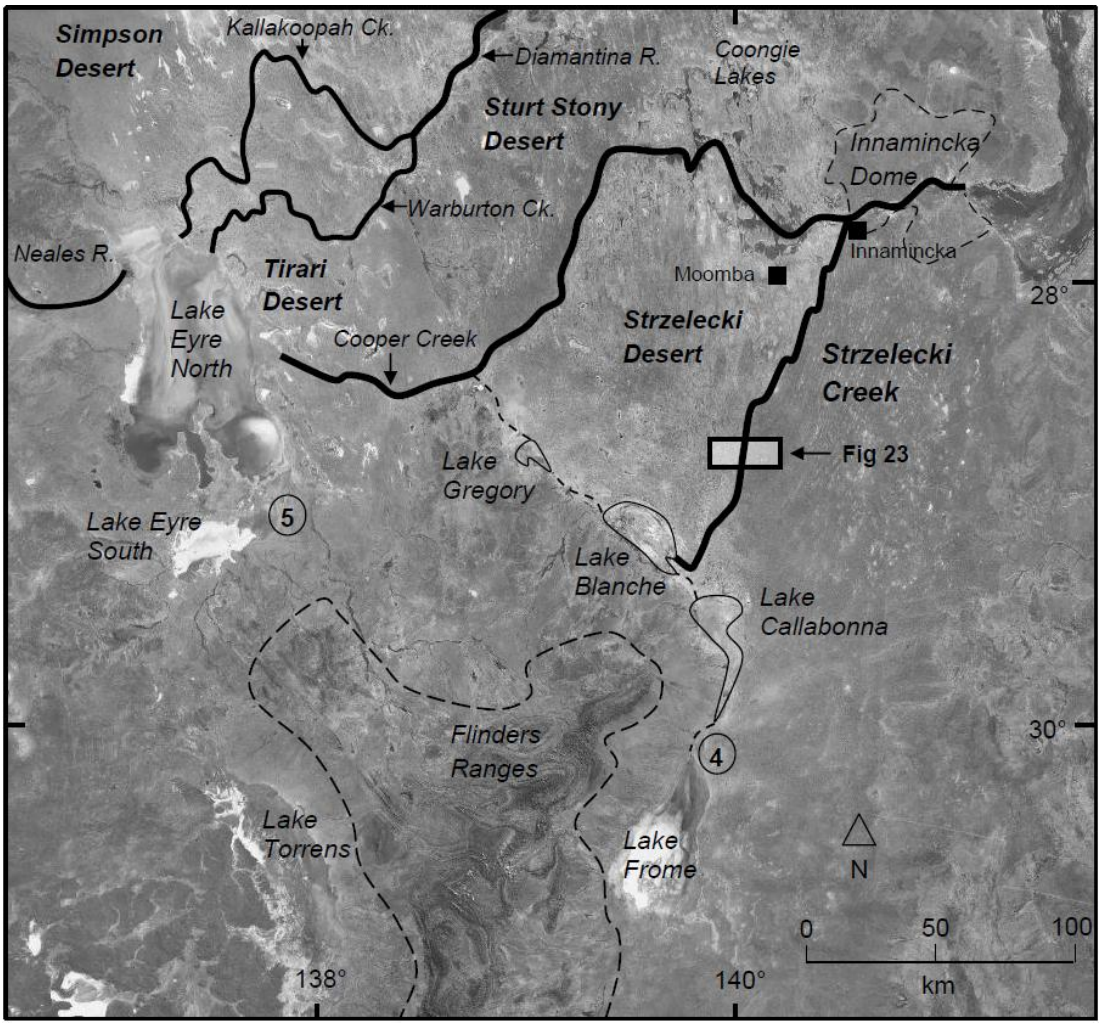

Figure 21. The lower Lake Eyre Basin, which shows the major river networks that supply the terminal lake systems. Strzelecki Creek begins near Innamincka and flows south to Lake Blanche, with the location of stratigraphic and chronological investigated in Figure 23 also shown. The Flinders Ranges is the only other source of runoff for the Lake Mega-Frome system, with all other drainage flowing to Lake Eyre.

The Cooper Creek catchment is also able to supply runoff to Lake Eyre, however its tortuous path through the Strzelecki Desert means transmission losses capture almost all the flood waters in the contemporary setting, although there is considerable evidence for the direct supply of runoff at various times in the Late Quaternary (Nanson et al., 2008). Lakes Gregory, Blanche, Callabonna, and Frome form an arc of terminal lakes around the northeastern edge of the Flinders Ranges, with Lake Frome being the largest (Figure 21). In the Quaternary, when their water achieves

depths great than ~10m, these fours lakes have coalesced into a single large lake, termed Mega-Frome. When Mega-Frome has filled to in excess of ~16m, it has overflowed into Cooper Creek and Lake Eyre. In combination, when full, these two lakes represented the two largest interconnected bodies of standing water able to be maintained on the Australian continent in the past 50 ka.These lakes today rarely contain significant surface water, although Strzelecki Creek provides a pathway for floodwaters from the Cooper Creek system to flow down the eastern edge of the Strzelecki Desert to Lake Blanche, which it has done several times in the historical record. The Flinders Ranges provide the only other source of runoff.

McMahon et al. (2008a) demonstrated that the rainfall in the LEB is dominated by long periods of dry conditions followed by long periods of wet conditions, and that both these trends are longer than what would be expected from a random rainfall distribution. The length of these trends is also longer in the north of the LEB, and although there is no consistent dominance of trend length in the catchment, there is a strong bias towards dryer trends or droughts. Moreover, such a bias is not consistent with the timescales of ENSO, suggesting other mechanisms such as the inter-decadal pacific oscillation (IPO), are controlling the drought dominating conditions (McMahon et al., 2008a). Nonetheless, the mechanisms of large rainfall events are clearer, since they are controlled by the incursion of summer monsoon troughs into the basin, which themselves are generally more intense during wet phases of ENSO (Kotwicki and Allan, 1998a).

5.3.2 The alluvial record of Strzelecki Creek

Prior flow regimes have been assessed in the LEB on the basis of how laterally extensive are the alluvial sequences that remain (e.g. Nanson et a., 2008). So as to assess changes in the Quaternary flow regime to Lake Meg-Frome, a series of large ~5-6 m deep pits were excavated with a large tracked-excavator into Strzelcki Creek’s floodplain and adjacent terraces and dunes (Figure 23). Whereas the present creek is small with a barely-defined channel, there is clear evidence from these exposures that it was a much more powerful and laterally active system feeding the Lake Mega-Frome system at certain times in the past, and forms the first part of this investigation.

5.4 Field sampling and laboratory methods

Fluvial sediment samples for optically stimulated luminescence (OSL) analysis were collected using light-proof steel tubes hammered into freshly excavated pit faces. Sealed samples for the determination of the environmental dose rate and water content were also collected from the same exposure. Care was taken to ensure mottled layers or any layers with evidence of iron mobilisation were not sampled, so as to avoid potential dose-rate disequilibrium. In addition, samples were taken exclusively from layers composed of at least ~ 0.5 m thick coarse to fine sand fluvial bodies, and therefore without significant proximity to fine sediment deposits which may contribute different dose rates to the sample than those estimated from the sand samples alone.

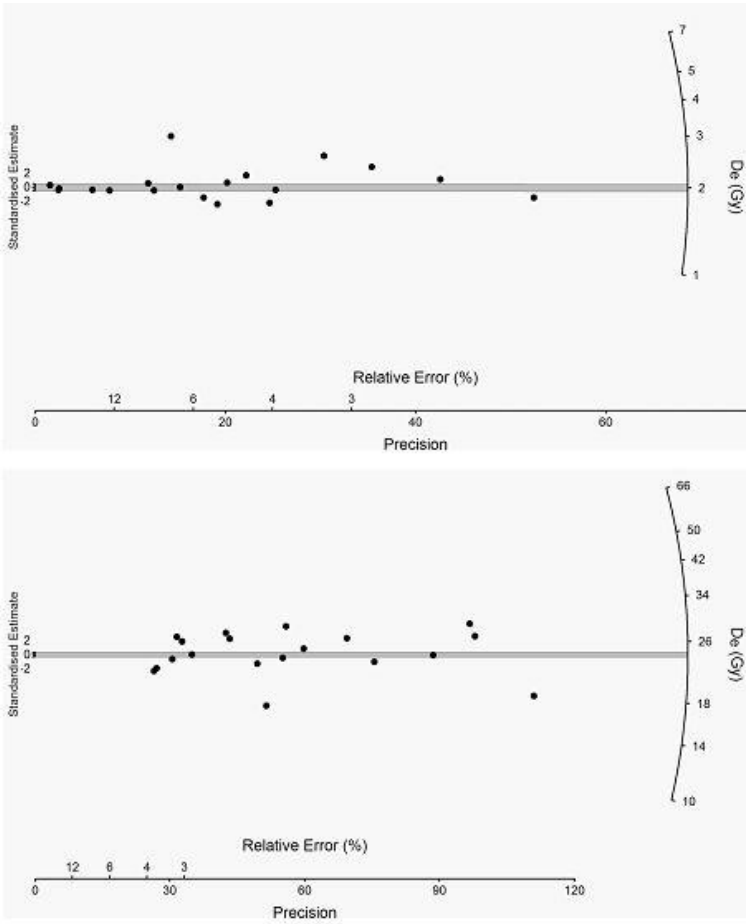

Figure 22. Radial plots of the D_e distributions for OSL measurements from Strzelecki Creek samples (a) Pit 3 1.6m and (b) Pit 6 3.7m, which are representative of the general D_e distributions from all samples in this study. In both cases, the grey line represents the D_e calculated using the central age model.

Under subdued orange light, all samples were first sieved to recover the 180–250 μm grain size fraction and any carbonates were then dissolved in HCl (10%) for 24 hours, followed by treatment with H_2O_2 (10%) for 24 hours to remove organic material, and finally with HF (40%) for 1 hour to remove any feldspar grains and to etch the surface of the quartz grains which may contain an enriched α-dose. Following the 1 hour HF treatment, a final treatment with HCl (10%) for 40 min was used to remove any residual fluorides. The resulting quartz-rich extracts were then re-sieved and checked for the absence of feldspars using infrared (IR) stimulated luminescence to confirm the purity of the extract. The clean quartz grains were mounted on 1 mm or 0.5 mm diameter stainless steel discs using a thin layer of silicone oil, resulting in a single layer of grains ~ 0.5 mm in diameter, and then measured in an automated Risø TL/OSL reader. A single aliquot regenerative (SAR) dose protocol was used to measure the palaeo-dose (D_e) according to Murray and Wintle (2000, 2003) for each aliquot, with the final D_e for each sample estimated using the central age model (CAM) (Galbraith et al., 1999). Examples of the D_e and error distribution for these samples, as well as the estimated D_e using the central age model are shown in Figure 22, with the final D_e results of all samples shown in Table 10. In the case where a D_e could not be estimated due to dose saturation (sample Pit 8b 5.6 m), the $2D_0$ value was calculated in order to provide a minimum age (Wintle and Murray, 2006).

For dosimetry measurements the bulk samples were firstly heated at 450 °C for 24 h and subsequently homogenized by grinding. The samples were then mixed with wax, cast in cup-shaped moulds and stored for three weeks to allow for the establishment of secular equilibrium between ^{222}Rn and ^{226}Ra. The cups were then counted on a high-resolution gamma-detector (Murray et al., 1987), and the activity concentrations of ^{238}U, ^{232}Th, and ^{40}K (Bq/ kg) were used to calculate dose rates (Gy / ka) by multiplication of the emitted energy per decay using the conversion factors of Olley et al. (1996) (Table 10) The contribution of cosmic-ray radiation to the dose rate was calculated using the approach described of Prescott and Hutton (1988, 1994) and a fixed value of 0.06 ±0.03 Gy / ka was used as an estimate of the internal dose rate for the quartz grains. The water content of each sample was determined as the difference in sample weight following heating to 100 °C for 24 hours, and then incorporated into the dose rate calculation assuming an error of 20%, which is necessarily high

given the potentially large fluctuations in the degree of water saturation that have occurred since deposition in this environment. These results and the final age calculation (D_e / dose rate) of each sample are listed in Table 10.

Sample	Depth (cm)	H_2O (%)	n	U^{238} (Bq / kg)	Ra^{226} (Bq / kg)	Th^{232} (Bq / kg)	K^{40} (Bq / kg)	Dose rate (Gy / ka)	D_e (Gy)	Age (ka)
Pit 1			2		7.41 ±	8.44 ±			12.6 ±	17.7 ±
5.2m	520	0.6	1	8.84 ± 4.0	0.29	0.32	84 ± 4	0.71 ± 0.13	1.0	3.5
Pit 3			2		7.96 ±	9.17 ±				
1.6m	160	0.8	1	8.40 ± 3.0	0.24	0.28	82 ± 3	0.78 ± 0.13	6.9 ± 0.3	8.8 ± 1.5
Pit 3			3		4.74 ±	6.02 ±				16.5 ±
4.2m	420	0.7	6	3.99 ± 2.5	0.20	0.20	49 ± 3	0.52 ± 0.08	8.6 ± 0.4	2.7
Pit 4			2		3.81 ±	4.20 ±			1.99 ±	
5m	430	0.2	0	< 0.1 ± 3.1	0.22	0.25	31 ± 2	0.39 ± 0.06	0.1	5.1 ± 0.8
Pit 6			1		4.19 ±	3.90 ±			24.2 ±	48.4 ±
3.7m	370	0.5	9	0.25 ± 3.4	0.25	0.28	37 ± 3	0.50 ± 0.08	1.9	8.4
Pit 6			2		5.39 ±	6.73 ±			23.7 ±	41.4 ±
4.4m	440	5.1	1	< 0.1 ± 4.5	0.33	0.38	73 ± 4	0.57 ± 0.09	1.3	7.0
Pit 7			1		5.61 ±	6.72 ±				46.3 ±
4.5m	450	0.5	9	6.04 ± 3.4	0.26	0.30	74 ± 4	0.63 ± 0.11	29 ± 2.0	8.5
Pit 8a			1		4.68 ±	6.02 ±			22.3 ±	34.2 ±
1.45m	145	0.9	5	1.63 ± 2.4	0.20	0.20	80 ± 3	0.65 ± 0.10	0.8	5.3
Pit 8a			1		4.35 ±	4.79 ±			18.1 ±	39.2 ±
5.4m	540	1.9	3	< 0.1 ± 5.8	0.40	0.46	54 ± 5	0.46 ± 0.07	1.6	7.2
Pit 8b					11.43 ±	8.67 ±	14 5 ±			
5.6m	560	6.4	-	14.86 ± 6.7	0.50	0.52	6	0.92 ± 0.17	~180[a]	> 195
Pit 10			2		7.83 ±	9.74 ±	11 6 ±			77.2 ±
2.2m	220	4.1	0	10.22 ± 3.4	0.28	0.31	4	0.86 ± 0.14	66 ± 3.0	13.5
Pit 10			2		10.72 ±	13.65 ±	147 ±			163.4 ±
5.5m	550	4.0	1	16.02 ± 6.1	0.48	0.55	7	1.03 ± 0.20	169 ± 7.0	32.0

Table 10. Sample depth, water content, dose rate, estimated palaeodose, and final age calculation for Strzelecki Creek, the actual stratigraphic position of the sample is shown in Figure 23. [a]Calculated as a minimum D_e using the $2D_0$ estimate following Wintle and Murray (2006), the resulting age estimate is therefore also a minimum value only.

5.5 Strzelekci Creek chronology, stratigraphy and palaeoenvironmental significance

Within the confinement of the Strzelecki Crossing, we find a large body of Late Quaternary channel and floodplain alluvium with an inset modern channel and associated annabranch bar development. The stratigraphy can be divided into an aeolian unit and five distinct fluvial units, with highly weathered sandstone bedrock occurring at the base of some sections on the western side (Figure 23). The five fluvial units are distinguished primarily on the basis of chronology (Figure 23, Table 10), and clearly visible stratigraphic discontinuities.

The oldest fluvial unit is composed of medium-coarse white sands, with well-developed channel cross-bedding, however, because of environmental dose saturation, only a minimum age of > 195 ka could be obtained. Overlying these sands is a homogeneous undated mud layer of variable thickness, which like the

underlying sands, has an erosional boundary with the western floodplain. This is in turn overlain by ~9-10 m of massive fine sand to silt aeolian dune deposits with upward declining silt, clay, and carbonate concretion concentrations. The age of the base of the dune is 163.4 ± 32 ka whereas that at ~ 2 m depth is 77.2 ± 13.5 ka. This indicates that the bulk of this dune is broadly consistent in age with the range of dune ages already obtained from the Strzelekci Desert (Cohen et al., 2010; Fitzsimmons et al., 2007; Lomax et al., 2003).

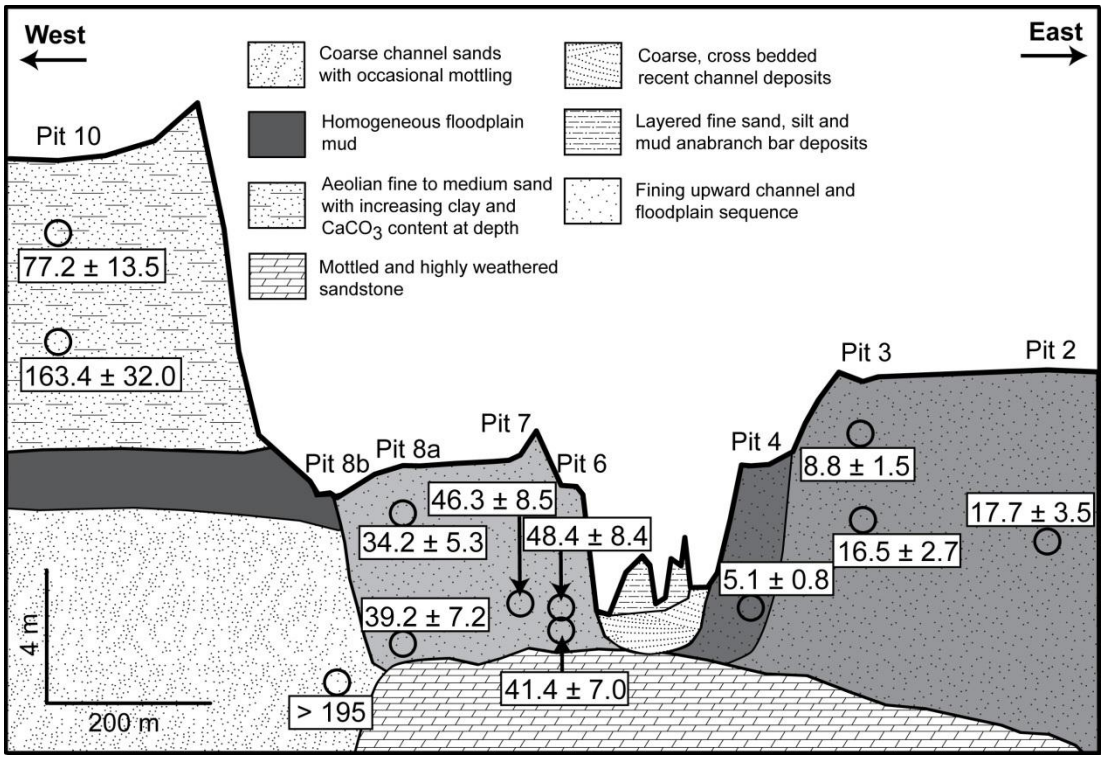

Figure 23. Fluvial and aeolian chrono-stratigraphy of Strzelecki Creek, showing the location of the excavated pit sites and the depth from which OSL ages were obtained. The three grey scale fining upward channel and floodplain units (distinct from the dark grey floodplain muds) are distinguished on the basis of relative age and topographic variation. Depth to bedrock on the eastern side of the modern channel is hypothetical.

The remaining fluvial deposits associated with Strzelekci Creek are set at a lower elevation than the western aeolian dune, with the western floodplain slightly lower than the eastern, and both containing smaller inset terraces adjacent to the modern channel. The alluvial deposits preserved between the modern channel and the aeolian dune on the western side of Strzelecki Creek are all within the age range 34.2 ± 5.3 – 48.4 ± 8.4 ka, despite a wide range of sampling depths across the whole width of the floodplain. Pit 6, located on the small inset terrace adjacent to the modern creek on

the western side, exhibits the only stratigraphic age inversion in the dataset, however the estimated ages are still within the 1 σ error margin (41.4 ± 7 and 48.4 ± 8.4). This age bracket for deposition is narrow compared to similar stratigraphic sections in the LEB (Nanson et al., 2008), yet nonetheless entirely feasible. This does not include the very top ~ 0.2 m of the floodplain, which displays occasional evidence of aeolian reworking and deposition.

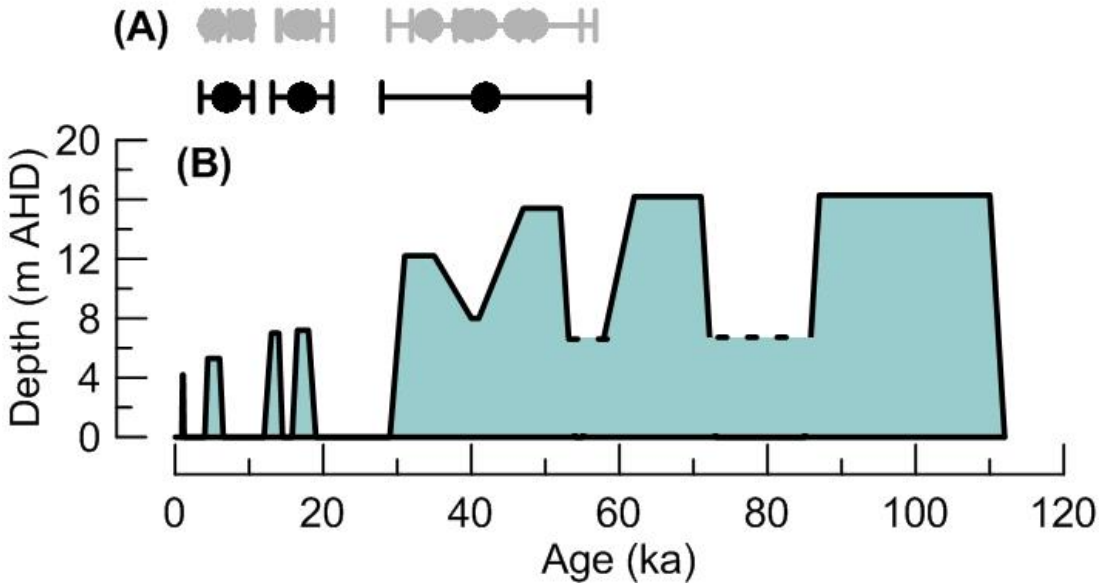

Figure 24. Composite fluvial and lacustrine records for Strzelecki Creek and Lake Frome. (a) Strzelecki Creek fluvial ages (light grey), with the mean and standard error of the three separate age clusters shown below (black). (b) Lake Frome shoreline ages (Cohen et al., in press).

The lower inset western terrace does not have distinguishably younger ages from the rest of the western floodplain alluvium despite a clear topographic break, and suggests that the bulk of this channel and floodplain sediment was deposited within a similar hydrological phase. The simplest explanation is that the western floodplain section had most of its sediment excavated prior to ~50 ka and up to the dune boundary, followed by re-deposition of channel and floodplain sequences from about 35 to 45 ka, with the inset terrace (Pit 6) representing the culmination of this phase. Interestingly, this depositional phase also corresponds to the 30 – 45 ka series of shoreline high stands in the Lake Frome system (Cohen et al., in press), suggesting the channel forming discharge at this time on Strzelecki Creek was part of the same hydrological phase responsible for the maintenance of high lake levels downstream,

including the last full connection between the Lake Frome and Lake Eyre systems (Figure 24).

On the eastern side of the channel, the alluvium is not constrained by any visible topographic features, and the stratigraphy was investigated over roughly the same floodplain width as the western side. The stratigraphy is similar to the opposite side of the modern channel, with fining upwards sequences with basal coarse channel sands and rising to 2 – 3 m of poorly laminated fine sandy floodplain deposit. Despite excavating to similar depths, we were unable to reach any basal bedrock, suggesting the bedrock surface dips, or is more incised, towards the east. In addition, the similar stratigraphy is not matched by a similar chronology, with the eastern alluvium considerably younger than the western. Basal ages for Pit 2 and Pit 3 from cross-bedded channel sands are similar (17.7 ± 3.5 and 16.5 ± 2.7 ka, respectively), with the overlying floodplain deposits in Pit 3 being approximately half that age (8.8 ± 1.5 ka). A further feature of the eastern side is the clear chronological break of the lower terrace or what is probably the contemporary floodplain on the eastern side with the rest of the alluvial sequence, the base of which is mid-Holocene in age (5.1 ± 0.8 ka).

The chronology of the fluvial deposits to the east of Strzelecki Creek reveals a break in deposition from ~34 – 18 ka, nevertheless, during this time the excavation of any pre-existing alluvium on the eastern side also had to be achieved. A problem is that an interpretation of hydrological inactivity on the basis of an absence of ages from 34-18 ka is difficult to sustain. It is possible that possible that most of the excavation of this material occurred at the same time as the deposition of its replacement, which would mean that there was relatively little fluvial activity between ~34 ka and the Last Glacial Maximum (LGM), and this area was excavated and reformed as an alluvial surface after the LGM. Interestingly, the ages for fluvial deposition on the eastern side coincide well with the remaining lake shoreline record from Lake Mega-Frome, in particular the shoreline at the termination of the last glacial maximum (LGM) and the mid-Holocene (Cohen et al., in press). Although are is no fluvial deposits that directly match the ~ 13 ka shoreline on Lake Frome, deposits of this age almost certainly occur within the continuous ~16 – 8 ka channel and floodplain stratigraphic sequence recorded within Pit 3. Likewise, fluvial ages matching the

youngest recorded lake activity on Lake Frome are likely to be found within the deposits of the modern incised channel, and which have not been investigated here.

The good correspondence between the fluvial archive from Strzelecki Creek and the palaeo-shorelines of the Lake Frome system demonstrates the ability of the Strzelecki and presumably Cooper Creek that was its source to supply sufficient volumes of water to transport an abundant sandy bedload in laterally reworking channel. The precise volumes under which this would occur are not possible to determine with the data available, however the largest historical flood recorded on Strzelecki Creek in 1974 did not produce any perceivable changes to the overall channel structure or move any significant bedload, even at its delta with Lake Blanche (May, Unpublished data). Strzelecki Creek has only had flow along its reach recorded ~ 6 times in the last 50 years, with only the floods in 1974, 1990, and 2010 managing to flow from the beginning of the channel near Innamincka until its termination at Lake Blanche. None of these events caused Lake Blanche to overflow into Lake Frome, although satellite imagery indicates Lake Frome did have a large portion of its surface area covered by water following these flood events (Cohen et al., in press), suggesting some combination of local rainfall, runoff from the eastern Flinders Ranges, and groundwater equalisation with Lake Balanche and Lake Callabonna was able to reach the lake.

5.6 Hydrological comparison of lake records

Clearly, the modern hydrological conditions require significant modifications if the palaeo-environmental evidence recorded within Strzelecki Creek, and the Lake Eyre and Lake Mega-Frome lacustrine systems are to be met. Although the fluvial record presented above does contribute some evidence for the supply of water from the north-eastern parts of the LEB, which in turn would be expected to be dominated by monsoonal rainfall, it does not answer questions regarding the scale of hydrological change. Furthermore, if Strzelecki Creek, and indeed other rivers throughout the LEB were able to effectively supply water to the terminal lake systems from the north of the basin, the comparison of lake depths thus far in the literature (Cohen et al., in press) may not provide an accurate means of comparison, since basin morphology itself may be a large component of any perceived correlation or differences in lake levels. This is important because the construction and preservation of shoreline records are entirely dependent on the depth of the lake

achieved through changes in volume, and therefore in order to compare the records of hydrological change between Lake Eyre and Lake Mega-Frome it is important to develop the basis for an equivalent hydrological understanding.

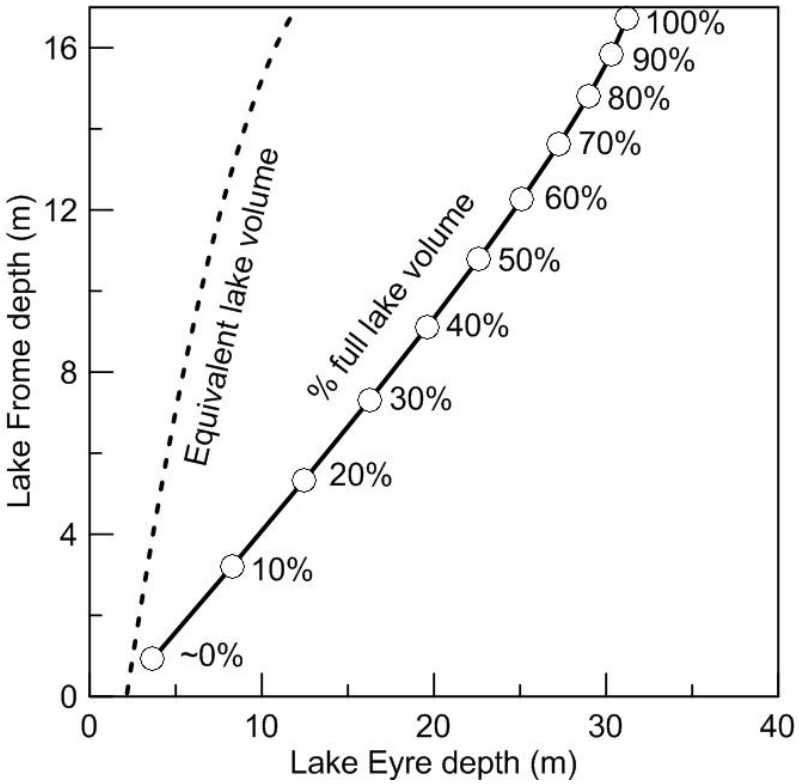

Figure 25. Absolute depth (m) of Lake Eyre (x-axis) and Lake Mega-Frome (y-axis). Solid black line compares the depth at which increasing lake volumes (%) are attained, with the white circles showing 10% increments. The dashed line represents the depths at which the volumes (km^3) in the two lakes are equivalent.

Using the hypsometric data of (Leon and Cohen, submitted), a comparison of the absolute lake depths (m) of Lake Eyre and Lake Mega-Frome yields two interesting curves (Figure 25). The first is the depth at which a given percentage of lake full volume is reached in both lakes, which demonstrates that a 10m deep lake on Lake Eyre would be ~13 % full, while an equivalent depth on Lake Mega-Frome would be ~45% full. The second curve, and the most relevant for palaeo-hydrological interpretations, is the point at which the lake volumes (km^3) are equivalent for any given lake depth. This demonstrates that if the highest shoreline in the Lake Mega-Frome record was established by an increased inflow of water, the equivalent volume of water in Lake Eyre under the same conditions would only reach the -10 m (AHD) shoreline. However, this is only a hypothetical scenario for comparative purposes, since it is unrealistic to expect both lakes to consistently have equivalent inflow, and

therefore ever obtain equivalent lake volumes. Nevertheless, it establishes that high lake levels on Lake Mega-Frome cannot necessarily be placed in the same hydrological context as high lake levels on Lake Eyre.

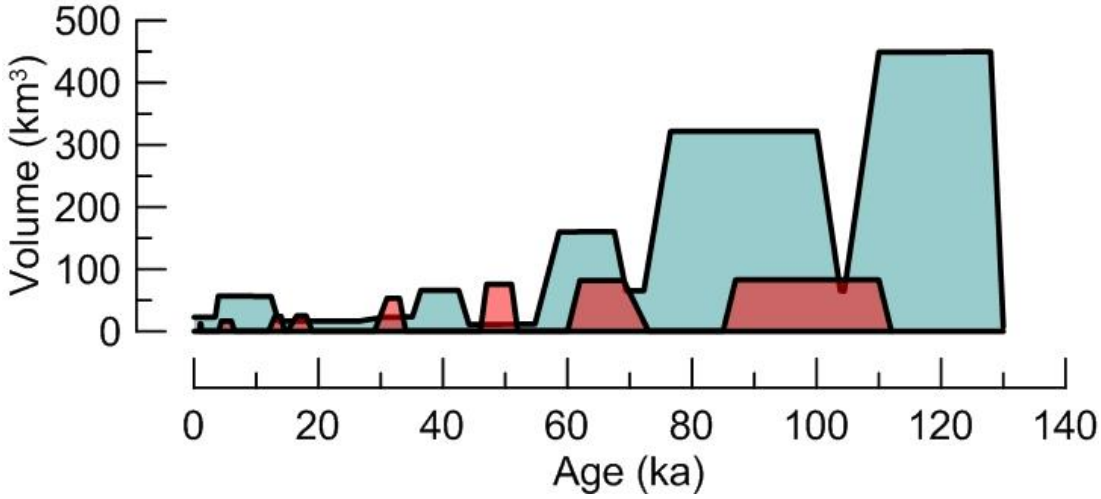

Figure 26. Estimated changes in lake volume over the Late Quaternary for the Lake Eyre (blue), and Lake Mega-Frome (red) basins.

This last point can be demonstrated more effectively by converting the lake depth records in Figure 24 into their equivalent lake volumes (Figure 26). The high stands on Lake Eyre are clearly the result of much larger hydrological inputs than any of the high stands on Lake Mega-Frome, although it is important to remember that the highest shoreline on Lake Frome is also the upper limit to lake size, after which higher shorelines are not possible since any extra water will be diverted through the Warrawoocara Chanel to Lake Eyre (Nanson et al., 1998). Moreover, it is now difficult to infer differences between the two records, given the uncertainty surrounding what the lake levels may have been between the large high stands, and because the younger records are of increasingly smaller volume. Although the out of phase high lake volumes on Lake Eyre and Lake Mega-Frome between ~30 – 55 ka, as well as the comparatively minor events over the last ~ 20 ka (Figure 26), could still be interpreted in terms of changing moisture sources which preferentially provide inflow to one lake or another (Cohen et al., in press), a simpler explanation might instead be related to shoreline preservation. That is, the record of consistently declining lake volumes over the Late Quaternary may easily be an artefact of the decreasing preservation probability of shorelines with decreasing height, a mechanism which guarantees younger ages for progressively smaller shorelines.

Thus, the presence of a high stand on Lake Mega-Frome in the absence of a similar 'peak' in Lake Eyre (e.g. ~50 ka) may simply be the result of shoreline reworking by younger events on Lake Eyre that filled to a similar volume (e.g. at ~40 ka).

5.7 Theoretical framework for hydrological and climatic change

5.7.1 The catchment water and energy balance

Irrespective of the exact timing of lake high stands, the construction and maintenance of elevated shorelines on Lake Eyre and Lake Mega-Frome at any time in the Late Quaternary must have still occurred under a consistent water and energy balance between the land surface and the atmosphere. Since this balance does not permit significant water bodies for more than approximately two annual flood cycles in the current climate, there must be some aspect(s) of the past climate that is (are) distinct from the present one that has enabled such differences.

In order to estimate these conditions, the basic catchment water balance is first considered, which can be formulated as:

$$Q = P - E + \Delta S \qquad (1)$$

where the available surface runoff (Q) is a function of the water provided by the atmosphere (P), the water extracted by the atmosphere (E), and any surplus provided by changes in catchment water storage (ΔS). Over the large inter-annual timescales of interest we can assume that ΔS is not significant, especially compared to the magnitude of P, E, and Q, and Equation (1) therefore reduces to $Q = P - E$.

This can be connected with the energy balance, in which incoming shortwave (S) and long wave (L_{in}) radiation provides the net radiation (R_n) available at the earth's surface:

$$R_n = S(1 - \alpha) + L_{in} - L_{out} \qquad (2)$$

where S is partitioned according to the surface albedo (α), and R_n is diminished by outgoing long wave radiation (L_{out}). The energy balance achieved between R_n and the surface moisture and heat fluxes can then be written as:

$$R_n = \lambda E + H + G + F \qquad (3)$$

where λE is the latent heat flux, H is the sensible heat flux, G is the soil heat flux, and F is the energy consumed by plant respiration and photosynthesis. The largest surface fluxes in Equation (8) are λE and H, and their partitioning is also the most critical for the water balance, which will be discussed later. For simplicity, we assume that for long time scales Equation (8) becomes $R_n = \lambda E + H$, and that λE adequately approximates the total moisture fluxes from the surface to the atmosphere, or $\lambda E = E$.

For the water balance of the modern LEB, it is difficult to measure E directly, and since estimates of evaporative demand (E_0) are more readily available, a suitable framework in which the two can easily be related is required. E_0 is typically estimated from net radiation or pan evaporation data (Roderick and Farquhar, 2011; Yang et al., 2006) and in this study we use the gridded mean annual areal potential evapotranspiration provided by the Australian Bureau of Meteorology. This differs from the Penman definition of potential evaporation since the areal potential evapotranspiration is calculated assuming the area under investigation is large enough that any local variations can be considered part of a regional areal average (Morton, 1983), and rejects the assumption of the Penman equations that when an environment is energy limited, $E \propto E_0$ (Nash, 1989). A full comparison of the two approaches to potential evaporation is provided by Nash (1989) and Hobbins et al. (2001), with the main advantages of the areal estimate being that it requires fewer calibration parameters, and the main limitation being the assumption that the vapour transfer co-efficient is independent of wind speed. In addition, the areal estimates of E_0 are almost half that of pan evaporation estimates within the LEB (McMahon et al., 2005), which will lead to a discrepancy for estimates of E depending on which is used. However, since the areal estimate of E_0 for the LEB is still much larger than P, the resulting estimates of E are not especially sensitive to the choice of E_0 measurement, which is similar to the results found in the Murray-Darling Basin in south-east Australia (Roderick and Farquhar, 2011).

In terms of the Late Quaternary water and energy balance, it is possible to also make further simplifications, and assume that $R_n \sim E_0$, which then results in the difference between E_0 and E being solely in terms of H. The validity of such an approximation is not apparent if the atmospheric water demand (E_0) is not affected by surface changes in the same way as R_n is, which will almost certainly be the case unless the

surface partitioning of water fluxes can be included as a function of the water balance. In order to do so, it is more useful to consider the how the ratios of atmospheric water demand and supply (E_0/P) and actual water fluxes (E/P) are balanced. This can be achieved using a 'Budyko' style framework (Budyko, 1974), which states that:

$$\frac{E}{P} = \left[\frac{E_0}{P}\tanh\left(\frac{E_0}{P}\right)^{-1}\left(1-\cosh\frac{E_0}{P}+\sinh\frac{E_0}{P}\right)\right]^{0.5} \qquad (4)$$

and has become widely applied in catchment water balance studies (Fu, 1981; Yang et al., 2006; Zhang et al., 2004), and for which an analytical basis has recently been developed (Gerrits et al., 2009). We can also evaluate E/P as a function of E_0/P (the aridity index) with the inclusion of a partitioning parameter, which Zhang et al. (2004) write as:

$$\frac{E}{P} = 1+\frac{E_0}{P}-\left[1+\left(\frac{E_0}{P}\right)^{\omega}\right]^{1/\omega} \qquad (5)$$

Thus given good estimates of annual P and E_0, it is possible to establish a reasonable estimate of E/P. We can also re-write Equation (5) solely in terms of E, according to Choudhury (1999):

$$E = \frac{P\,E_0}{(P^n + E_0^n)^{1/n}} \qquad (6)$$

with the parameters ω and n in equations (5) and (6) partitioning atmospheric moisture supply (P) and demand (E_0) between Q and E within a catchment according to slope, soils, vegetation etc., and can be related to each other according to (Yang et al., 2008) as:

$$\omega \approx n + 0.75 \qquad (7)$$

Using Equation (6) to obtain E, it then follows that an estimate of Q can be obtained with Equation (1), which is provided here for the contemporary LEB using the average climate variables listed in Table 11. Using n = 1.8 (Choudhury, 1999; Roderick and Farquhar, 2011), we obtain a mean annual Q of 24.43 mm/yr, which is within 7% of the actual mean value of 22.92 mm/yr, which is estimated using the

mean annual discharge of all available stations in the LEB (n = 18) summarised in McMahon et al. (2005) (Table 11). Adjusting n to 1.84 we can estimate Q within > 0.1 %, and this value is adopted in further analysis. We can also check the accuracy of the mean climate values and n by first solving Equation (4) for E_0/P = 1, which yields E/P = 0.694 (Donohue et al., 2011). Secondly, incorporating Q to Equation (6) results in:

$$Q = P - \frac{P\,E_0}{(P^n + E_0^n)^{1/n}} \tag{8}$$

which can then be solved numerically for $P = E_0$ and $Q = P - (0.694P)$ (Donahue et al. 2011) according to:

$$Q = P - \left(\frac{2}{n} P^2 \frac{P^n}{n}\right) \tag{9}$$

This allows n to be to be estimated directly from Equations (4) and (6), and yields n = 1.89 using the mean values in Table 11. This is very close to our adjusted estimate of n, and alters Q to 21.1 (mm/yr), suggesting our estimates of mean P and E_0 are very good, with the mean annual Q derived fromMcMahon et al. (2005) perhaps slightly too high, however in the absence of better data we use the mean LEB data in Table 11 with n = 1.84 in the remaining analysis. A full description of the sensitivity of n and its derivation is provided by Donohue et al. (2011).

Location	P (mm/yr)[a]	E_0 (mm/yr)[a]	E (mm/yr)[b]	Q (P-E) (mm/yr)[a]
North-East	650 - 700	1500 - 1600	585 - 629	65.2 - 71.3
South - Central	200 - 300	1000 - 1100	195 - 286	5.4 - 14.0
Flinders Ranges	330 – 470[c]	1100 – 1200[c]	327 – 460[c]	2.9 – 9.1[c]
LEB Mean	408	1338	385	22.9[b]

Table 11. Range and mean of climate and hydrology parameters for the LEB used in this study. [a] P, E_0, and Q data from McMahon et al. (2005). [b] Mean Q and all E values are calculated using n = 1.84 to match the mean Q estimate for the LEB from McMahon et al. (2005). [c] Values for P and E_0 are estimates from the Bureau of Meteorology annual average data, and adjusted to match the available values of Q from McMahon et al. (2005). In addition, the considerable decrease in catchment scale changes the portioning parameter n significantly, and is here given as n = 3.

For the purposes of later comparisons, an estimate of the modern P, E_0, E, and Q mean annual conditions for the Flinders Ranges are also calculated. These Ranges

are a potential source of runoff for many of the terminal lakes in the Lake Mega-Frome system, and in particular Lake Frome itself, and therefore it is useful to consider this area separately. Climate and hydrology data is unfortunately not well covered in this area, however the two estimates of mean annual Q from this area (9.1 and 2.9 mm/yr) demonstrate very low runoff conditions compared to the range of P and E_0 estimates (Table 11). In order for such low Q to be accounted for in the above framework, it is necessary to increase the relative fluxes of E through the partitioning parameter n, and given the considerably smaller catchment size of the Flinders Ranges compared to the LEB as a whole, values closer to ~ 3 have been found to be reasonable as catchment area decreases (Donohue et al., 2011), and is therefore adopted here. The resulting runoff ratios (Q/P) are extremely low (~ 1%), and are probably realistic given that on average most of the rainfall in the Flinders Ranges does not provide significant runoff past the apex of the alluvial fans on the mountain front boundary.

We can visualise the relationship between E_0/P and E/P for the range and mean climate estimates for the LEB using the Budyko curve (Figure 27). Budyko (1974) proposed that differences in E_0/P can divide climates into: forests ($0.33 < E_0/P < 1$) which are generally energy limited ($Q > E$), and the water limited climates ($E > Q$): savannah ($1 < E_0/P < 2$), semi-arid ($2 < E_0/P < 3$) and arid ($3 < E_0/P$). Based on the data in Table 11, the LEB centre-south and basin average E_0/P values fall within the arid climate state, with the north and east E_0/P values in the semi-arid climate state. The range of E_0/P estimates for the Flinders Ranges places this area on the boundary between semi-arid and arid, which is likely a reflection of the northward trend towards aridity in this area. In each of these cases however, $E_0 >> P$, and therefore in Figure 27 all LEB E/P values have $E \rightarrow P$, which is typical of arid environments where E is strongly limited by water supply.

5.7.2 Lake area and the water balance

It is possible using the catchment water balance described above to estimate the inflow to Lake Eyre and Lake Mega-Frome, provided accurate information on transmission losses and actual lake E_0/P and E/P conditions surrounding the lake can be included. However, since this information is poorly known, an alternative approach is to assume the extent of surface water in a lake is in itself indicative of

catchment water supply and local climatic conditions. In this respect, the ratio of lake area (A_L) to catchment area (A_C) has been a used extensively for the estimation of palaeoclimates from lake records around the world (Benson and Paillet, 1989; Bowler, 1981; Kutzbach, 1980; Mason et al., 1994). Here, we define this ratio (A_R) as:

$$A_R = \frac{A_L}{A_L + A_C} \tag{10}$$

One limitation faced in the implementation of the catchment water balance for palaeo-lakes using the framework in section (6.1) is that we have no way of independently evaluating values for a catchment parameter such as n. Therefore, a simpler formulation of the water supplied to lakes is more appropriate. An alternative to the Budyko framework for evaluating Q as a function of catchment climate was first provided by Schreiber (1904)

$$Q = P \exp\left(-\frac{E_o}{P}\right) \tag{11}$$

based on an evaluation of annual runoff and precipitation in European river basins. Recently, Fraedrich (2010) demonstrated this can also be applied to problems concerning catchment E_0/P and E/P ratios, whereby:

$$\frac{E}{P} = 1 - \exp\left(-\frac{E_0}{P}\right) \tag{12}$$

If we consider the simplified catchment water and energy balance from Equations (1) and (3) and that A_L must be a function of a range of catchment E_0/P conditions , assuming that all water inflow into a lake is equal to the relevant catchment Q, and that P over the lake is the same as the relevant catchment area, then according to Fraedrich and Sielmann (in press) we can write

$$A_R = \frac{1 - \frac{E}{P}}{\frac{E_0}{P} - \frac{E}{P}} \tag{13}$$

However, since we cannot distribute E and Q according to n using Equation (11), it is more useful to express A_R solely in terms of E_0/P (Fraedrich and Sielmann, in press):

$$A_R = \frac{\exp(-\frac{E_0}{P})}{\left(\frac{E_0}{P} - 1\right) + \exp(-\frac{E_0}{P})} \quad (14)$$

Clearly, the assumption of equivalence between catchment and lake precipitation does not hold in the current climate of the LEB, even for the mean basin conditions. It is also difficult to make this assumption at any time in the Late Quaternary, however, using Equation (14) it is possible to compare the A_R values expected using modern E_0/P conditions with the known modern A_R, and therefore interpret any difference as a contrast between the wider modern catchment E_0/P and the E_0/P conditions directly surrounding Lake Eyre and Lake Mega-Frome themselves.

Extending the framework of the Budyko curve in Figure 27, we can include a function for A_R and E_0/P and ask two related questions: 1. what is the predicted A_R given the range of modern E_0/P value? and 2. what can we predict about the E_0/P from actual estimates of modern A_R? This last question can be addressed by re-arranging equation (14) to find:

$$\frac{E_0}{P} \approx W\left(\frac{1 - A_R}{e \cdot A_R}\right) + 1 \quad (15)$$

where W is the product log function of the bracketed terms. The predicted values of A_R are shown at the ends of the arrows descending from the modern climate E_0/P estimates in Figure 27, and the highlighted grey range refers to the E_0/P range of the modern Flinders Ranges and the modern South – Central LEB. These results indicate that each estimate of A_R for Lake Eyre fits within the range of the South – Central climate conditions, ($E_0/P \approx 4.05 – 4.51$). For the estimates of Lake Mega-Frome A_R, the equivalent E_0/P ($\approx$ 4.80 or 3.07), depends on the assumed contributing catchment area. For Lake Eyre A_C is always very large regardless of the inclusion or exclusion of the Cooper Creek catchment as a runoff contributor (AR # 1 and AR # 2 respectively), and the area of water generally contained within modern Lake Eyre (A_L) is consistent with the current E_0/P conditions of the South – Centre portion of the basin. On the other hand, A_C for Lake Mega-Frome can be comparatively small if

only the Flinders Ranges is used, or quite large if the contributing area of Cooper and Strzelecki Creeks is included, thus leading to large differences in calculated A_R values.

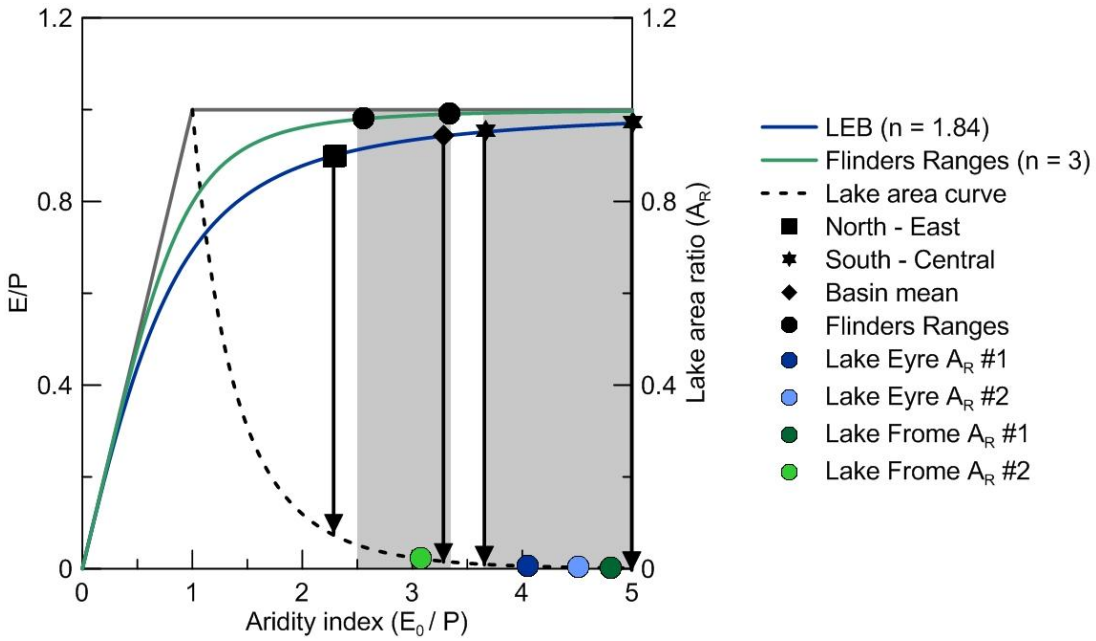

Figure 27. A Budyko framework for the modern climate and lakes of the Lake Eyre Basin. The blue and green lines represent the Budyko curves for the Lake Eyre Basin and Flinders Ranges respectively, with the calculation of parameters discussed in the text and Table 12. The dotted black line is the lake area curve predicted using equation (14) for changing values of E_0/P. The grey lines which border the space in which these curves plot are the energy limit ($E_0 = P$), water limit (E/P = 1), and also lake area limit (A_R = 1) common to any catchment. Black symbols refer to the range of modern climate conditions in the LEB (plotted on the blue curve), and the separate consideration of the Flinders Ranges are plotted on the green curve. Black arrows descending from these points indicate the position on the lake area curve that a lake existing under those exact climate conditions would be predicted to plot, and the grey shaded areas highlight the climatic range of the Flinders Ranges and South – Central LEB across the lake area curve. The modern A_R values for Lake Eyre and Lake Frome are plotted as the coloured circles, with the different A_R values for each lake based on separate assumptions of contributing catchment areas (A_R # 1 and # 2 for each lake). For Lake Eyre, A_R # 1 assumes runoff is only received from the Georgina and Diamantina catchments, while A_R # 2 includes the additional catchment area provided by Cooper Creek. For Lake Frome, A_R # 1 assumes runoff can be sourced from the Cooper Creek catchment and the Flinders Ranges, while A_R # 2 assumes the only contributing catchment is from the Flinders Ranges. For modern Lake Eyre, A_L is assumed to be on average 2055 km^2, which corresponds to a ~1 m deep lake, and for Lake Frome A_L is assumed to have an average value of 708 km^2. These values are difficult to estimate given the lack of monitoring, and may therefore be slight overestimates.

Using only the Flinders Ranges as the contributing catchment area (AR # 2), then the resulting A_R estimate is very close to the A_R expected under the current Flinders Ranges E_0/P conditions. This is consistent with the historical observation that Strzelecki Creek has never contributed flow to Lake Frome, and the Flinders Ranges are therefore likely to be the only modern contributor of runoff. However, it is important to remember that modern Lake Frome rarely, if ever, receives direct runoff from river channels, and thus local rainfall and equilibration with groundwater levels are the main hydrological drivers of the small contemporary A_R estimate. Nonetheless, these results demonstrate that the simple Budyko framework developed here for comparing the climate parameters of the catchment, and those of the lake, are consistent under modern climatic conditions and can therefore be applied with reasonable confidence to climate changes of the past.

5.7.3 Lake and climate conditions of the Late Quaternary

If river discharge and lake volumes have changed substantially throughout the Late Quaternary, a deceptively simple yet fundamental question is how much the basic climatic parameters have to change in order to cause the inferred hydrological changes. If we assume that the E_0/P conditions required to maintain a large lake at any time in the past to be the result of some changes in the surrounding catchment climate conditions, including vegetation (n), then the change required can be estimated by determining the likely response of all catchment inputs and outputs to the changed climate conditions experienced over the Late Quaternary. The response of these parameters are potentially very complex, however we can simplify this considerably by first predicting the likely direction of change given simple climate scenarios. For example, if there was a uniform decrease in the mean LEB E_0 during glacial times as a result of reduced solar forcing (R_n), then we would initially expect lower E and therefore also higher Q. However, lower E_0 will also have an effect on catchment vegetation and therefore provide feedback to n, which may increase as a result, and therefore cause overall catchment Q to decrease. In reality, such feedbacks are likely to be more complicated since the basin is very large, and each part will not necessarily respond in the same way. In addition, the changes may be temporal, with summer P increasing or decreasing, yet with the mean P conditions remaining the same if there is an equal and opposite change in winter P. Therefore,

these potential changes (spatial, temporal, and vegetation) to catchment climate forcings (P and E_0) and the likely directional responses of n, E, and Q are summarised in Table 12, and forms the basis of the remaining analysis regarding potential feedbacks.

Change	n	E	Q
Spatial Distribution [a]			
E_0			
↑ N – E, ↓ S – C	↓	↓	↑
↓ N – E, ↑ S – C	↑	↑	↓
P			
↑ N – E, ↓ S – C	↓	↓	↑
↓ N – E, ↑ S – C	↑	↑	↓
Temporal distribution			
E_0			
↑ summer, ↓ winter	↑	↑	↓
↓ summer, ↑ winter	↓	↓	↑
P			
↑ summer, ↓ winter	↑	↑	↓
↓ summer, ↑ winter	↓	↓	↑
Vegetation			
↓ CO_2 and LAI	↓	↓	↑
Trees to grasses	↓	↓	↑

Table 12. Summary of the predicted direction of change for parameters in the catchment water balance for the LEB during the Late Quaternary. [a] Refers to the distribution of E_0 and P separately within the North – East (N – E) and South – Central (S – E) sections of the basin as described in Table 11.

Using the estimated A_L and A_R of the major filling events of both lakes during the Late Quaternary (Figure 26), we can estimate changes in the local E_0/P conditions required for these lakes to exist at for each A_R or high stand (Figure 28). For Lake Eyre, the range of A_R (0.015 – 0.041) is an order of magnitude higher than the modern A_R (0.003), which is a similar result to Quaternary Lake Mega-Frome A_R (0.011 – 0.022) if Cooper Creek/ Strzelecki Creek and the Flinders Ranges are both considered to contribute to A_C (A_R # 1). A larger hydrological change is required of Lake Mega-Frome A_R if only the Flinders Ranges are considered to contribute runoff to the lake (A_R # 2). Although the range of Quaternary high stand A_R (0.104 – 0.188) values are still only one order of magnitude higher than the modern estimate (0.022),

the resulting change in E_0/P is much larger than for the other lake scenarios (Figure 28). Interestingly, the range of E_0/P values for Lake Mega-Frome AR # 1 catchment conditions (Flinders Ranges + Cooper/Strzelecki Creek) are all lower than the modern E_0/P for AR # 2 (Flinders Ranges only) even at the largest lake filling events, suggesting that although it is possible for the Flinders Ranges to be the sole supplier of runoff to Lake Mega-Frome, the change in local and catchment E_0/P required would indicate that the Flinders Ranges became a fairly humid savannah landscape many times throughout the last ~ 120 000 years, for which there is thus far no substantial palaeoclimatic evidence (Draper and Jensen, 1976; Haberlah et al., 2010; Singh and Luly, 1991).

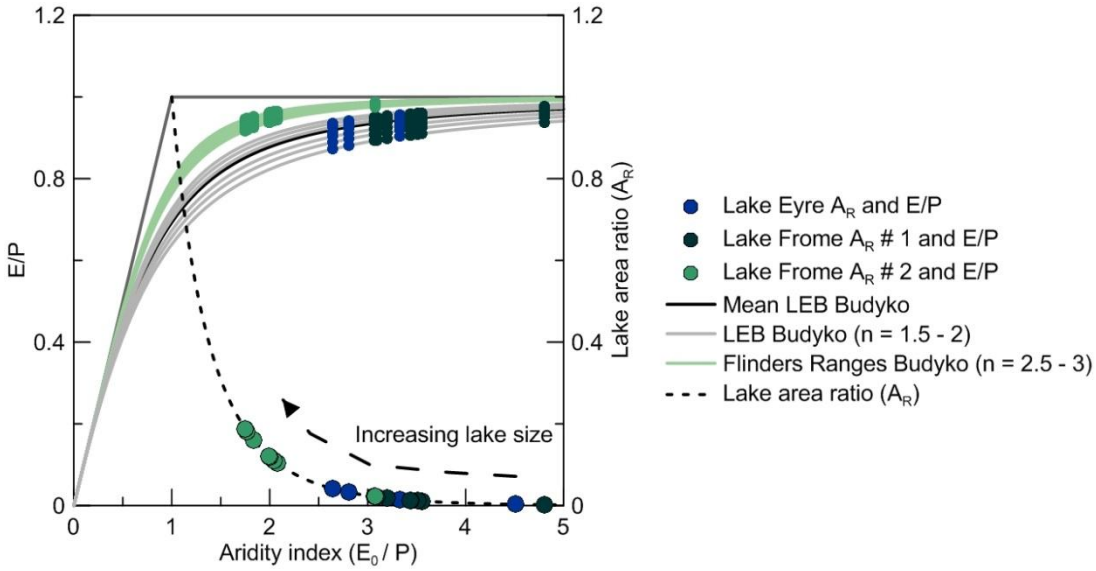

Figure 28. The Budyko and lake area ratio curves for the Late Quaternary high stands on Lake Eyre and Lake Frome. The Budyko curves are the same as for Figure 27, except now a range of n values are used in order to account for any feedbacks between E_0, P, and n, which are in turn used in the estimation of the range of catchment E/P conditions corresponding to lake high stand values of A_R. As was found in the modern lake conditions, the A_R estimates of Lake Eyre are not sensitive to the inclusion or exclusion of the Cooper Creek catchment, and since extensive Quaternary fluvial deposits have been recorded in the lower reaches of this system (Nanson et al., 2008), the A_C of Cooper Creek is included in the calculation of past A_R estimates for Lake Eyre. In the case of Lake Mega-Frome however, scenarios of contributing A_C are given separately for the Cooper Creek and Flinders Ranges combined (A_R # 1), and the Flinders Ranges alone (A_R # 2).

In contrast, the maintenance of high lake levels through the contribution of runoff from the Cooper Creek/Strzelecki Creek catchment to Lake Mega-Frome, and the large lake conditions on Lake Eyre, have E_0/P conditions still within the semi-arid

to arid climatic range. The E_0/P requirements of Late Quaternary lake areas presented in Figure 28 can in turn be used to estimate a range of realistic catchment E/P conditions using Equation (5). Given the feedbacks between E_0, P, and n, it is necessary to consider a range of values for n within the LEB (1.5 – 2) and the Flinders Ranges (2.5 – 3) in which P might be partitioned into E and Q. The resulting E/P ratios are likely to be slightly lower than the modern estimates, however they must remain roughly similar given that E is still limited by P in most cases (Figure 28).

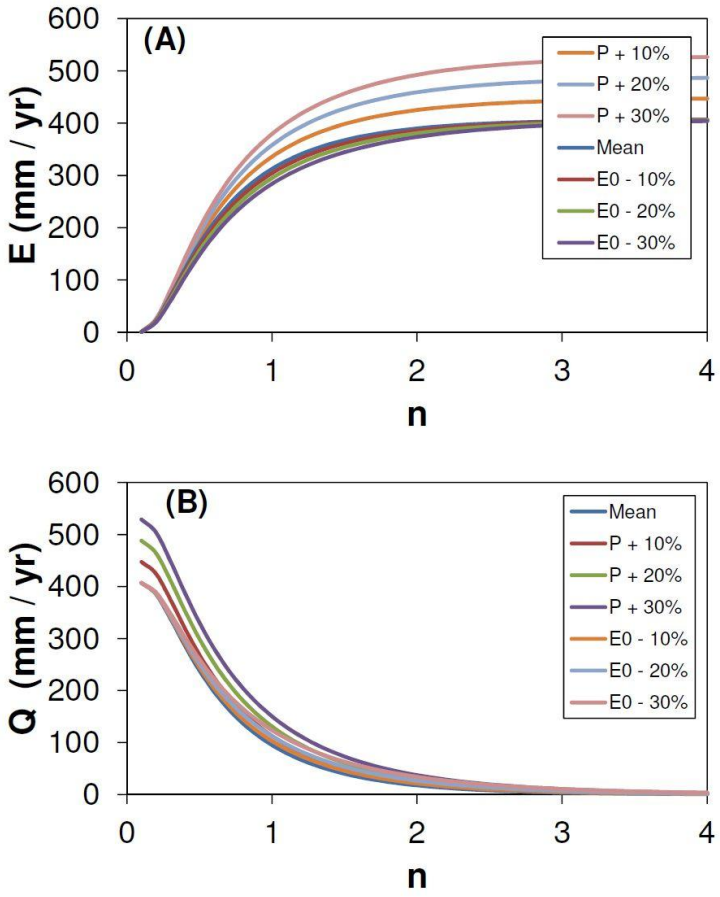

Figure 29. Sensitivity analysis of Q and E to changing values of n for different LEB climate change scenarios: P + 10 – 30% and E_0 - (10 – 30) %.

In order to explore these relations further, the sensitivity of catchment water fluxes (E and Q) to a wide range of catchment conditions (n) is calculated in Figure 29, assuming mean LEB climate conditions in which P and E_o are progressively increased or decreased respectively (± 10 – 30%). Although these fluxes are certainly sensitive to changing values of n, this is not especially the case for n > 1.5, and

values below this would suggest that catchments are no longer able to return water to the atmosphere as E and hence any water fluxes from P are dedicated almost completely to Q, a situation which is probably rare for most catchments on earth. Therefore, the range of n values considered in Figure 28 are most likely valid for any changes in E_0 or P during the Late Quaternary, which may include decreases due to the conversion of forest to grassland, lower CO_2 and leaf area (LAI), or increases due to the opposite effects (Table 12). In any case, Figure 29 demonstrates that changes in Q within this range of n are not so large for increasing P or decreasing E_0 relative to E, although an increase in P is slightly more effective than a corresponding decrease in E_0 in generating an increase in Q. This is because the LEB has $E_0 >> P$ even for those E_0/P conditions required to sustain large lake levels, meaning that any increase in P will be mostly delivered back to the atmosphere as an increase in E with a much smaller amount available to be transmitted as Q, and that any decrease in E_0 only results in minor reductions (gains) in E (Q). Nevertheless, small changes in Q, and potentially large changes in E, appear to be sufficient within this climatic framework to sustain even the largest lake levels observed in central Australia throughout the last ~130 000 years.

5.7.4 Assessing relative change

Now that the likely catchment and lake E_0/P and E/P conditions required to produce large lake conditions have been determined, it is possible to more fully address the question posed at the beginning of the last section: just how different was the climate? Although the previous section hinted that the differences need not be large on the basis of E_0/P ratios, it is possible to take a step further and attempt to quantify the relative (%) changes in Q and E as a result of changes in catchment E_0 and P. Using Equation (6) we can calculate the changes in E for any given changes to the climatic forcings (P and E_0) according to the following first order derivations (equations 16 – 19) from Roderick and Farquhar (2011):

$$dE = \frac{\partial E}{\partial P} dP + \frac{\partial E}{\partial E_0} dE_0 + \frac{\partial E}{\partial n} dn \qquad (16)$$

with the respective partial differentials :

$$\frac{\partial E}{\partial P} = \frac{E}{P}\left(\frac{E_0^n}{P^n + E_0^n}\right) \quad (17a)$$

$$\frac{\partial E}{\partial E_0} = \frac{E}{E_0}\left(\frac{P^n}{P^n + E_0^n}\right) \quad (17b)$$

$$\frac{\partial E}{\partial n} = \frac{E}{n}\left(\frac{\ln(P^n + E_0^n)}{n} - \frac{(P^n \ln P + E_0^n \ln E_0)}{P^n + E_0^n}\right) \quad (17c)$$

Assuming also that changes in catchment water storage are minimal (Equation 1), the change in Q can then be formulated as:

$$dQ = dP - dE \quad (18)$$

Combining Equations (16) and (18), an analytical expression for the relative change in Q is therefore:

$$\frac{dQ}{Q} = \left[\frac{P}{Q}\left(1 - \frac{\partial E}{\partial P}\right)\right]\frac{dP}{P} - \left[\frac{E_0}{Q}\frac{\partial E}{\partial E_0}\right]\frac{dE_0}{E_0} - \left[\frac{n}{Q}\frac{\partial E}{\partial n}\right]\frac{dn}{n} \quad (19)$$

Using Equation (19) we can now evaluate the hydrological change relative to the present conditions that is required to match the climate conditions indicated by past lake high stands. Although changes in n do not influence E_0/P, they do impact on E/P and therefore the range of n values considered in Figure 28 are also used in the estimation of the effect of dP and dE_0 on dQ/Q in Equation (19).

Although E_0 has almost certainly varied throughout the Late Quaternary as a result of changes in solar forcing and the partitioning of R_n into E and H through Equation (3), Figure 29 demonstrates that even large changes (~ 30% below modern) have only minor effects on the major fluxes of the water balance (since modern E_0 -30 % is still >> P). Therefore, the most critical changes in the Quaternary climate and catchment forcings are likely to be dP and dn, in which case it is possible to test what percentage (%) change in P will be sufficient to sustain the Quaternary lake high stands for given values of n.

Plotting the range of lake high stand E_0/P for both Lake Eyre and Lake Mega-Frome with E_0/P values calculated at increasing increments of P (5 – 30%) demonstrates that the largest lake levels on Lake Mega-Frome can be achieved with only a ~ 9%

increase in catchment P, assuming Cooper Creek / Strzelecki Creek are also contributing catchment areas (Figure 30). For Lake Eyre, the largest recorded lake levels can be maintained with a ~ 27 % increase in catchment P, and in both cases (Lake Mega-Frome and Lake Eyre) this increase is relative to the modern mean LEB conditions in Table 11. As expected, the response of dQ/Q to dP and dn is non-linear, however if we consider n = 1.6 – 1.8 to be a realistic range over the Late Quaternary, then the ~ 9% increase in catchment P corresponds to a 28 – 55 % increase in Q, and the maximum 27 % increase in catchment P (for Lake Eyre) corresponds to a 70 – 88% increase in Q (Figure 30). These results demonstrate that the relative change in catchment climate conditions does not need to be large to effect a large relative change in catchment hydrology and the terminal lake systems to which they drain.

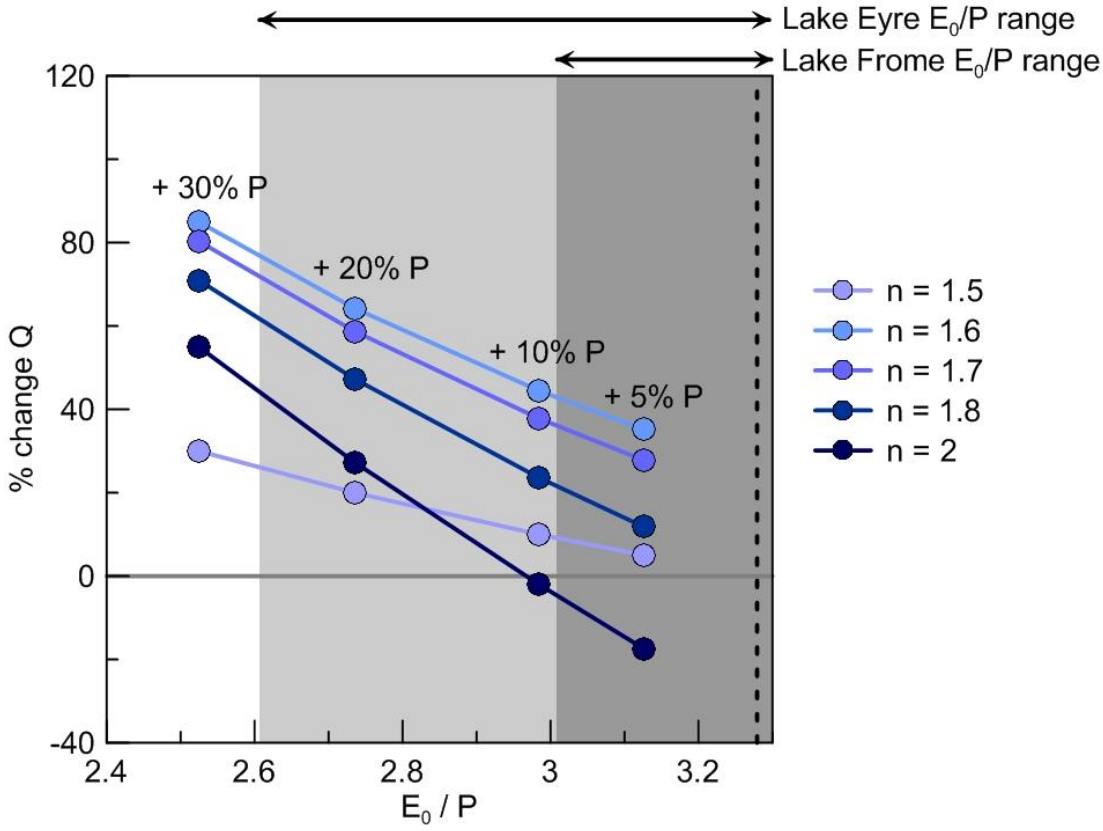

Figure 30. Estimated E_0/P and dQ/Q (% change Q) for increasing catchment precipitation at different catchment parameter n values. The mean modern LEB E_0/P conditions are shown as the dashed vertical line, and the range of E_0/P conditions for the entire filling range of Lake Mega-Frome and Lake Eyre are shown with the dark and light grey sections respectively.

An alternative mechanism for the presence of some high stands on Lake Mega-Frome was proposed by Cohen et al. (in press) wherein an expanded westerly wind system was suggested to deliver moisture from the Southern Ocean to the catchment area of the Flinders Ranges, which then provided all the necessary runoff to sustain Lake Mega-Frome. The same formulation used above can be applied assuming the Flinders Ranges are the only contributing catchment area to Lake Mega-Frome (AR # 2), and again considering changes in E_0 to have little effect on the overall water balance, then the dP/P required to maintain the catchment and lake E_0/P conditions in Figure 28 is ~ 50%. This result is significantly larger than the change required if the Strzelecki Creek / Cooper Creek system was able to contribute runoff (~ 9%), and it is difficult to envisage such a large change impacting only upon the Flinders Ranges, and not also a broader region throughout the southern LEB. Therefore, although the Flinders Ranges almost certainly contributed runoff to an expanded Lake Frome system, the idea that they could have been the sole runoff contributor due to the presence of westerly frontal systems is a difficult and somewhat climatically irreconcilable task.

A final consideration is the potential effects of seasonality on dP, dE, and dQ which are not addressed specifically under the mean annual climate conditions. Table 12 considers these potential changes and their likely direction to be equal and opposite in terms of summer and winter effects on P or E_0, which may of course not necessarily be the case. However, knowing that E_0 can always be assumed to be higher in summer than winter in this environment, a relative reduction in summer P will have a much larger impact on E and Q than any offset provided by an increase in winter P. Thus it is intuitively critical that for large lake levels to be maintained, an increase in winter P will have little effect on the catchment and lake water balance unless high summer P can also be provided. Although this does not exclude the contribution of southern moisture sources such as the westerlies to the overall water balance throughout the Late Quaternary, since they are winter dominated rainfall patterns that are hypothesised to extend northwards, their ability to provide the required increase in mean catchment precipitation for high lake levels will always be limited.

5.8 Implications for the interpretation of Quaternary climatic and hydrological change

The results of this study are pertinent to several debates regarding changes in the climate and water resources of central Australia throughout the Late Quaternary. To date, this debate is mostly centred on a dichotomous hydrological interpretation, whereby central Australia is either 'wet' or 'dry' (Nanson et al., 1992; Williams et al., 2009), and is complemented with a somewhat cryptic use of climatic definitions. For example, both the monsoon and continental aridity have been suggested to have an 'onset' (Chen and Barton, 1991; Wyrwoll and Miller, 2001), with no explanation for how these phenomena should be devoid of transitional behaviour, and this is despite the availability of clear definitions and indexes for both these terms in the modern context (e.g. the shift in wind shear for monsoon onset, and E_0/P for aridity). These issues are not simply semantic, since the arrival of humans in Australia at ~50 ka (Bowler et al., 2003; Roberts et al., 1994) has been suggested to have caused the rapid extinction of the Australian megafauna by ~46 ka (Miller et al., 2005b; Roberts et al., 2001) , which contains the premise that climatic changes were not so dramatic during this period as to be a possible alternative explanation for their demise. Prideaux et al. (2007) and Prideaux et al. (2010) formulated this argument more explicitly when they suggest that the survival of megafauna during previously arid periods in the Pleistocene means that their subsequent extinction at ~46 ka must be due to humans as they were already adapted to arid climates. This general argument appears to neglect the interactions between climate and the hydrological cycle throughout the Quaternary, and the results presented here demonstrate that even within the broad context of arid and semi-arid climate states, small changes in precipitation are sufficient to drive large changes in catchment water fluxes and lake levels. Thus the complete exclusion of climate from the cause of large mammal extinction at this time in already water limited environments seems to result from a fundamental oversight of the non-linear feedbacks between climate and hydrology.

Miller et al. (2005a) extended this potential human impact to atmospheric water fluxes by suggesting that the conversion of forested landscapes in northern Australia to grassland as a consequence of aboriginal burning reduced the penetration of the monsoon into the interior of the continent through the reduction of E and increase in H (Equation 3). The effects of such a response by the atmosphere to the land surface

have been subsequently shown to be very minimal (Pitman and Hesse, 2007). This has been recently been confirmed by Notaro et al (2011), although these authors do suggest some minimal impact on precipitation during the shoulder monsoon season that results in a delay to the monsoon onset. Moreover, these revised conclusions regarding the atmospheric response to land surface changes are consistent with interpretations of current large scale catchment hydroclimatology, whereby the majority of continental precipitation has only a small component derived from vegetation transpiration (Angelini et al., 2011), and is globally dominated by oceanic sources (Gimeno et al., 2010).

The potential sources of oceanic precipitation within the LEB during the Late Quaternary remains a considerable challenge with most arguments still rooted in speculation. Magee et al. (2004) posited that the Holocene monsoon 'failed' because of the lack of recorded lake high stands on Lake Eyre during this time, which was in contrast with the presence of the largest recorded lake phases during the previous interglacial. In addition, Cohen et al. (in press) suggested that the monsoon may only play a minor role in the hydrology of Lake Mega-Frome because of a contrast between the Lake Eyre and Lake Mega-Frome depth records, arguing that Lake Mega-Frome was instead able to fill from Southern Ocean weather sources. The work presented here demonstrates that both these interpretations are misleading, and highlights the risk posed by contrasting 'wet' and 'dry' interpretations of past climates that make no attempt to actually quantify this perceived change. If this study is correct and only minor changes in mean catchment precipitation are required (9 – 27 %) to induce large changes in surface water availability (28 – 88% increase in runoff), then in the absence of direct evidence for the switching of moisture sources a slight enhancement of the current climatic regime of monsoon-dominated precipitation, or some combination that incorporates greater input from other northern source such as precipitation from the western Pacific (Coral Sea), is the simplest and most parsimonious explanation for the hydrological changes required in central Australia over the last ~130 000 years. Of course the synoptic conditions generated by the Southern Ocean throughout this time almost certainly varied from their current arrangement and frequency, and this may indeed be the cause of documented hydrological changes throughout other areas of Australia (Williams et

al., 2009), however on the basis of the work presented here this is not likely to be significant for the LEB.

5.9 Conclusions

This study presents the first evidence for the existence of Quaternary fluvial activity from Cooper Creek via Strzelecki Creek, a record that broadly matches in timing the high stands on Lake Mega-Frome. This demonstrates that the headwater catchments in the north and northeast of the LEB were capable of transporting flood waters down Strzelecki Creek and directly into Lake Mega-Frome. Comparing the high stands on Lake Mega-Frome and Lake Eyre demonstrates much larger hydrological inputs have driven changes in the latter, as well as the difficultly in inferring hydrological differences between the two records. This means that a direct comparison of lake depths based on evidence of Late Quaternary high stands between the two systems is not necessarily hydrologically meaningful.

An evaluation the current hydroclimatology and surface water hydrology within the framework of a simple connected water and energy balance accurately compares key climate ratios using separate estimates derived from catchment parameters and lake areas. When this is then extended to the Quaternary climate by using the lake area ratios from high-stand records for Lakes Eyre and Mega-Frome, it reveals that the ratio of potential evaporation to precipitation, an index of aridity, does not need to be shifted beyond the semi-arid climate state in order for these expanded lake systems to exist. Importantly, it is apparent that potential evaporation is likely to have been very much greater than precipitation at all times in the Late Quaternary, and therefore the sensitivity of the changes in catchment water fluxes resides within increases in precipitation. This means that the most dramatic change in the water budget is actual evaporation returned to the atmosphere. A final calculation provides the first quantitative estimate of the change in precipitation required to maintain large Late Quaternary lake levels. A ~ 9% increase in mean catchment precipitation results in a 22 – 55 % increase in runoff, and is sufficient to maintain the highest recorded extent of Lake Mega-Frome, including its connection to an expanded Lake Eyre. However, in order to maintain the largest lake levels on Lake Eyre, a ~ 27 % increase in precipitation with a resultant ~70 – 88 % increase in runoff is necessary.

These changes are relatively small, keep the overall climate of the Lake Eyre Basin within a semi-arid to arid setting, and demonstrate the extreme sensitivity of water

resources upon the land surface in these environments to very small changes in climate. This suggests that previous interpretations involving contrasting ‘wet’ and ‘dry’ conditions are misleading, and that arguments concerning the origin of moisture for these lakes, and the role of climate in the extinction of megafauna, or the impact of humans on the climate, generally fail to quantify any perceived change in climate, and are therefore unable to accurately account for the non-linear feedbacks between the water and energy budgets which are critical for realistic hydrological interpretations.

6 SUMMARY OF CONCLUSIONS

Although the specific problems addressed in this thesis, and tools used in their investigation are varied, a general theme between them has been the desire to better understand the nature of the water budget in dryland environments, both for understanding the modern context and for interpreting the environmental changes that occurred during the Late Quaternary. A summary of the major conclusions of each chapter, and possible avenues for further study, are given below.

The major controls on surface water quality and the origin of dissolved ions in dryland environments are poorly understood, and Chapter 2 demonstrates that the effects of evaporation on flow are not detectable at most locations in the LEB, despite large transmission losses. Instead, these losses can be attributed mainly to recharge of the shallow groundwater table and other water storages (i.e. floodplain soils and terminal wetlands), a proposal which is investigated in greater detail in Chapter 3. An evaluation of all the potential major ion sources contributing to the dissolved load in the LEB demonstrates that rain and dust contribute between 22 – 75%, with the remaining ions being derived from silicate weathering and carbonate dissolution which is separated on the basis of generic silicate and carbonate mineral stoichiometry. Silicate weathering therefore accounts for 10 – 70% of the dissolved load, a process not previously quantified in dryland environments. This provides a simple explanation for the dominance of HCO_3 and the high concentrations of SiO_2 in the rivers of the LEB. These results have important implications for our understanding of silicate weathering processes, research for which has usually focused on tropical rivers or tectonically active terrains. Since at least one third of the world's land surface is arid to semi-arid, a lack of knowledge about weathering processes in these environments results in a large deficit in our understanding of chemical weathering processes as a whole, a deficit which further research can easily address.

Groundwater from the shallow semi-confined aquifer system of Cooper Creek, the second largest catchment in the Lake Eyre Basin, is investigated in Chapter 3 and was found to exhibit marked changes in salinity and water quality with increasing distance from waterholes, however the exact recharge pathways and mechanisms controlling these changes are not straightforward. Exploring the losses to the surface water budget discussed in Chapter 2 in greater detail, three main groundwater

recharge pathways have been identified: 1. via segments of large channels where the base can be easily scoured, 2. via smaller channels, probably only during exceptional flood events, and 3. through desiccation cracks on the mud floodplain surface. Each of these pathways is distinguished on the basis of tracer (^{14}C and ^{3}H) derived recharge rates, major ions and stable isotopes, and redox chemistry. The first two preferential pathways are largely determined by channel morphology, and the last by antecedent conditions. This explains variation in the large transmission losses both along this section of Cooper Creek in particular, and within mud dominated systems in dryland environments more generally. Given the dominance of preferential flow pathways, mean recharge-rate estimates probably do not capture the true nature of such fluxes in this environment, and it is instead suggested that recharge be considered in terms of the sum of the probability of recharge via these distinct pathways. These results also have implications for the development of saline groundwater systems, since in this study it appears that surface evaporation plays a very minor role because of protection from confining layers. Slow dispersion of recharge waters and fractional leaching in the unsaturated zone in the absence of isotopic enrichment appears to be the best explanation, a process not commonly documented in dryland environments. Furthermore, if these results can be generalised, they suggests that groundwater recharge in semi-confined alluvial settings is likely to be dominated by preferential flow processes. This is important if the water balance of dryland environments is to be determined with a higher degree of certainty. Future work can use these results to investigate preferential flow processes in groundwater recharge more generally, and also attempt to quantify the uncertainty surrounding losses in the water balance.

In order to account for the changes interpreted from palaeo-hydrological records, Chapter 4 discusses the general problem surrounding which climate factors are likely to have changed in the past, and it addresses the considerable confusion surrounding the role of evaporation. The LGM is used as an extreme example, and it is suggested that the well-established drop in mean annual temperatures at that time may not have led to the corresponding drop in mean annual evaporation that researchers have generally assumed. If there was a decrease in precipitation during the LGM, then this would certainly limit the amount of actual evaporation, particularly for the majority of Australia's land surface that is not permanently wet. However, for surfaces such as

wetlands or lakes, whose palaeo-records are used to infer climatic conditions during the LGM, there appears to be no *a priori* reason to suspect that evaporation would have been significantly lower.

These conclusions highlight the lack of a robust conceptual model for palaeo-hydrological processes and feedbacks more generally, since precipitation and evaporation are almost always considered to be uniformly lower, and the role of vegetation is rarely considered. The difficulty of course is quantifying precisely how much, and for how long, these processes impact the terrestrial water balance, and an attempt is made in Chapter 5 to address some of these problems.

In this attempt, the first task of Chapter 5 is to bolster the existing proxy record for river activity in the Lake Eyre Basin, which is known to have experienced considerable hydrological changes during the Late Quaternary. The first evidence for the existence of Quaternary fluvial activity from Strzelecki Creek is presented and is found to match the broad range of lake high stands recently recorded for Lake Mega-Frome. This demonstrates that the headwater catchments of the LEB were capable of transporting flood waters from Cooper Creek down Strzelecki Creek and directly into Lake Mega-Frome, a possibility that was previously only speculated upon. If these floodwaters and their associated rainfall were indeed responsible for the raising and maintaining the high lake levels recorded in the LEB, a simple analysis of lake volumes reveals that much larger hydrological inputs have driven changes in Lake Eyre compared to changes in Lake Mega-Frome. This highlights the difficulty in inferring hydrological differences between lake records, and it is therefore suggested that a direct comparison of lake depths between the two systems is not necessarily hydrologically meaningful.

The last section of Chapter 5 uses climate ratios calibrated to the contemporary conditions to quantitatively examine changes in lake areas and catchment water fluxes. This is extended to the Late Quaternary climate by using the lake area ratios of the lake high stand records from Lake Eyre and Lake Mega-Frome, and reveals that the ratio of potential evaporation to precipitation, an index of aridity, does not need to be shifted beyond the semi-arid climate state in order for these greatly expanded lake systems to exist. Importantly, it is apparent that potential evaporation is always likely to be much greater than precipitation throughout the Late Quaternary, and therefore the sensitivity of the water fluxes to changes in climate

forcings resides mostly within increases to mean precipitation. Because of this, the most dramatic change to the water budget is expected to be in terms of actual evaporation returning water to the atmosphere. A final calculation provides the first quantitative estimate of the changes in precipitation required to maintain large Late Quaternary lake levels. A ~ 9% increase in mean catchment precipitation results in a 22 – 55 % increase in runoff, and is sufficient to maintain the highest recorded extent of Lake Mega-Frome, including its connection to an expanded Lake Eyre. In order to maintain the largest lake levels on Lake Eyre however, a ~ 27 % increase in precipitation with a resultant ~70 – 88 % increase in runoff is necessary. These results demonstrate the extreme sensitivity to very small changes in climate of water resources upon the land surface. This suggests that previous interpretations involving contrasting 'wet' and 'dry' conditions are generally misleading, and that arguments concerning the origin of moisture for these lakes, the role of climate in the extinction of megafauna, or the impact of humans on the climate, generally fail to quantify any perceived change in climate. They are therefore unable to accurately account for the non-linear feedbacks between the water and energy budgets which are critical for realistic hydrological interpretations. It is hoped that this work identifies new approaches for future research to combine field data and modelling for investigations of the modern and Late Quaternary water balances.

REFERENCES

Acworth, R.I., Jankowski, J., 2001. Salt source for dryland salinity - evidence from an upland catchment on the Southern Tablelands of New South Wales. Australian Journal of Soil Research 39, 39-59.

Alley, N.F., 1998. Cainozoic stratigraphy, palaeoenvironments and geological evolution of the Lake Eyre Basin. Palaeogeography, Palaeoclimatology, Palaeoecology 144, 239-263.

Allison, G.B., 1982. The relationship between ^{18}O and deuterium in water in sand columns undergoing evaporation. Journal of Hydrology 55, 163-169.

Amiaz, Y., Sorek, S., Enzel, Y., Dahan, O., 2011. Solute transport in the vadose zone and groundwater during flash floods. Water Resources Research 47, W10513.

Angelini, I., Garstang, M., Davis, R., Hayden, B., Fitzjarrald, D., Legates, D., Greco, S., Macko, S., Connors, V., 2011. On the coupling between vegetation and the atmosphere. Theoretical and Applied Climatology 105, 243-261.

Appelo, C.A.J., Postma, D., 2005. Geochemistry, Groundwater, and Pollution, Second Edition. A.A. Balkema, Amsterdam.

Assayag, N., Rivé, K., Ader, M., Jézéquel, D., Agrinier, P., 2006. Improved method for isotopic and quantitative analysis of dissolved inorganic carbon in natural water samples. Rapid Communications in Mass Spectrometry 20, 2243-2251.

Benson, L.V., Paillet, F.L., 1989. The use of total lake-surface area as an indicator of climatic change: Examples from the Lahontan basin. Quaternary Research 32, 262-275.

Biggs, A.J.W., 2006. Rainfall salt accessions in the Queensland Murray-Darling Basin. Australian Journal of Soil Research 44, 637-645

Bowler, J.M., 1981. Australian salt lakes: a palaeohydrological approach. Hydrobiologia 81-82, 431-444.

Bowler, J.M., 1986. Spatial variability and hydrologic evolution of Australian lake basins: Analogue for pleistocene hydrologic change and evaporite formation. Palaeogeography, Palaeoclimatology, Palaeoecology 54, 21-41.

Bowler, J.M., Hope, G.S., Jennings, J.N., Singh, G., Walker, D., 1976. Late Quaternary climates of Australia and New Guinea. Quaternary Research 6, 359-394.

Bowler, J.M., Johnston, H., Olley, J.M., Prescott, J.R., Roberts, R.G., Shawcross, W., Spooner, N.A., 2003. New ages for human occupation and climatic change at Lake Mungo, Australia. Nature 421, 837-840.

Bowser, C.J., Jones, B.F., 2002. Mineralogic controls on the composition of natural waters dominated by silicate hydrolysis. American Journal of Science 302, 582-662.

Brutsaert, W., Parlange, M.B., 1998. Hydrologic cycle explains the evaporation paradox. Nature 396, 30-30.

Bryan, S.E., Constantine, A.E., Stephens, C.J., Ewart, A., Schön, R.W., Parianos, J., 1997. Early Cretaceous volcano-sedimentary successions along the eastern Australian continental margin: Implications for the break-up of eastern Gondwana. Earth and Planetary Science Letters 153, 85-102.

Budyko, M.I., 1974. Climate and life. Academic press.

Bullard, J.E., McTainsh, G.H., Martin, P., 2007. Establishing Stage-Discharge Relationships in Multiple-Channelled, Ephemeral Rivers: a Case Study of the Diamantina River, Australia. Geographical Research 45, 233-245.

Bunn, S.E., Thoms, M.C., Hamilton, S.K., Capon, S.J., 2006. Flow variability in dryland rivers: boom, bust and the bits in between. River Research and Applications 22, 179-186.

Burford, M.A., Cook, A.J., Fellows, C.S., Balcombe, S.R., Bunn, S.E., 2008. Sources of carbon fuelling production in an arid floodplain river. Marine and Freshwater Research 59, 224-234.

Calf, G.E., 1988. Tritium activity in Australian rainwater 1962-1986. Australian Nuclear Science & Technology Organisation.

Cartwright, Weaver, T.R., Fulton, S., Nichol, C., Reid, M., Cheng, X., 2004. Hydrogeochemical and isotopic constraints on the origins of dryland salinity, Murray Basin, Victoria, Australia. Applied Geochemistry 19, 1233-1254.

Cartwright, Weaver, T.R., Stone, D., Reid, M., 2007. Constraining modern and historical recharge from bore hydrographs, ^{3}H, ^{14}C, and chloride

concentrations: Applications to dual-porosity aquifers in dryland salinity areas, Murray Basin, Australia. Journal of Hydrology 332, 69-92.

Cendón, D.I., Larsen, J.R., Jones, B.G., Nanson, G.C., Rickleman, D., Hankin, S.I., Pueyo, J.J., Maroulis, J., 2010. Freshwater recharge into a shallow saline groundwater system, Cooper Creek floodplain, Queensland, Australia. Journal of Hydrology 392, 150-163.

Ceplecha, V.J., 1971. The distribution of the main components of the water balance in Australia. The Australian Geographer 11, 455-462.

Chen, X.Y., Barton, C.E., 1991. Onset of aridity and dune-building in central Australia: sedimentological and magnetostratigraphic evidence from Lake Amadeus. Palaeogeography, Palaeoclimatology, Palaeoecology 84, 55-73.

Choudhury, B.J., 1999. Evaluation of an empirical equation for annual evaporation using field observations and results from a biophysical model. Journal of Hydrology 216, 99-110.

Clark, I.D., Fritz, P., 1997. Environmental Isotopes in Hydrogeology. Lewis, New York.

Cohen, T.J., Nanson, G.C., Jansen, J.D., Jones, B.G., Jacobs, Z., Larsen, J.R., May, J.H., Treble, P., Price, D.M., Smith, A.M., in press. Late Quaternary mega-lakes fed by the northern and southern river systems of central Australia: Varying moisture sources and increased continental aridity. Palaeogeography, Palaeoclimatology, Palaeoecology.

Cohen, T.J., Nanson, G.C., Larsen, J.R., Jones, B.G., Price, D.M., Coleman, M., Pietsch, T.J., 2010. Late Quaternary aeolian and fluvial interactions on the Cooper Creek Fan and the association between linear and source-bordering dunes, Strzelecki Desert, Australia. Quaternary Science Reviews 29, 455-471.

Costelloe, Irvine, E.C., Western, A.W., Herczeg, A.L., 2009. Groundwater recharge and discharge dynamics in an arid-zone ephemeral lake system, Australia. Limnology and Oceanography 54, 86-100.

Costelloe, J., Payne, E., Woodrow, I., Irvine, E., Western, A., Leaney, F., 2008. Water sources accessed by arid zone riparian trees in highly saline environments, Australia. Oecologia 156, 43-52.

Costelloe, J.F., Shields, A., Grayson, R.B., McMahon, T.A., 2007. Determining loss characteristics of arid zone river waterbodies. River Research and Applications 23, 715-731.

Coventry, R.J., 1976. Abandoned shorelines and the late quaternary history of lake George, New South Wales. Journal of the Geological Society of Australia 23, 249 - 273.

Coventry, R.J., 1978. Late Cainozoic geology, soils, and landscape evolution of the Torrens Creek area, North Queensland. Journal of the Geological Society of Australia 25, 415 - 427.

Dahan, O., Shani, Y., Enzel, Y., Yechieli, Y., Yakirevich, A., 2007. Direct measurements of floodwater infiltration into shallow alluvial aquifers. Journal of Hydrology 344, 157-170.

Dahan, O., Tatarsky, B., Enzel, Y., Kulls, C., Seely, M., Benito, G., 2008. Dynamics of Flood Water Infiltration and Ground Water Recharge in Hyperarid Desert. Ground Water 46, 450-461.

Dogramaci, S.S., Herczeg, A.L., 2002. Strontium and carbon isotope constraints on carbonate-solution interactions and inter-aquifer mixing in groundwaters of the semi-arid Murray Basin, Australia. Journal of Hydrology 262, 50-67.

Donohue, R.J., Roderick, M.L., McVicar, T.R., 2011. Assessing the differences in sensitivities of runoff to changes in climatic conditions across a large basin. Journal of Hydrology 406, 234-244.

Dooge, J.C.I., 1992. Hydrologic models and climate change. Journal of Geophysical Research 97, 2677-2686.

Draper, J., Jensen, A., 1976. The geochemistry of Lake Frome, a playa lake in South Australia. BMR Journal of Australian Geology and Geophysics 1, 83-104.

Edmunds, W.M., Dodo, A., Djoret, D., Gaye, C.H., Goni, I.B., Travi, Y., Zouari, K., Zuppi, G.-M., Gasse, F., 2004. Groundwater as an archive of climatic and environmental change: Europe to Africa. Past Climate Variability through Europe and Africa, In: Battarbee, R.W., Gasse, F., Stickley, C.E. (Eds.). Springer Netherlands, pp. 279-306.

Edmunds, W.M., Guendouz, A.H., Mamou, A., Moulla, A., Shand, P., Zouari, K., 2003. Groundwater evolution in the Continental Intercalaire aquifer of

southern Algeria and Tunisia: trace element and isotopic indicators. Applied Geochemistry 18, 805-822.

Favreau, G., Leduc, C., Marlin, C., Dray, M., Taupin, J.-D., Massault, M., Le Gal La Salle, C., Babic, M., 2002. Estimate of Recharge of a Rising Water Table in Semiarid Niger from ^{3}H and ^{14}C Modeling. Ground Water 40, 144-151.

Feth, J.H., 1971. Mechanisms Controlling World Water Chemistry: Evaporation-Crystallization Process. Science 172, 870-872.

Fitzsimmons, K.E., Rhodes, E.J., Magee, J.W., Barrows, T.T., 2007. The timing of linear dune activity in the Strzelecki and Tirari Deserts, Australia. Quaternary Science Reviews 26, 2598-2616.

Fraedrich, K., 2010. A Parsimonious Stochastic Water Reservoir: Schreiber's 1904 Equation. Journal of Hydrometeorology 11, 575-578.

Fraedrich, K., Sielmann, F., in press. An equation of state for land surface climates. International Journal of Bifurcation and Chaos.

Freeze, A.R., Cherry, J.A., 1979. Groundwater. Prentice Hall, Upper Saddle River.

Fu, B., 1981. On the calculation of the evaporation from land surface. Scientia Atmospherica Sinica 5, 23-31.

Fujioka, T., Chappell, J., Honda, M., Yatsevich, I., Fifield, K., Fabel, D., 2005. Global cooling initiated stony deserts in central Australia 2-4 Ma, dated by cosmogenic ^{21}Ne-^{10}Be. Geology 33, 993-996.

Gaillardet, J., Dupré, B., Louvat, P., Allègre, C.J., 1999. Global silicate weathering and CO2 consumption rates deduced from the chemistry of large rivers. Chemical Geology 159, 3-30.

Galbraith, R.F., Roberts, R.G., Laslett, G.M., Yoshida, H., Olley, J.M., 1999. Optical dating of single and multiple grains of quartz from Jinmium rock shelter, northern Australia: Part 1, experimental design and statistical models. Archaeometry 41, 339-364.

Galloway, R.W., 1965. Late Quaternary Climates in Australia. The Journal of Geology 73, 603-618.

Garrels, R., M., Mackenzie, F., T., 1967. Origin of the Chemical Compositions of Some Springs and Lakes, In: Stumm, W. (Ed.), Equilibrium Concepts in Natural Water Systems. American Chemical Society, pp. 222-242.

Gerrits, A., Savenije, H., Veling, E., Pfister, L., 2009. Analytical derivation of the Budyko curve based on rainfall characteristics and a simple evaporation model. Water Resources Research 45, W04403.

Gibbs, R.J., 1970. Mechanisms Controlling World Water Chemistry. Science 170, 1088-1090.

Gibbs, R.J., 1971. Mechanisms Controlling World Water Chemistry: Evaporation-Crystallization Process: Reply. Science 172, 870-872.

Gimeno, L., Drumond, A., Nieto, R., Trigo, R.M., Stohl, A., 2010. On the origin of continental precipitation. Geophysical Research Letters 37, L13804.

Godsey, S.E., Kirchner, J.W., Clow, D.W., 2009. Concentration–discharge relationships reflect chemostatic characteristics of US catchments. Hydrological Processes 23, 1844-1864.

Gregory, J.W., 1906. The dead heart of Australia: A journey around Lake Eyre in the summer of 1901-1902, with some account of the Lake Eyre basin and the flowing wells of central Australia. J. Murray, London.

Gunn, R., Fleming, P., 1984. The estimated store of soluble salts in the Lake Eyre catchment in Queensland and their possible transport in streamflow to the lake. Australian Journal of Soil Research 22, 119 - 134.

Gunn, R., Richardson, D., 1979. The nature and possible origins of soluble salts in deeply weathered landscapes of eastern Australia. Australian Journal of Soil Research 17, 197-215.

Haberlah, D., Williams, M.A.J., Halverson, G., McTainsh, G.H., Hill, S.M., Hrstka, T., Jaime, P., Butcher, A.R., Glasby, P., 2010. Loess and floods: High-resolution multi-proxy data of Last Glacial Maximum (LGM) slackwater deposition in the Flinders Ranges, semi-arid South Australia. Quaternary Science Reviews 29, 2673-2693.

Hamilton, S.K., Bunn, S.E., Thoms, M.C., Marshall, J.C., 2005a. Persistence of Aquatic Refugia between Flow Pulses in a Dryland River System (Cooper Creek, Australia). Limnology and Oceanography 50, 743-754

Hamilton, S.K., Bunn, S.E., Thoms, M.C., Marshall, J.C., 2005b. Persistence of Aquatic Refugia between Flow Pulses in a Dryland River System (Cooper Creek, Australia). Limnology and Oceanography 50, 743-754.

Harrington, G.A., Cook, P.G., Herczeg, A.L., 2002. Spatial and Temporal Variability of Ground Water Recharge in Central Australia: A Tracer Approach. Ground Water 40, 518-527.

Herczeg, A.L., Dogramaci, S.S., Leaney, F.W.J., 2001. Origin of dissolved salts in a large, semi-arid groundwater system: Murray Basin, Australia. Marine and Freshwater Research 52, 41-52.

Herczeg, A.L., Simpson, H.J., Mazor, E., 1993. Transport of soluble salts in a large semiarid basin: River Murray, Australia. Journal of Hydrology 144, 59-84.

Hesse, P.P., Magee, J.W., van der Kaars, S., 2004. Late Quaternary climates of the Australian arid zone: a review. Quaternary International 118-119, 87-102.

Hobbins, M.T., Dai, A., Roderick, M.L., Farquhar, G.D., 2008. Revisiting the parameterization of potential evaporation as a driver of long-term water balance trends. Geophysical Research Letters 35, L12403.

Hobbins, M.T., Ramírez, J.A., Brown, T.C., 2001. The complementary relationship in estimation of regional evapotranspiration: An enhanced advection-aridity model. Water Resources Research 37, 1389-1403.

Hua, Q., Barbetti, M., 2004. Review of tropospheric bomb 14C data for carbon cycle modeling and age calibration purposes. Radiocarbon 46, 1273-1298.

Jacobson, A.D., Blum, J.D., Chamberlain, C.P., Craw, D., Koons, P.O., 2003. Climatic and tectonic controls on chemical weathering in the New Zealand Southern Alps. Geochimica et Cosmochimica Acta 67, 29-46.

Jacobson, P.J., Jacobson, K.M., Angermeier, P.L., Cherry, D.S., 2000. Variation in material transport and water chemistry along a large ephemeral river in the Namib Desert. Freshwater Biology 44, 481-491.

Johnson, F., Sharma, A., 2010. A Comparison of Australian Open Water Body Evaporation Trends for Current and Future Climates Estimated from Class A Evaporation Pans and General Circulation Models. Journal of Hydrometeorology 11, 105-121.

Jolly, I., Walker, G., Narayan, K., 1994. Floodwater recharge processes in the Chowilla Anabranch system, South Australia. Australian Journal of Soil Research 32, 417-435.

Jolly, I.D., Williamson, D.R., Gilfedder, M., Walker, G.R., Morton, R., Robinson, G., Jones, H., Zhang, L., Dowling, T.I., Dyce, P., Nathan, R.J.,

Nandakumar, N., Clarke, R., McNeill, V., 2001. Historical stream salinity trends and catchment salt balances in the Murray-Darling Basin, Australia. Marine and Freshwater Research 52, 53-63.

Kemp, J., Rhodes, E.J., 2010. Episodic fluvial activity of inland rivers in southeastern Australia: Palaeochannel systems and terraces of the Lachlan River. Quaternary Science Reviews 29, 732-752.

Kershaw, A.P., Nanson, G.C., 1993. The last full glacial cycle in the Australian region. Global and Planetary Change 7, 1-9.

Kiefert, L., 1995. Characteristics of wind transported dust in eastern Australia. Griffith University, Brisbane, Australia.

Knighton, A.D., Nanson, G.C., 1994. Flow transmission along an arid zone anastomosing river, cooper creek, australia. Hydrological Processes 8, 137-154.

Knighton, A.D., Nanson, G.C., 2001. An event-based approach to the hydrology of arid zone rivers in the Channel Country of Australia. Journal of Hydrology 254, 102-123.

Kotwicki, V., 1986. Floods of Lake Eyre. Engineering and Water Supply Dept., Adelaide.

Kotwicki, V., Allan, R., 1998a. La Niña de Australia -- contemporary and palaeo-hydrology of Lake Eyre. Palaeogeography, Palaeoclimatology, Palaeoecology 144, 265-280.

Kotwicki, V., Allan, R., 1998b. La Niña de Australia — contemporary and palaeo-hydrology of Lake Eyre. Palaeogeography, Palaeoclimatology, Palaeoecology 144, 265-280.

Kutzbach, J.E., 1980. Estimates of past climate at Paleolake Chad, North Africa, based on a hydrological and energy-balance model. Quaternary Research 14, 210-223.

Lamontagne, S., Leaney, F.W., Herczeg, A.L., 2005. Groundwater–surface water interactions in a large semi-arid floodplain: implications for salinity management. Hydrological Processes 19, 3063-3080.

Lange, J., 2005. Dynamics of transmission losses in a large arid stream channel. Journal of Hydrology 306, 112-126.

Larsen, J.R., Cendón, D.I., Nanson, G.C., McTainsh, G.H., Jones, B.G., submitted. What determines the dissolved load of dryland rivers? The case for weathering, rain, dust, and absence of evaporation in the Lake Eyre Basin, central Australia. Global Biogeochemical Cycles.

Le Gal La Salle, C., Marlin, C., Leduc, C., Taupin, J.D., Massault, M., Favreau, G., 2001. Renewal rate estimation of groundwater based on radioactive tracers (^{3}H, ^{14}C) in an unconfined aquifer in a semi-arid area, Iullemeden Basin, Niger. Journal of Hydrology 254, 145-156.

Leigh, C., Sheldon, F., Kingsford, R.T., Arthington, A.H., 2010. Sequential floods drive "booms" and wetland persistence in dryland rivers: a synthesis. Marine and Freshwater Research 61, 896-908.

Leon, J., Cohen, T.J., submitted. An improved bathymetric model for the modern and palaeo Lake Eyre. Geomorphology.

Likens, G.E., Keene, W.C., Miller, J.M., Galloway, J.N., 1987. Chemistry of Precipitation From a Remote, Terrestrial Site in Australia. J. Geophys. Res. 92, 13299-13314.

Lomax, J., Hilgers, A., Wopfner, H., Grün, R., Twidale, C.R., Radtke, U., 2003. The onset of dune formation in the Strzelecki Desert, South Australia. Quaternary Science Reviews 22, 1067-1076.

Magee, J.W., Miller, G.H., Spooner, N.A., Questiaux, D., 2004. Continuous 150 k.y. monsoon record from Lake Eyre, Australia: Insolation-forcing implications and unexpected Holocene failure. Geology 32, 885-888.

Małoszewski, P., Zuber, A., 1982. Determining the turnover time of groundwater systems with the aid of environmental tracers: 1. Models and their applicability. Journal of Hydrology 57, 207-231.

Maroulis, J.C., Nanson, G.C., 1996. Bedload transport of aggregated muddy alluvium from Cooper Creek, central Australia: a flume study. Sedimentology 43, 771-790.

Maroulis, J.C., Nanson, G.C., Price, D.M., Pietsch, T., 2007. Aeolian–fluvial interaction and climate change: source-bordering dune development over the past 100 ka on Cooper Creek, central Australia. Quaternary Science Reviews 26, 386-404.

Marshall, J.C., Sheldon, F., Thoms, M., Choy, S., 2006. The macroinvertebrate fauna of an Australian dryland river: spatial and temporal patterns and environmental relationships. Marine and Freshwater Research 57, 61-74

Mason, I.M., Guzkowska, M.A.J., Rapley, C.G., Street-Perrott, F.A., 1994. The response of lake levels and areas to climatic change. Climatic Change 27, 161-197.

McMahon, T.A., Murphy, R.E., Peel, M.C., Costelloe, J.F., Chiew, F.H.S., 2008a. Understanding the surface hydrology of the Lake Eyre Basin: Part 1--Rainfall. Journal of Arid Environments 72, 1853-1868.

McMahon, T.A., Murphy, R.E., Peel, M.C., Costelloe, J.F., Chiew, F.H.S., 2008b. Understanding the surface hydrology of the Lake Eyre Basin: Part 2--Streamflow. Journal of Arid Environments 72, 1869-1886.

McMahon, T.A., Murphy, R.E., Peel, M.C., Costelloe, J.F., Chiew, F.H.S., 2008c. Understanding the surface hydrology of the Lake Eyre Basin: Part 2—Streamflow. Journal of Arid Environments 72, 1869-1886.

McMahon, T.M., Murphy, R., Little, P., Costelloe, J.F., Peel, M.C., Chiew, F.H.S., Hayes, S., Nathan, R., Kandel, D.D., 2005. Hydrology of the Lake Eyre Basin. Sinclair Knight Merz.

McNeil, V.H., Cox, M.E., Preda, M., 2005. Assessment of chemical water types and their spatial variation using multi-stage cluster analysis, Queensland, Australia. Journal of Hydrology 310, 181-200.

McTainsh, G.H., 1989. Quaternary aeolian dust processes and sediments in the Australian region. Quaternary Science Reviews 8, 235-253.

Meredith, K.T., Hollins, S.E., Hughes, C.E., Cendón, D.I., Hankin, S., Stone, D.J.M., 2009. Temporal variation in stable isotopes (^{18}O and ^{2}H) and major ion concentrations within the Darling River between Bourke and Wilcannia due to variable flows, saline groundwater influx and evaporation. Journal of Hydrology 378, 313-324.

Meybeck, M., 2003. Global Occurrence of Major Elements in Rivers, In: Heinrich, D.H., Karl, K.T. (Eds.), Treatise on Geochemistry. Pergamon, Oxford, pp. 207-223.

Miller, G., Mangan, J., Pollard, D., Thompson, S., Felzer, B., Magee, J., 2005a. Sensitivity of the Australian Monsoon to insolation and vegetation:

Implications for human impact on continental moisture balance. Geology 33, 65-68.

Miller, G.H., Fogel, M.L., Magee, J.W., Gagan, M.K., Clarke, S.J., Johnson, B.J., 2005b. Ecosystem Collapse in Pleistocene Australia and a Human Role in Megafaunal Extinction. Science 309, 287-290.

Morin, E., Grodek, T., Dahan, O., Benito, G., Kulls, C., Jacoby, Y., Langenhove, G.V., Seely, M., Enzel, Y., 2009. Flood routing and alluvial aquifer recharge along the ephemeral arid Kuiseb River, Namibia. Journal of Hydrology 368, 262-275.

Morton, F.I., 1983. Operational estimates of areal evapotranspiration and their significance to the science and practice of hydrology. Journal of Hydrology 66, 1-76.

Murray, A.S., Marten, R., Johnston, A., Martin, P., 1987. Analysis for naturally occuring radionuclides at environmental concentrations by gamma spectrometry. Journal of Radioanalytical and Nuclear Chemistry Articles 115, 263-288.

Murray, A.S., Wintle, A.G., 2000. Luminescence dating of quartz using an improved single-aliquot regenerative-dose protocol. Radiation Measurements 32, 57-73.

Murray, A.S., Wintle, A.G., 2003. The single aliquot regenerative dose protocol: potential for improvements in reliability. Radiation Measurements 37, 377-381.

Nanson, G.C., Callen, R.A., Price, D.M., 1998. Hydroclimatic interpretation of Quaternary shorelines on South Australian playas. Palaeogeography, Palaeoclimatology, Palaeoecology 144, 281-305.

Nanson, G.C., East, T.J., Roberts, R.G., 1993. Quaternary stratigraphy, geochronology and evolution of the Magela Creek catchment in the monsoon tropics of northern Australia. Sedimentary Geology 83, 277-302.

Nanson, G.C., Price, D.M., Jones, B.G., Maroulis, J.C., Coleman, M., Bowman, H., Cohen, T.J., Pietsch, T.J., Larsen, J.R., 2008. Alluvial evidence for major climate and flow regime changes during the middle and late Quaternary in eastern central Australia. Geomorphology 101, 109-129.

Nanson, G.C., Price, D.M., Short, S.A., 1992. Wetting and drying of Australia over the past 300 ka. Geology 20, 791-794.

Nanson, G.C., Rust, B.R., Taylor, G., 1986. Coexistent mud braids and anastomosing channels in an arid-zone river: Cooper Creek, central Australia. Geology 14, 175-178.

Nash, J.E., 1989. Potential evaporation and "The complementary relationship". Journal of Hydrology 111, 1-7.

Nativ, R., Adar, E., Dahan, O., Nissim, I., 1997. Water salinization in arid regions—observations from the Negev desert, Israel. Journal of Hydrology 196, 271-296.

Nêmec, J., Schaake, J., 1982. Sensitivity of water resource systems to climate variation. Hydrological Sciences Journal 27, 327-343.

Notaro, M., Wyrwoll, K.-H., Chen, G., 2011. Did aboriginal vegetation burning impact on the Australian summer monsoon? Geophysical Research Letters 38, L11704.

Nott, J., Price, D., 1994. Plunge pools and paleoprecipitation. Geology 22, 1047-1050.

Olley, J.M., Murray, A., Roberts, R.G., 1996. The effects of disequilibria in the uranium and thorium decay chains on burial dose rates in fluvial sediments. Quaternary Science Reviews 15, 751-760.

Parkhurst, D.L., Appelo, C.A.J., 1999. User's guide to PHREEQC (version 2) - A computer program for speciation, batch-reaction, one-dimensional transport, and inverse geochemical calculations. U.S. Geological Survey Water-Resources Investigations Report, p. 312.

Pillans, B., 2007. Pre-Quaternary landscape inheritance in Australia. Journal of Quaternary Science 22, 439-447.

Pitman, A.J., Hesse, P.P., 2007. The significance of large-scale land cover change on the Australian palaeomonsoon. Quaternary Science Reviews 26, 189-200.

Powell, D.M., 2009. Dryland Rivers: Processes and Forms, In: Parsons, A.J., Abrahams, A.D. (Eds.), Geomorphology of Desert Environments. Springer Netherlands, pp. 333-373.

Prescott, J.R., Hutton, J.T., 1988. Cosmic ray and gamma ray dosimetry for TL and ESR. International Journal of Radiation Applications and Instrumentation. Part D. Nuclear Tracks and Radiation Measurements 14, 223-227.

Prescott, J.R., Hutton, J.T., 1994. Cosmic ray contributions to dose rates for luminescence and ESR dating: Large depths and long-term time variations. Radiation Measurements 23, 497-500.

Prideaux, G.J., Gully, G.A., Couzens, A.M.C., Ayliffe, L.K., Jankowski, N.R., Jacobs, Z., Roberts, R.G., Hellstrom, J.C., Gagan, M.K., Hatcher, L.M., 2010. Timing and dynamics of Late Pleistocene mammal extinctions in southwestern Australia. Proceedings of the National Academy of Sciences 107, 22157-22162.

Prideaux, G.J., Roberts, R.G., Megirian, D., Westaway, K.E., Hellstrom, J.C., Olley, J.M., 2007. Mammalian responses to Pleistocene climate change in southeastern Australia. Geology 35, 33-36.

Rimon, Y., Dahan, O., Nativ, R., Geyer, S., 2007. Water percolation through the deep vadose zone and groundwater recharge: Preliminary results based on a new vadose zone monitoring system. Water Resources Research 43, W05402.

Roberts, R.G., Flannery, T.F., Ayliffe, L.K., Yoshida, H., Olley, J.M., Prideaux, G.J., Laslett, G.M., Baynes, A., Smith, M.A., Jones, R., Smith, B.L., 2001. New Ages for the Last Australian Megafauna: Continent-Wide Extinction About 46,000 Years Ago. Science 292, 1888-1892.

Roberts, R.G., Jones, R., Spooner, N.A., Head, M.J., Murray, A.S., Smith, M.A., 1994. The human colonisation of Australia: optical dates of 53,000 and 60,000 years bracket human arrival at Deaf Adder Gorge, Northern Territory. Quaternary Science Reviews 13, 575-583.

Roderick, M.L., Farquhar, G.D., 2011. A simple framework for relating variations in runoff to variations in climatic conditions and catchment properties. Water Resources Research 47, W00G07.

Roderick, M.L., Hobbins, M.T., Farquhar, G.D., 2009. Pan Evaporation Trends and the Terrestrial Water Balance. II. Energy Balance and Interpretation. Geography Compass 3, 761-780.

Roderick, M.L., Rotstayn, L.D., Farquhar, G.D., Hobbins, M.T., 2007. On the attribution of changing pan evaporation. Geophysical Research Letters 34, L17403.

Rotstayn, L.D., Roderick, M.L., Farquhar, G.D., 2006. A simple pan-evaporation model for analysis of climate simulations: Evaluation over Australia. Geophysical Research Letters 33, L17715.

Rust, B.R., Nanson, G.C., 1986. Contemporary and palaeo channel patterns and the late quaternary stratigraphy of Cooper Creek, Southwest Queensland, Australia. Earth Surface Processes and Landforms 11, 581-590.

Scanlon, B.R., 2004. Evaluation of methods of estimating recharge in semiarid and arid regions in the southwestern U.S, In: Hogan, J.F., Phillips, F.M., Scanlon, B.R. (Eds.), Groundwater recharge in a desert environment: the southwestern United States. American Geophysical Union, Washington, D.C, pp. 235-254.

Schreiber, P., 1904. Uber die Beziehungen zwischen dem Niederschlag und der Wasserfuhrung der Flusse in Mitteleuropa. Meteorologische Zeitschrift.

Senior, B.R., Mabbutt, J.A., 1979. A proposed method of defining deeply weathered rock units based on regional geological mapping in southwest Queensland. Journal of the Geological Society of Australia 26, 237-254.

Sharma, K.D., Choudhari, J.S., Vangani, N.S., 1984. Transmission losses and quality changes along a desert stream: the Luni Basin in NW India. Journal of Arid Environments 7, 255-262.

Sheldon, F., Fellows, C.S., 2010. Water quality in two Australian dryland rivers: spatial and temporal variability and the role of flow. Marine and Freshwater Research 61, 864-874.

Shentsis, I., Meirovich, L., Ben-Zvi, A., Rosenthal, E., 1999. Assessment of transmission losses and groundwater recharge from runoff events in a wadi under shortage of data on lateral inflow, Negev, Israel. Hydrological Processes 13, 1649-1663.

Shulmeister, J., Goodwin, I., Renwick, J., Harle, K., Armand, L., McGlone, M.S., Cook, E., Dodson, J., Hesse, P.P., Mayewski, P., Curran, M., 2004. The Southern Hemisphere westerlies in the Australasian sector over the last glacial cycle: a synthesis. Quaternary International 118-119, 23-53.

Simmers, I., 1997. Recharge of phreatic aquifers in (semi-) arid areas. AA Balkema, Rotterdam.

Simpson, H.J., Herczeg, A.L., 1994. Delivery of marine chloride in precipitation and removal by rivers in the Murray-Darling Basin, Australia. Journal of Hydrology 154, 323-350.

Singh, G., Luly, J., 1991. Changes in vegetation and seasonal climate since the last full glacial at Lake Frome, South Australia. Palaeogeography, Palaeoclimatology, Palaeoecology 84, 75-86.

Singh, G., Opdyke, N.D., Bowler, J.M., 1981. Late Cainozoic stratigraphy, palaeomagnetic chronology and vegetational history from Lake George, N.S.W. Journal of the Geological Society of Australia 28, 435 - 452.

Tooth, S., 2000. Process, form and change in dryland rivers: a review of recent research. Earth-Science Reviews 51, 67-107.

Turney, C.S.M., Haberle, S., Fink, D., Kershaw, A.P., Barbetti, M., Barrows, T.T., Black, M., Cohen, T.J., Corrège, T., Hesse, P.P., Hua, Q., Johnston, R., Morgan, V., Moss, P., Nanson, G., van Ommen, T., Rule, S., Williams, N.J., Zhao, J.X., D'Costa, D., Feng, Y.X., Gagan, M., Mooney, S., Xia, Q., 2006. Integration of ice-core, marine and terrestrial records for the Australian Last Glacial Maximum and Termination: a contribution from the OZ INTIMATE group. Journal of Quaternary Science 21, 751-761.

Tweed, S., Leblanc, M., Cartwright, I., Favreau, G., Leduc, C., 2011. Arid zone groundwater recharge and salinisation processes; an example from the Lake Eyre Basin, Australia. Journal of Hydrology 408, 257-275.

van Heerwaarden, C.C., Vilà-Guerau de Arellano, J., Teuling, A.J., 2010. Land-atmosphere coupling explains the link between pan evaporation and actual evapotranspiration trends in a changing climate. Geophysical Research Letters 37, L21401.

Walvoord, M.A., Plummer, M.A., Phillips, F.M., Wolfsberg, A.V., 2002. Deep arid system hydrodynamics 1. Equilibrium states and response times in thick desert vadose zones. Water Resources Research 38, 1308.

West, A.J., Galy, A., Bickle, M., 2005. Tectonic and climatic controls on silicate weathering. Earth and Planetary Science Letters 235, 211-228.

White, A.F., 2003. Natural Weathering Rates of Silicate Minerals, In: Heinrich, D.H., Karl, K.T. (Eds.), Treatise on Geochemistry. Pergamon, Oxford, pp. 133-168.

White, I., Macdonald, B.C.T., Somerville, P.D., Wasson, R., 2009. Evaluation of salt sources and loads in the upland areas of the Murray–Darling Basin, Australia. Hydrological Processes 23, 2485-2495.

Williams, M., Cook, E., van der Kaars, S., Barrows, T., Shulmeister, J., Kershaw, P., 2009. Glacial and deglacial climatic patterns in Australia and surrounding regions from 35 000 to 10 000 years ago reconstructed from terrestrial and near-shore proxy data. Quaternary Science Reviews 28, 2398-2419.

Williams, M., Prescott, J.R., Chappell, J., Adamson, D., Cock, B., Walker, K., Gell, P., 2001. The enigma of a late Pleistocene wetland in the Flinders Ranges, South Australia. Quaternary International 83-85, 129-144.

Wintle, A.G., Murray, A.S., 2006. A review of quartz optically stimulated luminescence characteristics and their relevance in single-aliquot regeneration dating protocols. Radiation Measurements 41, 369-391.

Wopfner, H., Twidale, C.R., 1967. Geomorphological history of the Lake Eyre basin, In: Jennings, J.N., Mabbutt, J.A. (Eds.), Landform Studies from Australia and New Guinea. A.N.U. Press, Canberra, pp. 118-143.

Wyrwoll, K.-H., Miller, G.H., 2001. Initiation of the Australian summer monsoon 14,000 years ago. Quaternary International 83-85, 119-128.

Yang, D., Sun, F., Liu, Z., Cong, Z., Lei, Z., 2006. Interpreting the complementary relationship in non-humid environments based on the Budyko and Penman hypotheses. Geophysical Reseach Letters 33, L18402.

Yang, H., Yang, D., Lei, Z., Sun, F., 2008. New analytical derivation of the mean annual water-energy balance equation. Water Resources Research 44, W03410.

Zhang, L., Hickel, K., Dawes, W., Chiew, F., Western, A., Briggs, P., 2004. A rational function approach for estimating mean annual evapotranspiration. Water Resources Research 40, W02502.

APPENDIX A

List of journal articles to which the candidate has contributed as an author

Cendón, D.I., Larsen, J.R., Jones, B.G., Nanson, G.C., Rickleman, D., Hankin, S.I., Pueyo, J.J., Maroulis, J., 2010. Freshwater recharge into a shallow saline groundwater system, Cooper Creek floodplain, Queensland, Australia. Journal of Hydrology 392, 150-163.

Cohen, T.J., Nanson, G.C., Jansen, J.D., Jones, B.G., Jacobs, Z., Larsen, J.R., May, J.H., Treble, P., Price, D.M., Smith, A.M., in press. Late Quaternary mega-lakes fed by the northern and southern river systems of central Australia: Varying moisture sources and increased continental aridity. Palaeogeography, Palaeoclimatology, Palaeoecology.

Cohen, T.J., Nanson, G.C., Larsen, J.R., Jones, B.G., Price, D.M., Coleman, M., Pietsch, T.J., 2010. Late Quaternary aeolian and fluvial interactions on the Cooper Creek Fan and the association between linear and source-bordering dunes, Strzelecki Desert, Australia. Quaternary Science Reviews 29, 455-471.

Ladd, B., Bonser, S.P., Peri, P.L., Larsen, J.R., Laffan, S.W., Pepper, D.A., Cendón, D.I., 2009. Towards a physical description of habitat: quantifying environmental adversity (abiotic stress) in temperate forest and woodland ecosystems. Journal of Ecology 97, 964-971.

Ladd, B., Larsen, J.R., Bonser, S.P., 2010. Effect of two types of tree guards (with and without weed control) on tree seedling establishment. Ecological Management & Restoration 11, 75-76.

Larsen, J.R., 2011. Was Evaporation Lower During the Last Glacial Maximum? Quaternary Australasia 28, 11.

Larsen, J.R., Cendón, D.I., Nanson, G.C., McTainsh, G.H., Jones, B.G., submitted. What determines the dissolved load of dryland rivers? The case for weathering, rain, dust, and absence of evaporation in the Lake Eyre Basin, central Australia. Global Biogeochemical Cycles.

Nanson, G.C., Price, D.M., Jones, B.G., Maroulis, J.C., Coleman, M., Bowman, H., Cohen, T.J., Pietsch, T.J., Larsen, J.R., 2008. Alluvial evidence for major climate and flow regime changes during the middle and late Quaternary in eastern central Australia. Geomorphology 101, 109-129.

APPENDIX B

PDF copies of articles listed in Appendix A